HUGHES TOOL COMPANY · AIRCRAFT DIVISION
Culver City, California

Report 285-9-8 (62-8)

CONTRACT NO. AF 33(600)-30271

HOT CYCLE ROTOR SYSTEM
RESULTS OF COMPONENT TEST PROGRAM

FINAL REPORT

March 1962

HUGHES TOOL COMPANY -- AIRCRAFT DIVISION
Culver City, California

for

Commander

Aeronautical Systems Division

Prepared by: G. D. Deveaux

G. D. Deveaux
Head, Structures Test

Approved by: C. R. Smith

C. R. Smith
Chief, Structures
Analysis and Test

J. L. Velazquez

J. L. Velazquez
Sr. Project Engineer

H. O. Nay

H. O. Nay
Manager, Transport Helicopter
Department

TABLE OF CONTENTS

SECTION 1

SUMMARY

This Component Test Program Report presents the results of the component tests conducted during the latter part of the Hot Cycle Rotor System development program. Prior component test results were submitted in HTC-AD reports 285-9-1 thru 285-9-6.

The Blade Fatigue Test, after modifications, gave a satisfactory service life. The Articulate Duct Outboard Seal Test and the Blade Flapping-Feathering Bearing Wear Test indicated satisfactory service life with negligible wear and leakage. The two Segment Duct Assembly Sealant Test demonstrated the ability of the RTV-601 silastic rubber compound to withstand the pressure and thermal environments of the Hot Cycle Rotor System.

SECTION 2

INTRODUCTION

This section presents the results of the Component Test Program in support of the Hot Cycle Rotor System performed by this Contractor.

The objectives of this program were to experimentally evaluate various materials and design concepts connected with the development of the Hot Cycle Rotor System concept, and to determine the reliability of the critical components of the Hot Cycle Rotor System to insure successful completion of the Whirl Test Program.

SECTION 3

ROTOR BLADE FULL SCALE FATIGUE TEST

3.1 PURPOSE

To determine a satisfactory service life for the rotor blade when subjected to primary loads of flapwise bending, centrifugal force and internal pressure.

3.2 TEST SETUP

3.2.1 Specimen

The test specimen consisted of a production blade from the root section to approximately midspan. Stations 19 to 159. This blade included the root retention straps, complete root structure modified titanium spars, five constant section segments, segment flexural couplings, trailing and leading edges and ducting from Stations 86 to 159. The segments discontinue at Station 159 and only modified spars extend outboard to Station 225. The test blade assembly Drawing 285-0200 is shown in Figure 3-1.

3.2.1.1 Modifications. Modifications to the test blade assembly were made to reduce fabrication costs and to eliminate the components which have a proven fatigue life, such as the feathering-flapping bearing and the articulate duct outboard seal (tests reported later herein).

The spars, between Stations 116 to 159, were modified to produce the same stresses under load as the critical section at Station 159 during flight. At Station 161 the spars are bent to converge at the quarter chord of Station 225. This convergence is intended to minimize differential bending that would be induced by blade torsion.

The internal ducts are closed off at Stations 86 and 159, forming a clos closed duct system. The bulkhead assembly added at Station 159 provides a duct system pressure bulkhead heater support, and a means of introducing the bending and torsion excitation loads into the blade.

3.2.1.2 Test Fixture

a. Loading Arrangement. The test blade assembly was mounted in the test fixture as a hinged beam under axial tension type loading or simulated centrifugal force. The fixture consisted of an I-beam base 40 feet long which supported load-reaction structures on each end. Figures 3-2 and 3-7 show this arrangement.

Centrifugal force is transmitted through a horizontal strap pack to a flexure at the tip end of the specimen. A hydraulic jack was used to apply the load to the strap. Variations in the centrifugal force due to flapwise bending were minimized by designing the jig base to act as a spring, mounted on two flexural pivots.

Flapwise bending was produced by excitation in the flapwise direction. A 5HP varidrive eccentric of adjustable stroke located at Station 159, (see Figure 3-8), was used to apply vertical force.

Torsion was induced by a four bar linkage arrangement at Station 159. The links restrained the blade, thus inducing torsion as flapwise bending was produced. Refer to Figure 3-2.

b. Heating Arrangement. Duct wall temperatures are simulated by internal banks of electrical heaters installed in each duct. The heaters consisted of strips of Nichrome ribbon installed on and insulated from cantilevered steel tubes. These tubes were supported at Station 159 and projected into the forward and aft ducts to Station 126. The heating elements provided a source of heat between Stations 126 and 148. This length included three (3) complete segments and two (2) flexural couplings.

The heaters were divided into separate banks to allow for a positive control of temperatures on the forward, upper, lower and aft portions of each duct. An external source of electrical power, a 120 amp DC generator, was used and control was achieved with ammeters and potentiometers. Figure 3-9 and Drawing 285-0916 show the heater details.

A centrifugal air blower located in front of the test area was used to prevent the outer skin from exceeding 420°F. Cooling air was also provided along the forward and aft spars by air hoses inserted into the leading and trailing edge fairings, as shown in the photograph in Figure 3-10.

c. Pressure Arrangement. The duct system, between Stations 86 and 159, formed a chamber which was pressurized to 24.0 psig. Pressure to the ducts was from nitrogen bottles during the first part of the test and from plant air supply during the remaining portion of the test. Nitrogen was first used to minimize the possibility of igniting the sealant compound at the duct high temperatures. Subsequent tests on the sealant compound demonstrated that this precaution was unnecessary and thereafter plant air was used. Leakage during the test was measured with a flowmeter.

3.2.1.3 Instrumentation

a. Strain Gage Installation. All loads and moments are measured

with electrical resistance strain gages or strain gaged devices. Axial load, input and output torsion couple, and input excitation load were measured with calibrated strain gaged load cells. Full bridge temperature compensated installations are made along the forward and aft spars as shown on Figures 3-10 and 3-3. The output of all strain gage bridges were recorded on an 18 channel oscillograph.

b. Thermocouple Installation. Iron-constantan and cromel-alumel thermocouples were installed in critical duct areas and outer skin areas. All thermocouple outputs were recorded on a Brown strip chart potentiometer through a switching unit. Figure 3-4 shows the thermocouple locations.

c. Calibration. Each load cell was calibrated in a Baldwin Test Machine utilizing a Baldwin SR-4 Strain Indicator. Bending strain gage bridges on the spars were calibrated with the test blade loaded as a simple beam. A vertical load was applied at Station 159 with zero centrifugal load. Bridge output was recorded on the oscillograph.

3.2.1.4 Test Load Conditions

The test conditions which were applied to the test blade assembly were as follows:

Flapwise bending (Stations 116-153.5) = $\pm$ 16,200 inch-pounds
Centrifugal force = 111,000 pounds
Torsion = $\pm$ 9,300 inch-pounds
Internal duct pressure = 24.0 psig
Simulated gas temperature = 1050°F.

The derivation of the test loads are given in HTC-AD Report 285-8-2S (61-14S).

3.2.1.5 Test Procedure

a. The centrifugal force and pressure were first applied to the test blade. Preliminary natural frequency tests were conducted by manually striking the blade and jig. An accelerometer mounted at Station 159 and connected to a Brush Recorder showed the blade's flapwise response.

b. Initial dynamic runs were then conducted without the heaters energized to attain the correct bending moments and torsion values. When these loads were established the accelerometer response was recorded and this "G" value was used to maintain the correct dynamic loading during the test.

c. For the actual test run the heaters were first energized and the temperature gradually increased. The duct pressure was applied during this temperature increase. When the temperature and pressure were stabilized the varidrive exciter was started and brought up to the proper flapwise bending values. All bending moments and loads were recorded on a recording C. E. C. oscillograph. All temperatures were recorded on the Brown Recorder. The loads and temperatures were recorded at thirty minute intervals during the test. The accelerometer response was continually monitored for any deviation which would indicate a possible malfunction.

3.3 TEST RESULTS

3.3.1 Phase I Tests

a. The test blade assembly was subjected to the test load conditions. Figures 3-11, 3-12 and 3-13 show the test blade assembly during the test. The temperatures attained within the duct area are shown in Figure 3-4. The bending moment distribution along the spars is shown in Figure 3-5.

b. At 266,000 cycles of load simulating the Weighted Fatigue Condition, the aft spar of the fatigue blade failed. The rupture consisted of a vertical break at Station 73 through two 5/16 inch bolt holes in the spar webs (Figures 3-14 and 3-15), which are provided for bolts that react the loads induced by a slight change in direction of the spars. Inspection of the failure area revealed that the fatigue crack had started at the upper hole (Figures 3-16 and 3-17) and worked out through the upper flange. The remainder of the failed section had the appearance of a ductile failure. Laboratory examination; showed normal Alpha structure for the Ti 6al-4V with no inclusions present. Burrs and galling were evident in the holes with minute cracks visible in the burrs at the edge of the hole. Figures 3-18, 3-19, 3-20 and 3-21. This condition was the result of a reaming operation on final assembly. Although it was intended that the ends of the holes through the spar web have rounded edges, the .005-.010 radius called out in Drawing No. 285-0170 was lost when it was found necessary to enlarge the holes during final assembly after the spars were partially attached to the blade structure. The burred and cracked condition discussed above escaped detection, particularly on the back side of the spar web where it bears against the blade segments and is not accessible to inspection except by removal of the spar.

c. Strain gage bending bridges were located on the spar at Stations 78, 112, 135, and 152.5. Extrapolation of recorded bending moments to Station 73 results in a cyclic moment of approximately $\pm$ 19,000 in-lbs. This gives a primary cyclic stress at the outer fiber of $\pm$ 10,000 psi with a steady stress of 36,000 psi. The corresponding cyclic stress at the edge of the bolt hole is $\pm$ 4,600 psi. The spar material,

Ti 6al-4V, in a polished specimen, has an endurance limit of 60, 000 psi or greater at the steady stress noted above. Although it is difficult to explain the initiation of a conventional fatigue failure at the low calculated stress levels, propagation of an existing crack that extends into the base material is readily understood even at the low calculated stress levels.

d. The aft spar takes a slight bend at this station (approximately 4. 5°) which induces secondary stresses. Although these secondary stresses are not considered to be appreciable in the whirl blades during actual operation, there is a possibility that these stresses may have been more severe in the full-scale fatigue specimen. The theoretical spar cap stresses calculated for combined flapwise and chordwise bending are simulated in the fatigue blade by applying, at Station 73, a flapwise bending moment of ± 19, 000 in-lbs., as mentioned above, in lieu of ± 9, 500 in-lbs. corresponding to the weighted fatigue condition at this station. Although this simplified procedure simulates the primary stresses, the secondary stresses may have been increased to an unknown degree, thus aggravating the fabrication discrepancy.

3. 3. 2 Repair Operation

The failed rear spar was replaced with a spare whirl test blade spar. The outboard portion of the rear spar was strengthened with a titanium doubler. HTC-AD Drawings 285-0224, 285-0225 and 285-0226 show the rework of the outboard portion of the rear spar. The rework of the inboard portion of the rear spar is shown in HTC-AD Drawing 285-0223. Figures 3-22 and 3-23 show the inboard reworked area. The front spar was reinstalled with new bolts replacing the bolts that were sheared due to secondary failure.

3. 3. 3 Phase II Test

The modified test blade assembly was subjected to cyclic flapwise bending, and centrifugal force loads. The cyclic flapwise bending was revised to ± 14, 200 inch-pounds at Station 73. 0 on the rear spar. Since the primary purpose of the phase II Testing was to evaluate structural integrity of the spars, including the rear spar reinforcement, at Station 73 the torsion load was deleted. All other load conditions remained constant. Figure 3-6 shows the flapwise bending moment distribution along the forward and aft spars. The fatigue test continued until 2, 049, 000 cycles on the blade assembly was accumulated. The total number of cycles on the modified rear spar was 1, 785, 000 cycles.

3. 3. 4 Inspection

Inspection of the test blade assembly revealed no indications of

fatigue cracks in the rear or front spars. The segments were not visibly damaged.

3.3.5 Material Evaluation Tests of the Failed Aft Spar

a. Static Tensile Tests. Tensile coupons were machined from the area adjacent to the fracture in the logitudinal direction. The coupon configuration was taken from the Federal Method Standard Number 151. The static tensile coupons were tested in a Baldwin-Hamilton 5,000 pound Test Machine. The results are shown in Table 3-1.

b. Fatigue Coupon Tests. Fatigue specimens were machined from material adjacent to the fracture area in a longitudinal direction. The specimens were subjected to tension-tension type loading in a resonant-beam fatigue machine. Two types of specimens were tested. The first type consisted of smooth specimens to check the endurance limit of the aft spar. The second type of specimens contained a hole at the reduced section. This hole was machined with a burr in an attempt to duplicate the hole conditions in the test spar. Other specimens of this type were radiused with a rubber impregnated abrasive to compare the fatigue life of the two hole conditions. The two specimen configurations are shown in Figure 3-24. The two hole conditions are shown in Figures 3-25 and 3-26.

The results of the failed aft spar specimen fatigue tests are shown in Table 3-2. Due to the limited number of specimens tested and the difficulty in reproducing the type of burr as shown in Figure 3-19 conclusive evidence of a marked decrease in the fatigue life cannot be stated. The limited data shows only that a trend in the reduction of fatigue life due to a burr is indicated.

c. Results of Laboratory Examination

Microstructure

(1) Normal Alpha structure
(2) No inclusion present
(3) Grain size 7-8

Hardness

Rockwell 15N 78-80
Converted to Rockwell C 35-39

Remarks:

(1) Burrs and galling present in holes.
(2) Minute cracks visible in burrs.

Material

Meets specification requirements.

TABLE 3-1

STATIC TENSILE PROPERTIES OF TITANIUM FAILED SPAR

Specimen No.	Area ($in.^2$)	Thickness (in.)	Load (lbs)	Ultimate Stress (psi)	Yield Stress .2% Elong.	Percent Elongation
A	.0638	.0255	9920	154,500	147,000	15
B	.0629	.0260	10,000	159,000	153,000	13

TABLE 3-2

FATIGUE TEST OF FAILED TITANIUM AFT SPAR SPECIMENS

Specimen No.	Specimen Configuration	Maximum Stress (PSI)	Mean Stress (PSI)	Total Cyclic Stress Variation (PSI)	Number of Cycles	Remarks
1 B	No hole	100, 000	55, 000	90, 000	3, 164, 000	No failure
2 B	No hole	120, 000	66, 000	108, 000	1, 748, 000	Failed
1	Burr on edge of . 313 in. hole	41, 000	36, 000	10, 000	3, 119, 000	No failure
1*	Burr on edge of . 438 in. hole	46, 000	36, 000	20, 000	559, 950	Failed
3	Burr on edge of . 403 in. hole	41, 000	36, 000	10, 000	2, 950, 000	No failure
3	Same as above	46, 000	36, 000	20, 000	336, 000	Failed
5	Burr on edge of . 403 in. hole	46, 000	36, 000	20, 000	391, 540	Failed
2 **	Polished . 403 in. hole	46, 000	36, 000	20, 000	440, 000	Failed (crack occurred in gall mark in hole.)

* Hole diameter increased from . 313 inch to . 438 inch to obtain a burr more closely simulating the aft spar hole condition.

** Specimen hole edges polished with coarse abrasive in rubber followed by fine abrasive in rubber.

TABLE 3-2 (continued)

FATIGUE TEST OF FAILED TITANIUM AFT SPAR SPECIMENS

Specimen No.	Specimen Configuration	Maximum Stress (PSI)	Mean Stress (PSI)	Total Cyclic Stress Variation (PSI)	Number of Cycles	Remarks
6***	Polished .406 in. hole	46,000		20,000	3,669,000	No failure
		51,000	36,000	30,000	1,142,000	No failure
		56,000		40,000	658,000	Failed in grip area

*** Specimen hole diameter increased from .313 inch to .406 inch in successive drilling operations of .030 inch per cut to .015 inch per cut until very small cuts were taken to the final hole diameter.

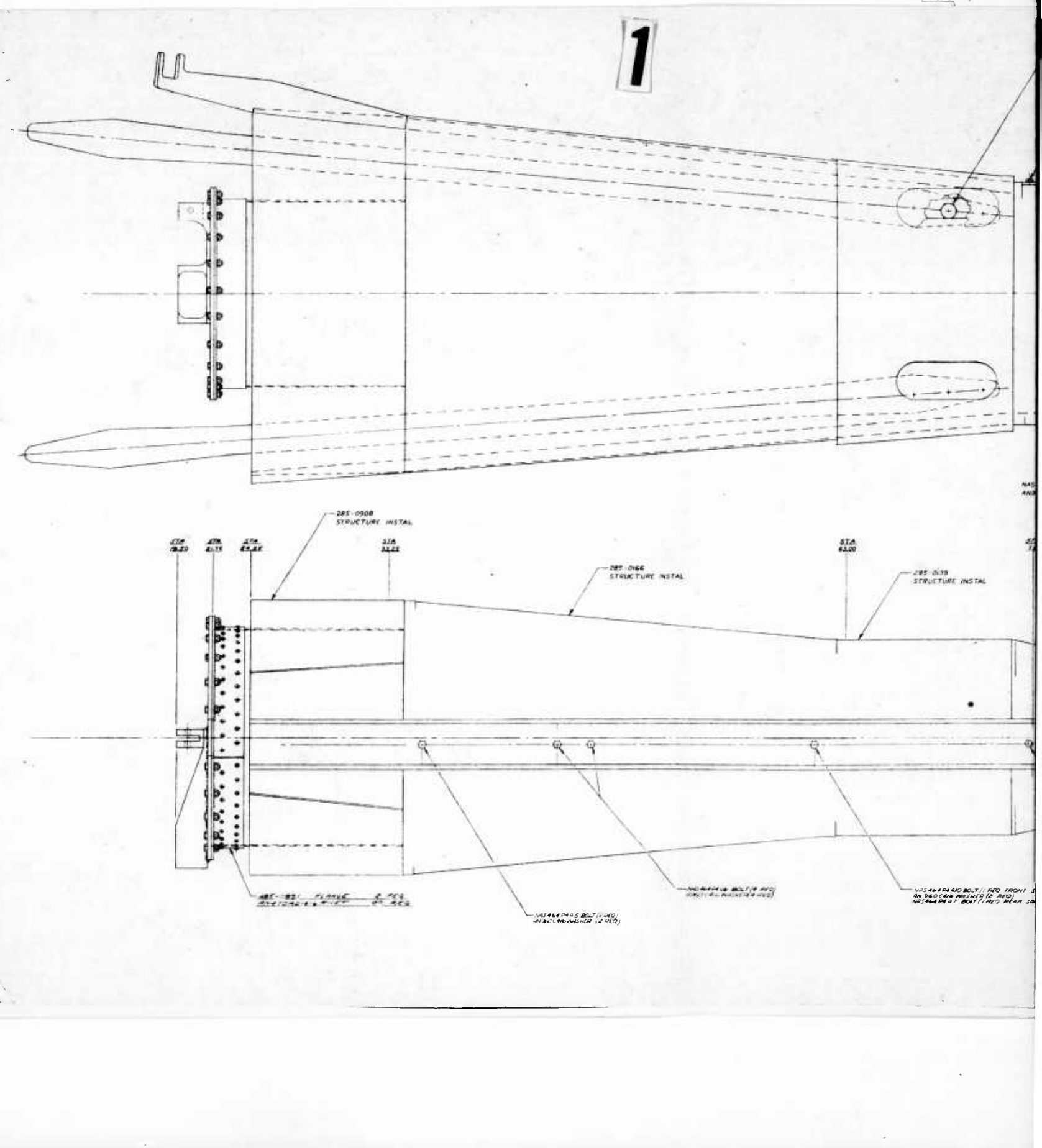
1
285-0908
STRUCTURE INSTAL
285-0966
STRUCTURE INSTAL
285-0639
STRUCTURE INSTAL

2

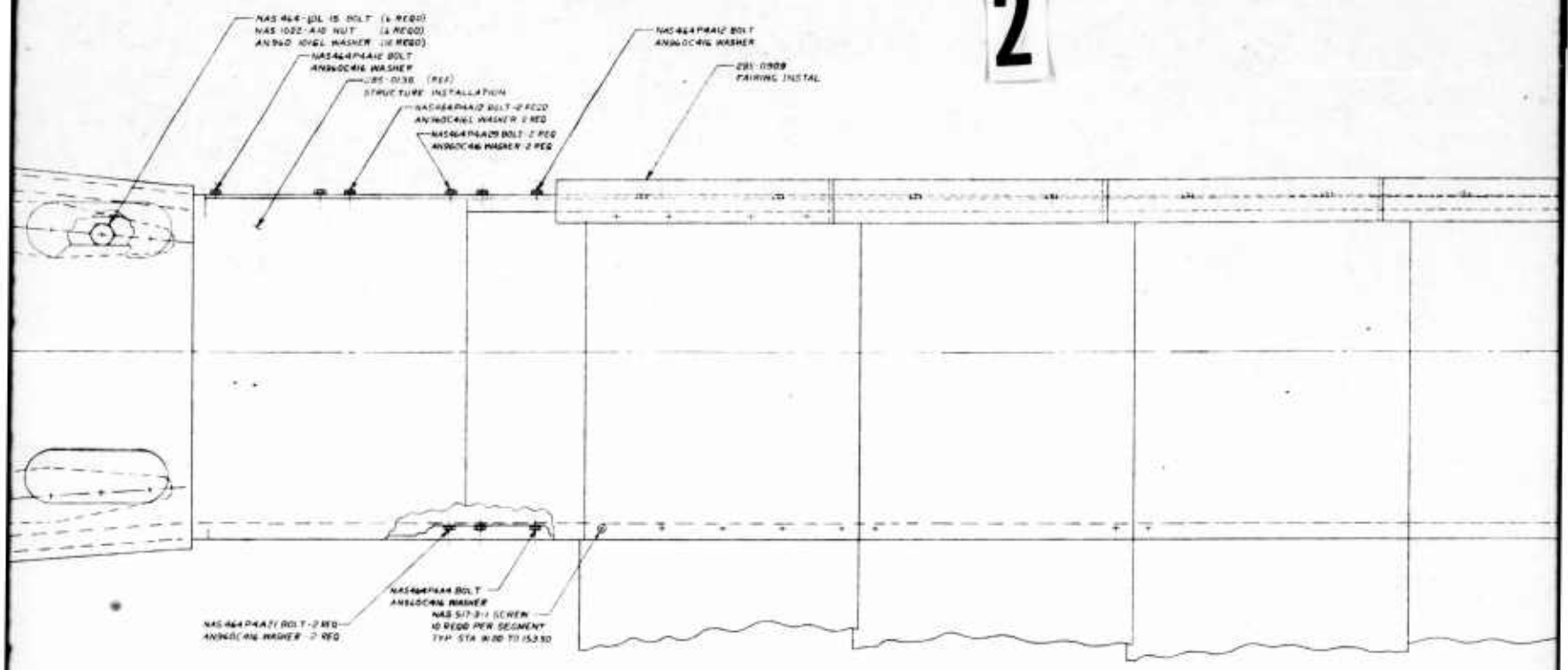
NAS 464-10L 15 BOLT (4 REQD)
NAS 1032-A10 NUT (4 REQD)
AN960 10VGL WASHER (10 REQD)
NAS464P4A12 BOLT
AN960C416 WASHER
285-0138 (REF)
STRUCTURE INSTALLATION
NAS464P4A12 BOLT-2 REQD
AN960C416L WASHER 2 REQ
NAS464P4A29 BOLT-2 REQ
AN960C416 WASHER 2 REQ
NAS464P4A12 BOLT
AN960C416 WASHER
285-0909
FAIRING INSTAL
NAS464P4A44 BOLT
AN960C416 WASHER
NAS 517-3-1 SCREW
10 REQD PER SEGMENT
TYP STA 14.00 TO 153.50
NAS464P4A17 BOLT-2 REQ
AN960C416 WASHER 2 REQ

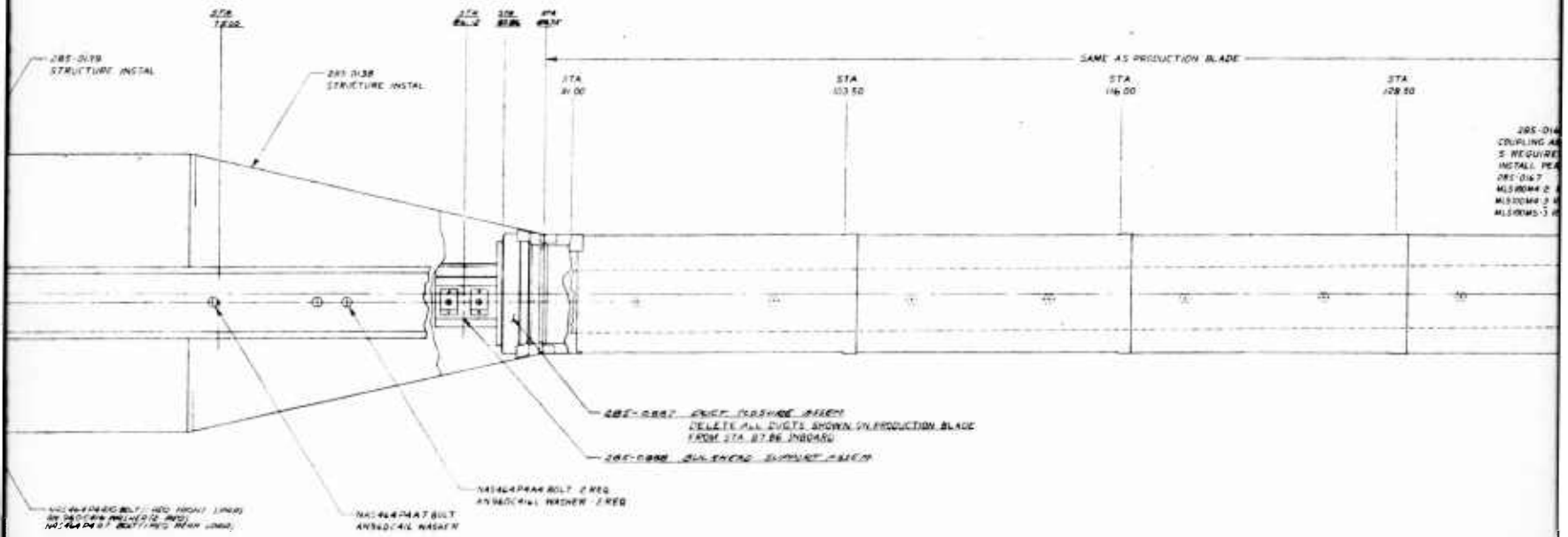
STA 7.00
STA 14.00
STA 28.00
285-0139
STRUCTURE INSTAL
285-0138
STRUCTURE INSTAL
SAME AS PRODUCTION BLADE
STA 14.00
STA 103.50
STA 146.00
STA 228.50
285-0867 DUCT (SHADE ASSY)
DELETE ALL DUCTS SHOWN ON PRODUCTION BLADE
FROM STA 87.86 INBOARD
285-0888 BULKHEAD SUPPORT ASSY
NAS464P4A6 BOLT-2 REQ
AN960C416L WASHER-2 REQ
NAS464P4A7 BOLT
AN960C416L WASHER

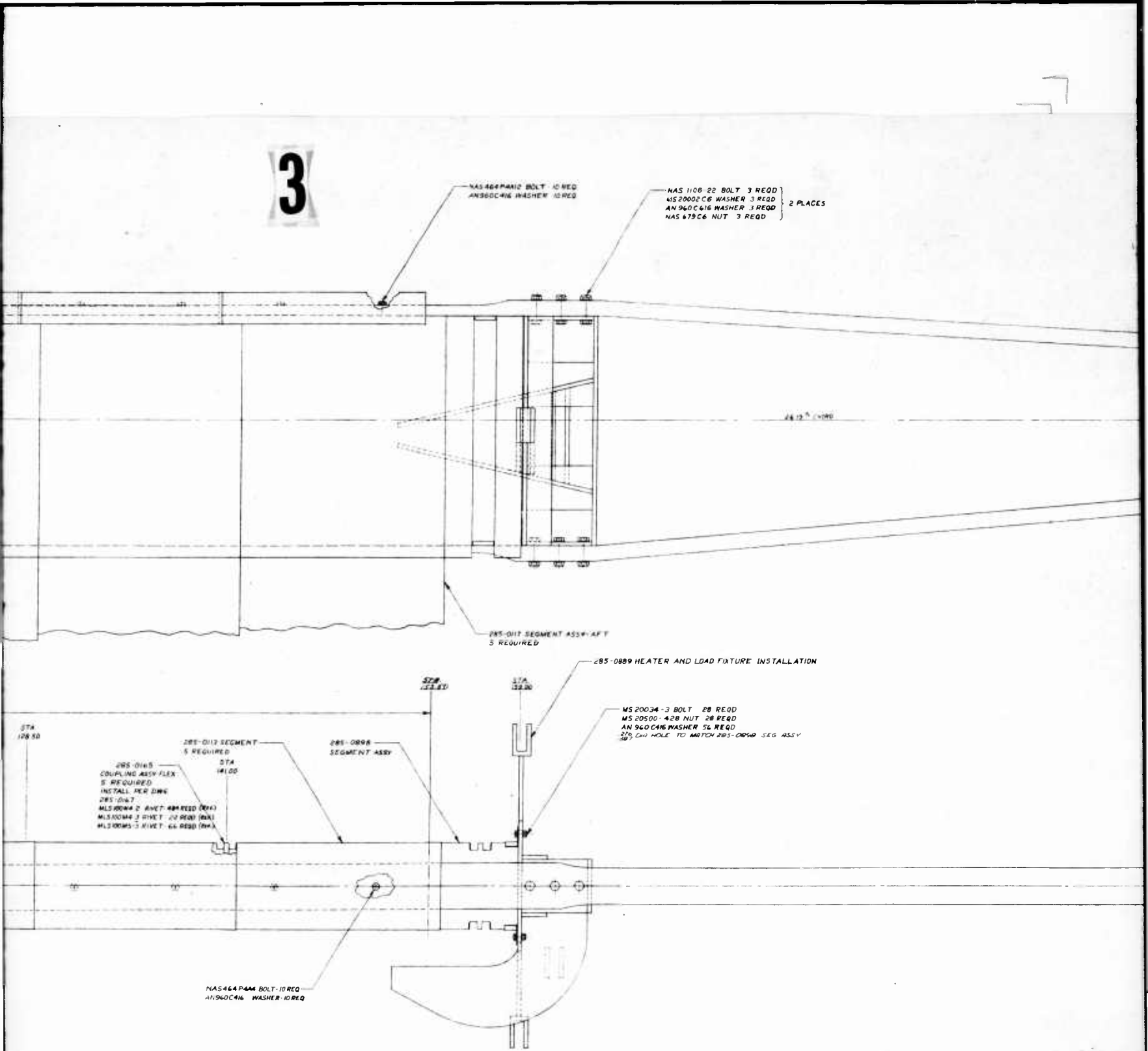
3
NAS 464 P4M12 BOLT - 10 REQ
AN960C416 WASHER - 10 REQ
NAS 1106-22 BOLT 3 REQD
MS 20002 C6 WASHER 3 REQD
AN 960 C 616 WASHER 3 REQD
NAS 679 C6 NUT 3 REQD
2 PLACES
285-0117 SEGMENT ASSY-AFT
5 REQUIRED
285-0889 HEATER AND LOAD FIXTURE INSTALLATION
MS 20034-3 BOLT 28 REQD
MS 20500-428 NUT 28 REQD
AN 960 C416 WASHER 56 REQD
STA 128.50
285-0113 SEGMENT
5 REQUIRED
285-0898
SEGMENT ASSY
285-0165
COUPLING ASSY FLEX
5 REQUIRED
INSTALL PER DWG
285-0147
MLS100W4-2 RIVET 484 REQD (BAX)
MLS100W4-3 RIVET 22 REQD (BAX)
MLS100W5-3 RIVET 66 REQD (BAX)
NAS464 P4M BOLT-10 REQ
AN960C416 WASHER-10 REQ

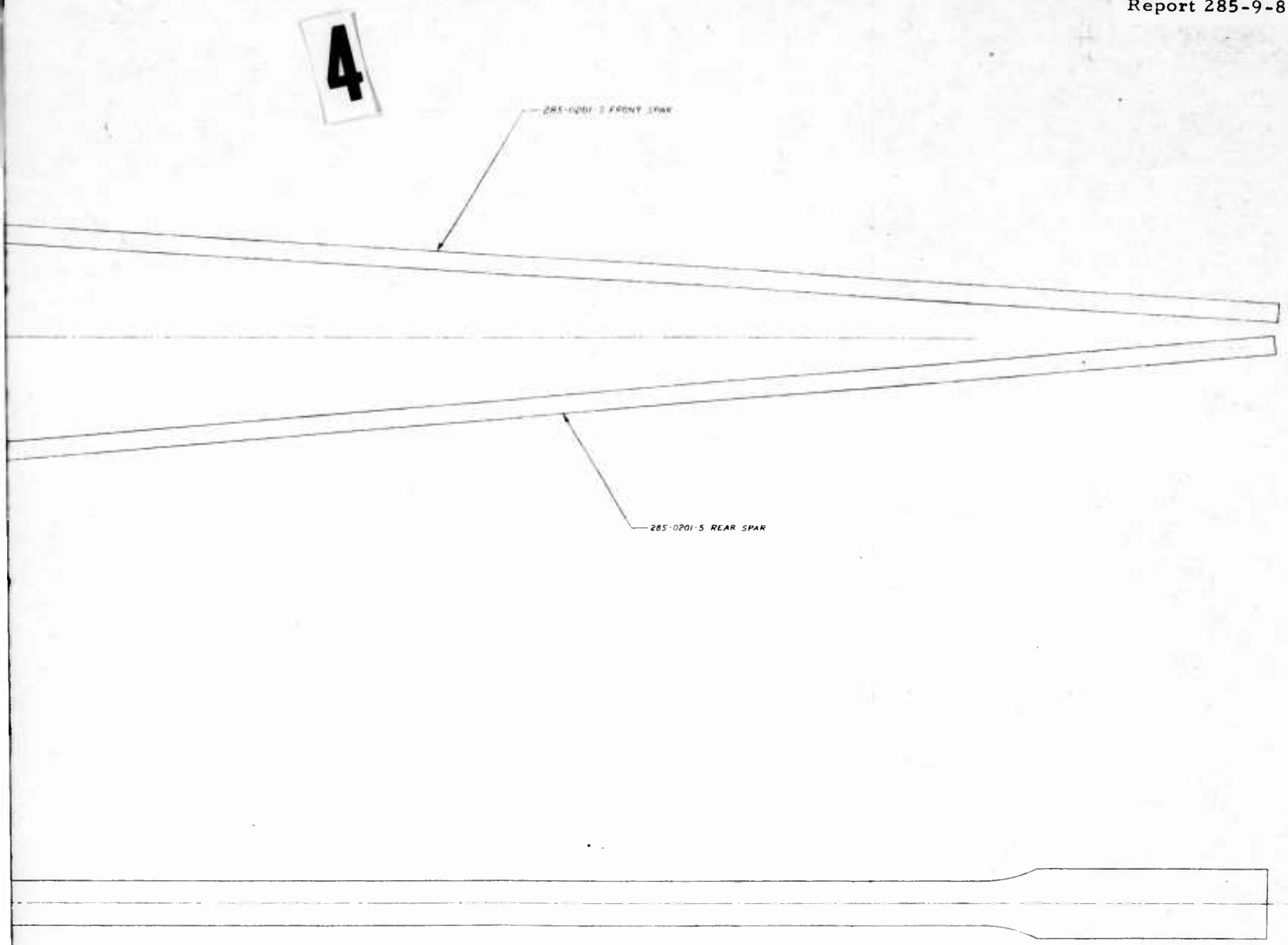

Figure 3-1. Full Scale Blade Fatigue Specimen.

2 DO NOT IMPRESSION STAMP
1 HOT CYCLE FATIGUE TEST BLADE SAME AS PRODUCTION BLADE ASSY 285-0100 EXCEPT AS SHOWN
NOTES: UNLESS OTHERWISE SPECIFIED

1

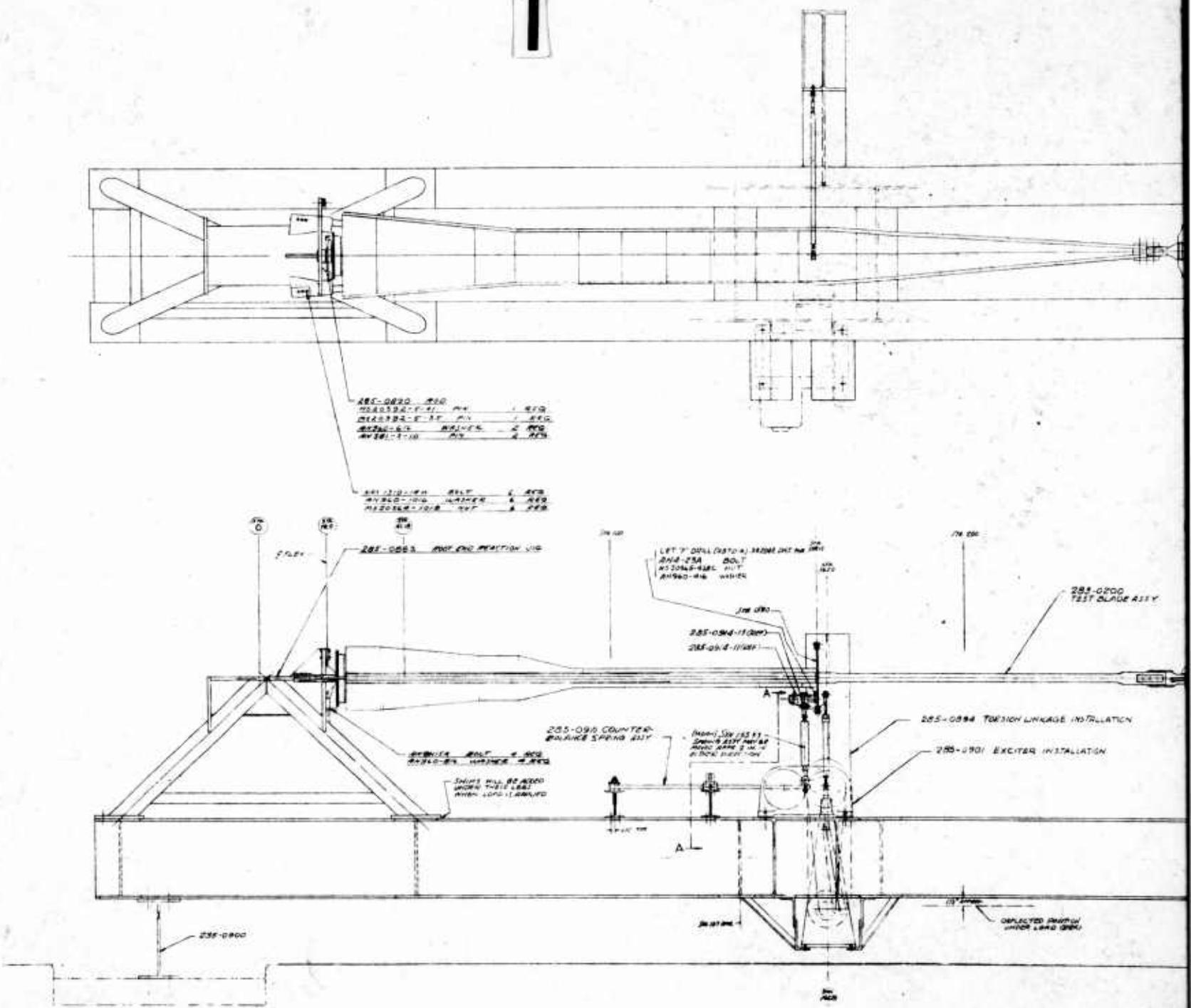
285-0200
TEST BLADE ASSY
285-0894 TORSION LINKAGE INSTALLATION
285-0901 EXCITER INSTALLATION
285-0910 COUNTER-
BALANCE SPRING ASSY
A
A
236-0900

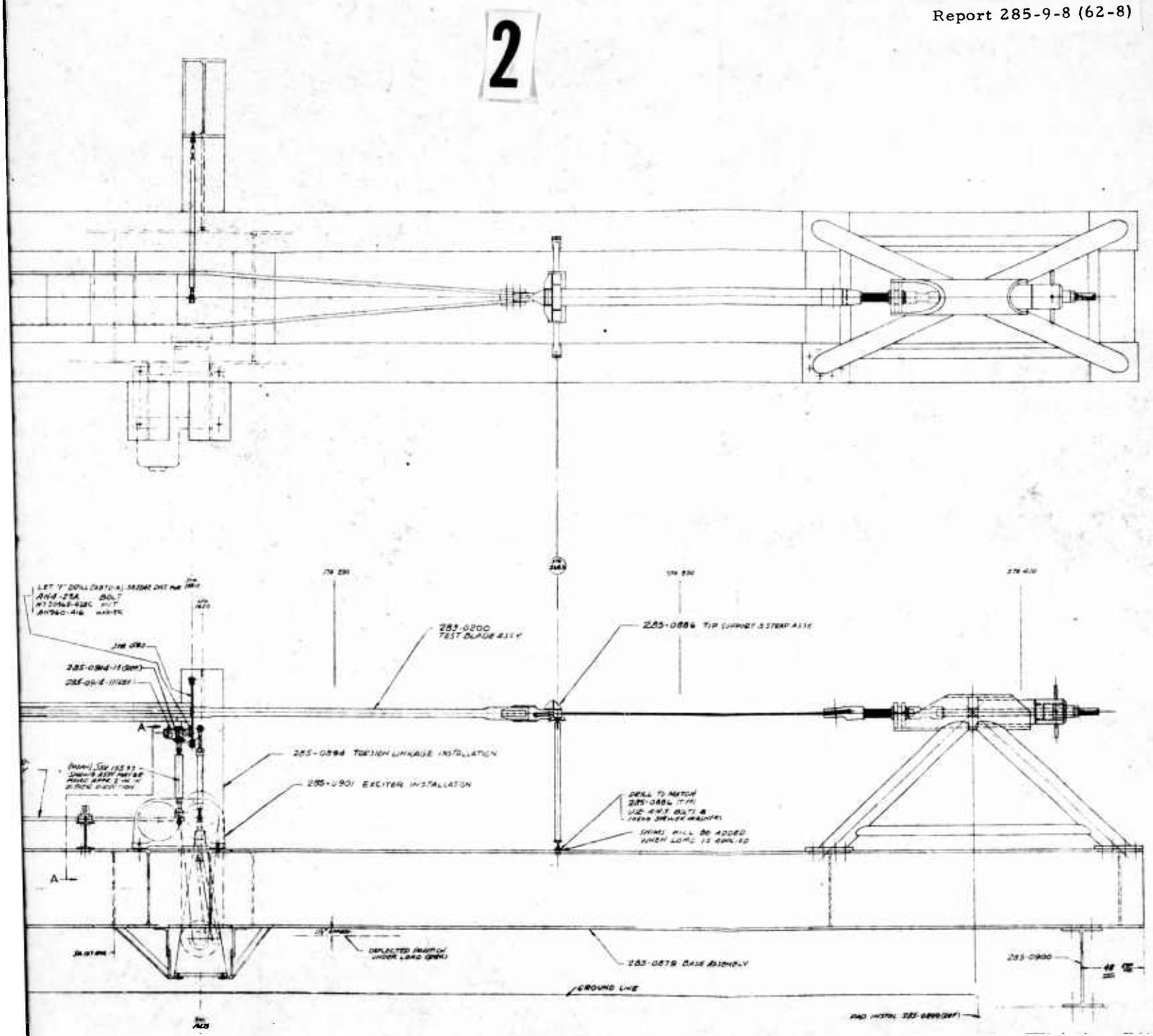

Figure 3-2. Fatigue Test Machine with Test Specimen installed.

1

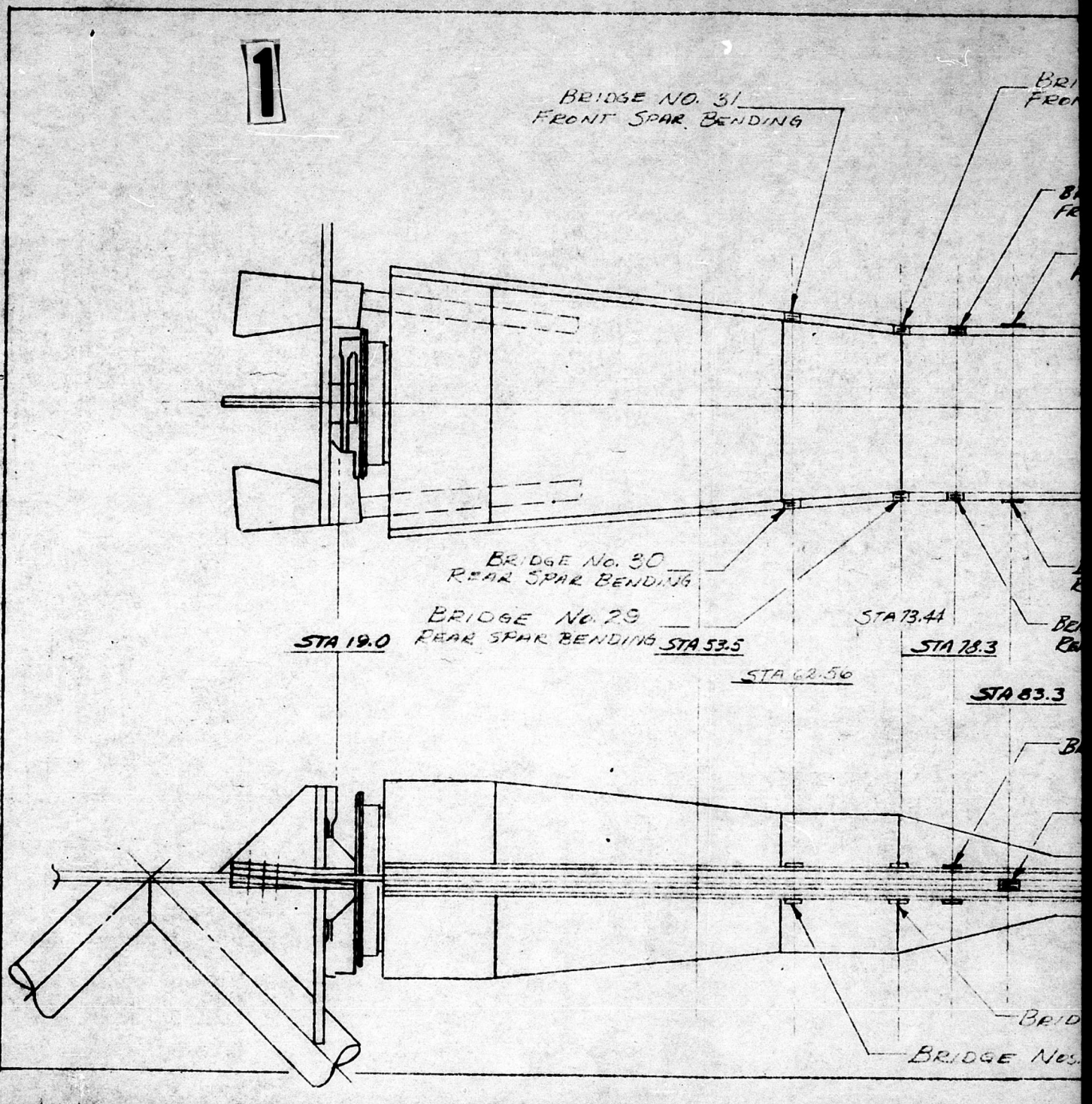
BRIDGE NO. 31
FRONT SPAR BENDING
BRIDGE NO. 30
REAR SPAR BENDING
BRIDGE NO. 29
REAR SPAR BENDING
STA 19.0
STA 53.5
STA 62.56
STA 73.44
STA 78.3
STA 83.3
BRIDGE NOS.

2

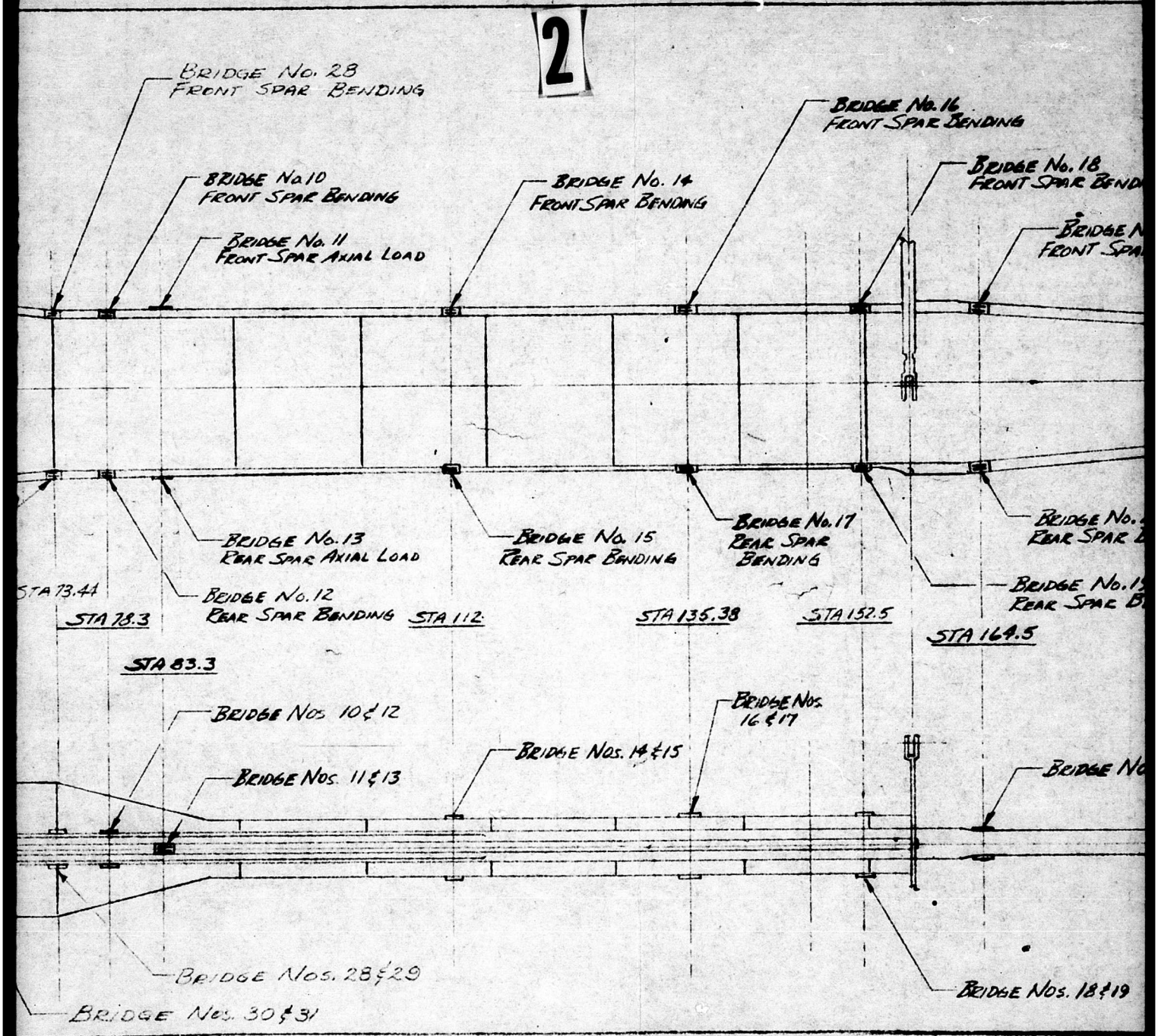
BRIDGE No. 28
FRONT SPAR BENDING
BRIDGE No. 10
FRONT SPAR BENDING
BRIDGE No. 11
FRONT SPAR AXIAL LOAD
BRIDGE No. 14
FRONT SPAR BENDING
BRIDGE No. 16
FRONT SPAR BENDING
BRIDGE No. 18
FRONT SPAR BENDI
BRIDGE N
FRONT SPA
BRIDGE No. 13
REAR SPAR AXIAL LOAD
BRIDGE No. 12
REAR SPAR BENDING
BRIDGE No. 15
REAR SPAR BENDING
BRIDGE No. 17
REAR SPAR
BENDING
BRIDGE No.
REAR SPAR
BRIDGE No.
REAR SPAR B
STA 73.41
STA 78.3
STA 112
STA 135.38
STA 152.5
STA 164.5
STA 83.3
BRIDGE NOS. 10 & 12
BRIDGE NOS. 11 & 13
BRIDGE NOS. 14 & 15
BRIDGE NOS.
16 & 17
BRIDGE NO
BRIDGE NOS. 28 & 29
BRIDGE NOS. 30 & 31
BRIDGE NOS. 18 & 19

3

BENDING

BRIDGE No. 18
FRONT SPAR BENDING

BRIDGE No. 22
FRONT SPAR BENDING

BRIDGE No. 24
FRONT SPAR BENDING

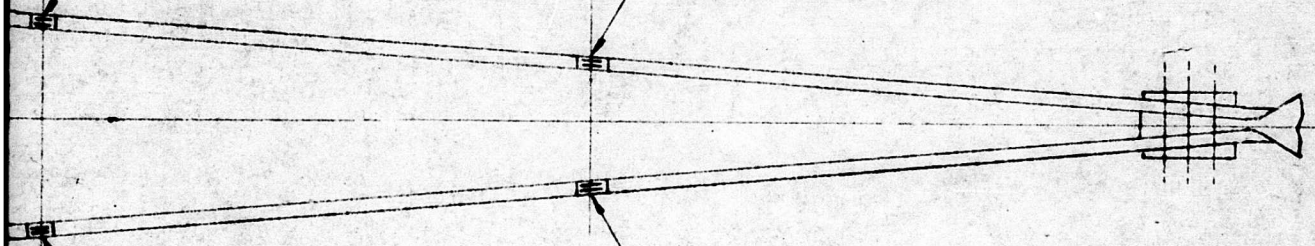

BRIDGE No. 23
REAR SPAR BENDING

BRIDGE No. 25
REAR SPAR BENDING

BRIDGE No. 19
REAR SPAR BENDING

STA 164.5

STA 206

BRIDGE Nos. 22 & 23

BRIDGE Nos 24 & 25

BRIDGE Nos. 18 & 19

STRAIN
HOT CYC

4

285-1006

Bridge No. 24
Front Spar Bending

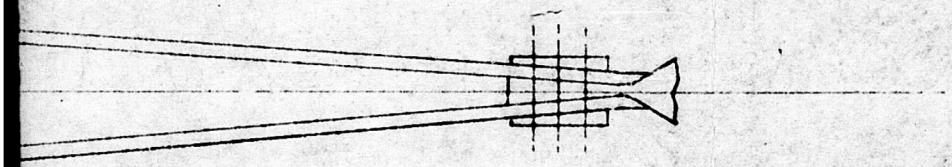

Bridge No. 25
Rear Spar Bending

Bridge Nos 24 & 25

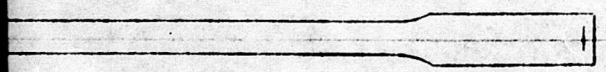

Figure 3-3.

STRAIN GAGE LOCATIONS
HOT CYCLE FATIGUE TEST BLADE

285-1006

Rev D.W.N. 3-6-62 L.L.E. 3-21-61

1

IRON - CONSTANTAN				CHROMEL - ALUMEL			
Box No.	T.C. IDENT.	STA. LOC.	TYP. TEMP FOR RUNS °F	Box No.	T.C. IDENT	STA. LOC.	TYP. TEMP FOR RUNS °F
1	S-1-1	125.4	800	33	FC-5-2	141	345
2	S-1-2	↓	800	34	FC-5-3	↓	460
3	S-1-3		640	35	FC-5-4		440
4	S-1-5		935	36	FC-5-5		440
5	S-1-6	125.4	625	37	FC-5-6		460
6	S-2-1	134.3	975	38	FC-5-7	141	515
7	S-2-2	↑	890	39	RS-13	83.3	AMBIENT
8	S-2-3		935	40	RS-15	112	195
9	S-2-5		1050	41	RS-17	135.38	370
10	S-2-6		820	42	RS-19	152.5	170
11	S-2-7		1050	43	RS-23	164.5	AMBIENT
12	S-2-8	↓	965	44	FS-11	83.3	AMBIENT
13	S-2-9	134.3	950	45	FS-14	112	140
14	S-2-9A	134.9	818	46	FS-16	135.38	230
15	S-2-11	134.3	915	47	FS-18	152.5	115
16	S-2-4	134.3	970	48	FS-22	164.5	AMBIENT
17	S-3-1	144.1	900				
18	S-3-2	144.1	1040				
19	S-3-3	144.1	790				
20	S-2-3A	134.9	840				
21	S-3-5	144.1	900				
22	S-3-6	144.1	765				
23	S-2-13	134.3	OUT				
24	S-2-14	134.9	210				
25	S-2-16	134.9	OUT				
26	S-2-18	134.3	210				
27	S-2-19	134.3	185				
28	S-2-20	134.9	275				
29	S-2-21	134.9	315				
30	S-2-22	134.9	340				
31	S-2-23	134.9	300				
32	AFT DUCT	134.3	OUT				

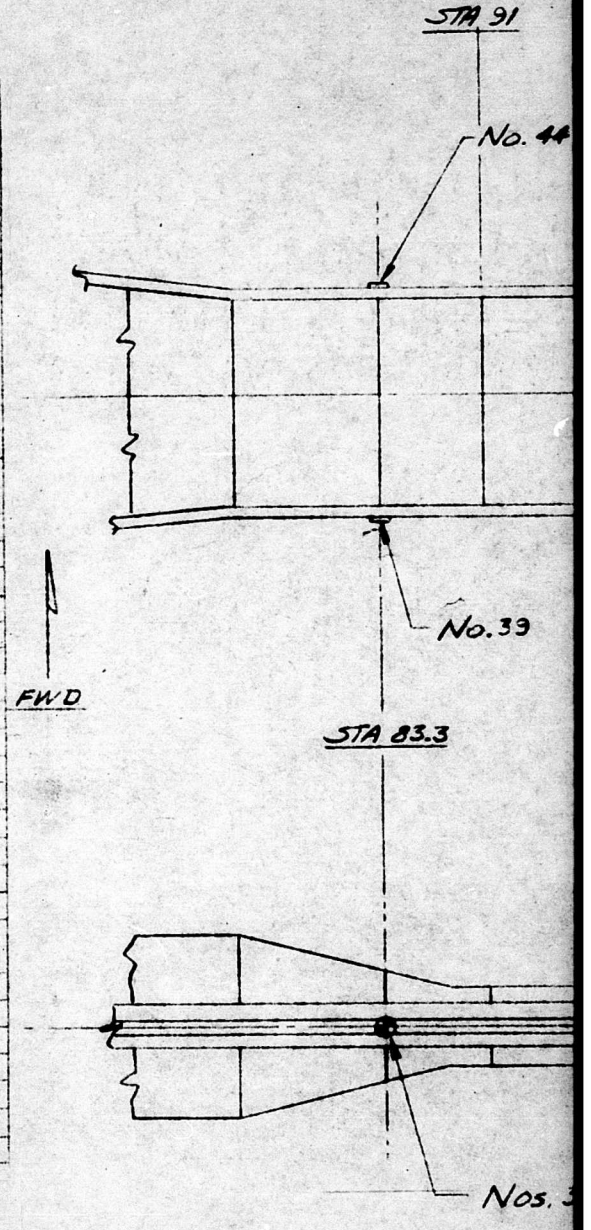

NOTES: 1. TC S-3-4 IS READ AT JUNCTION BOX

2

THERMOCOUPLE LOCATIONS - HOT CYCLE FATIGUE TEST BLADE

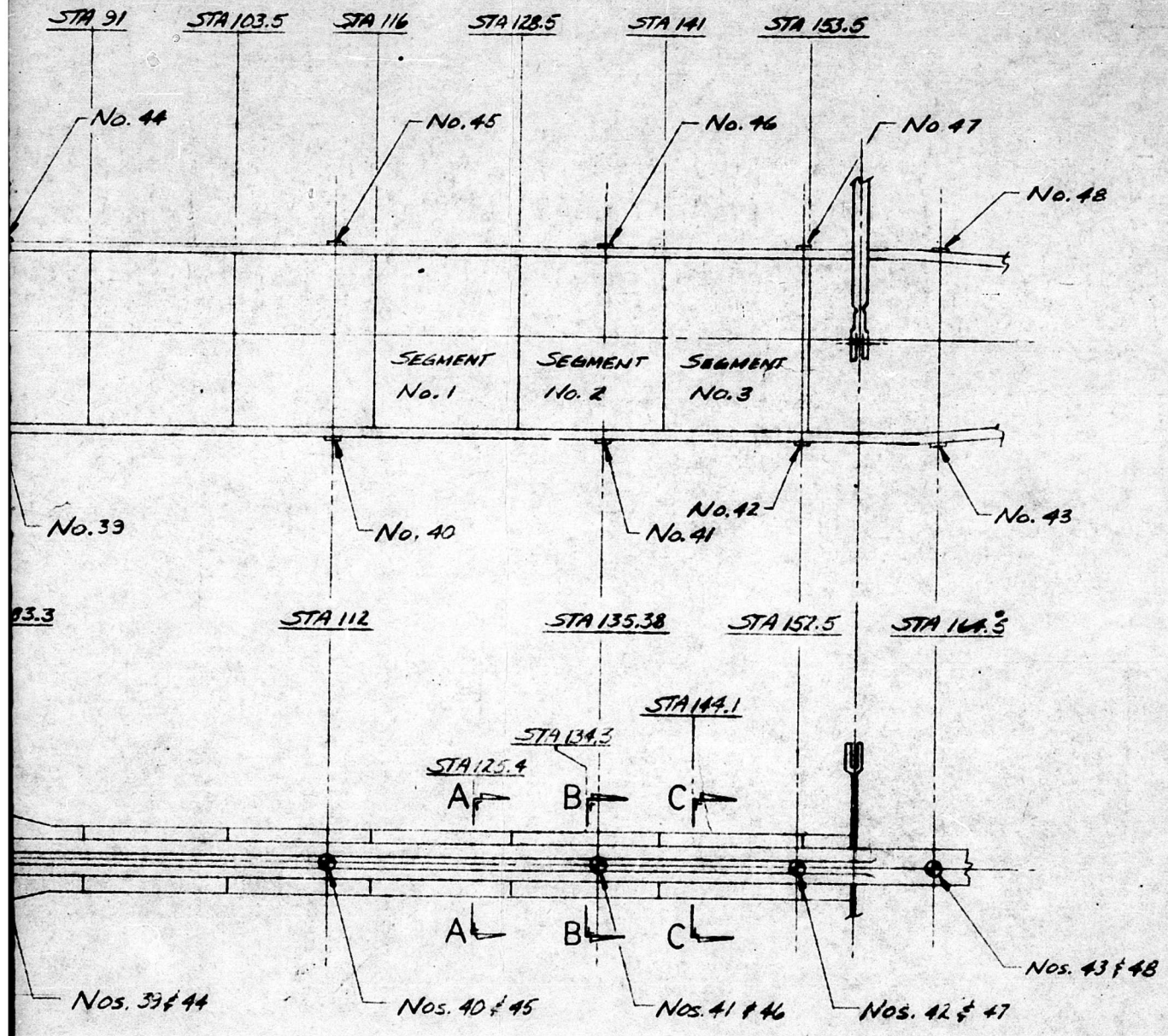

Report

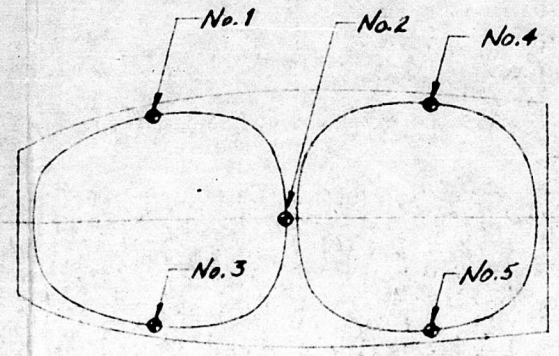

SECTION A-A
SEGMENT No. 1

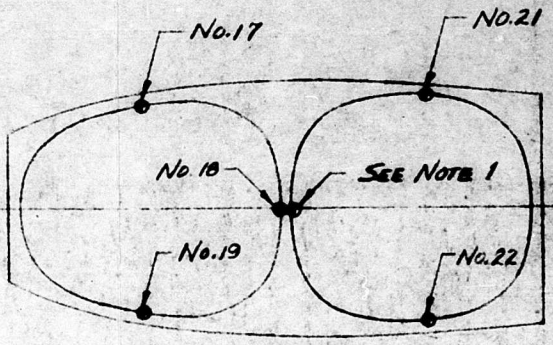

SECTION C-C
SEGMENT No. 3

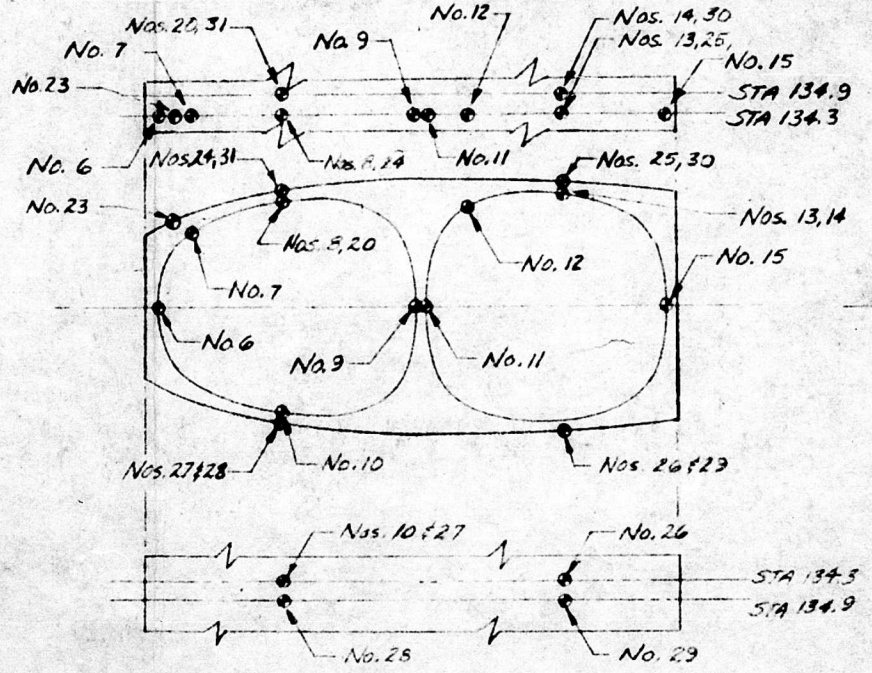

SECTION B-B
SEGMENT No 2

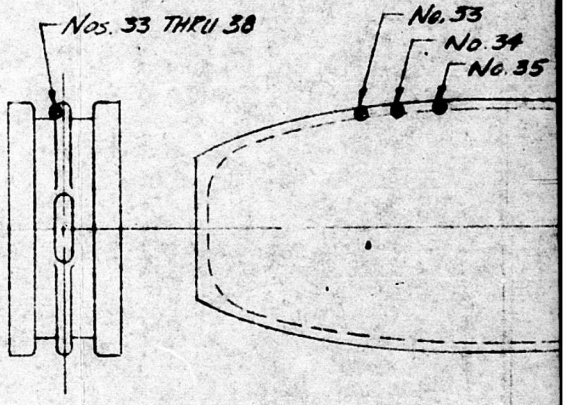

STATION 141 FLE

THERMOUPLE LOCAT
HOT CYCLE FATIGUE

28

DEI D.W

285-1005

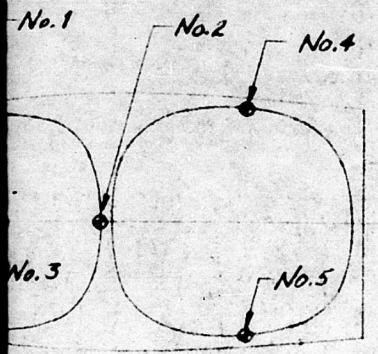

SECTION A-A
SEGMENT No. 1

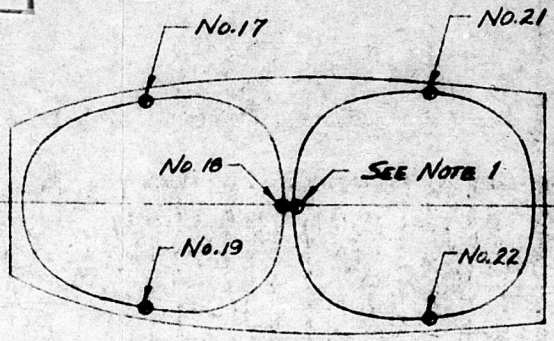

SECTION C-C
SEGMENT No. 3

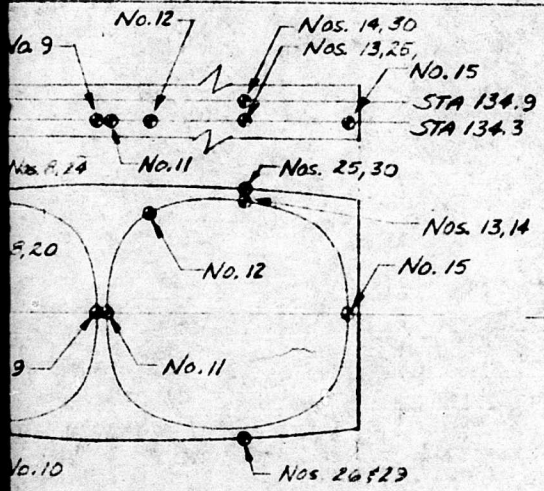

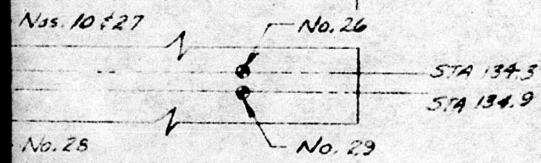

SECTION B-B
SEGMENT No 2

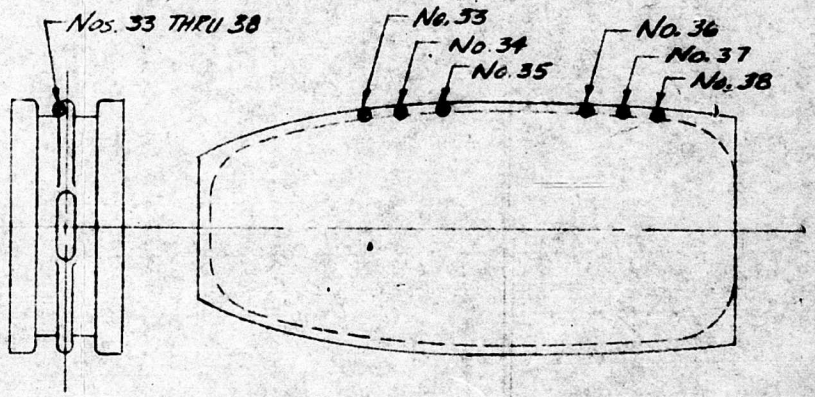

STATION 141 FLEXURE

Figure 3-4.

THERMOUPLE LOCATIONS
HOT CYCLE FATIGUE TEST BLADE
285-1005

REI D.W.N. 3-6-62 C.L.E 4-28-61

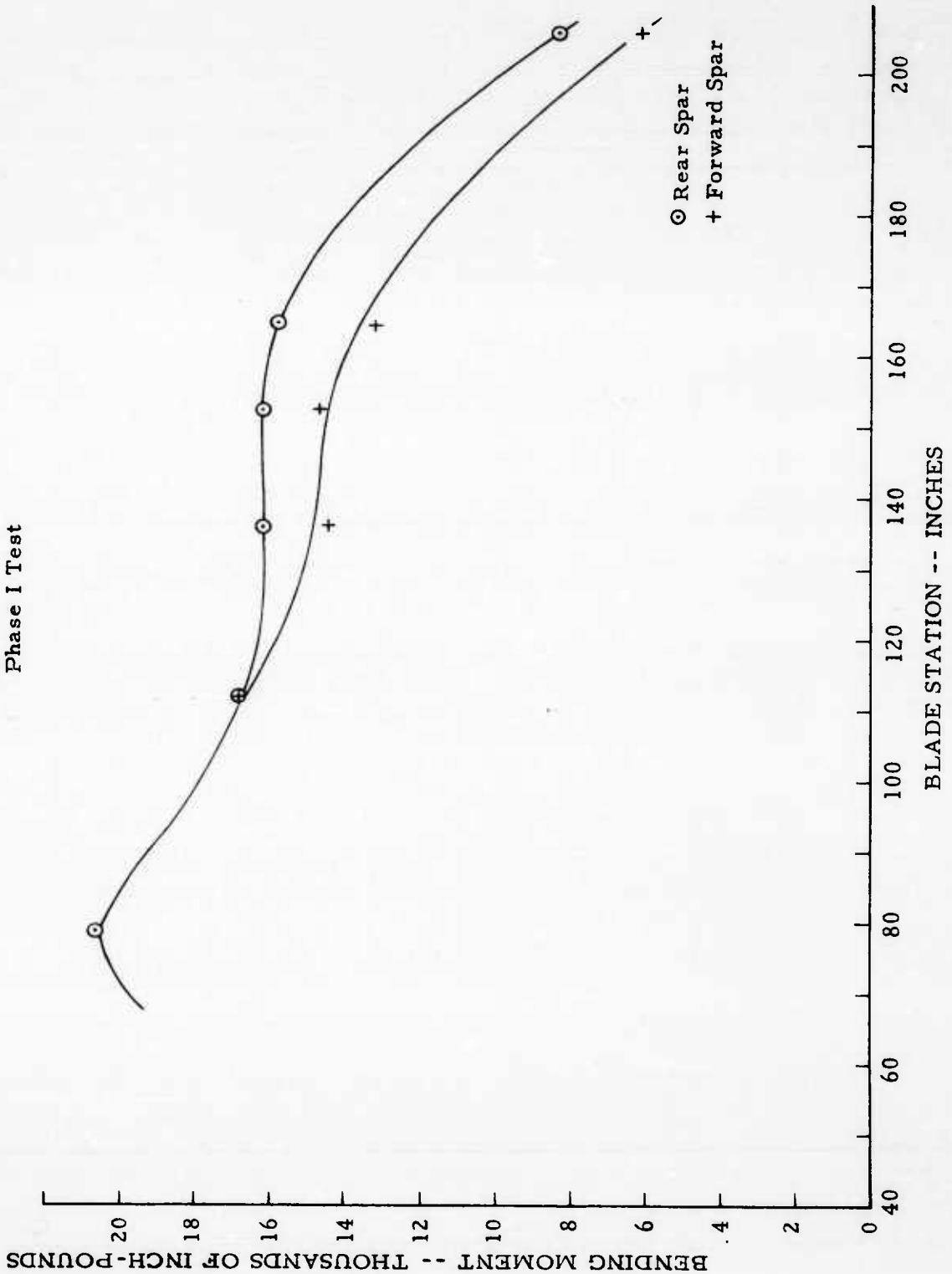

Figure 3-5. Bending Moment Distribution
Front and Rear Spar

Phase I Test

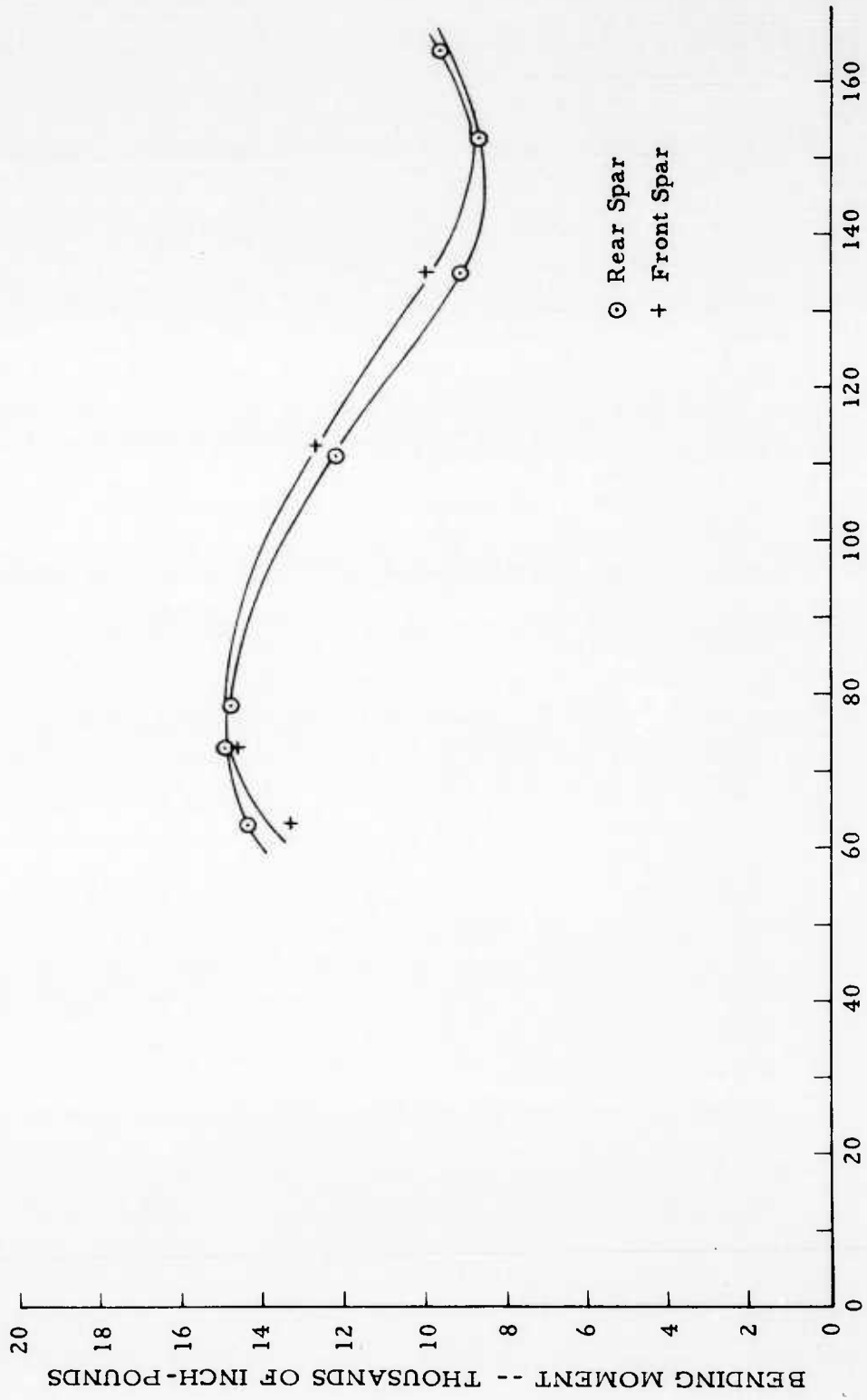

Figure 3-6. Bending Moment Distribution
Front and Rear Spar

Phase II Test

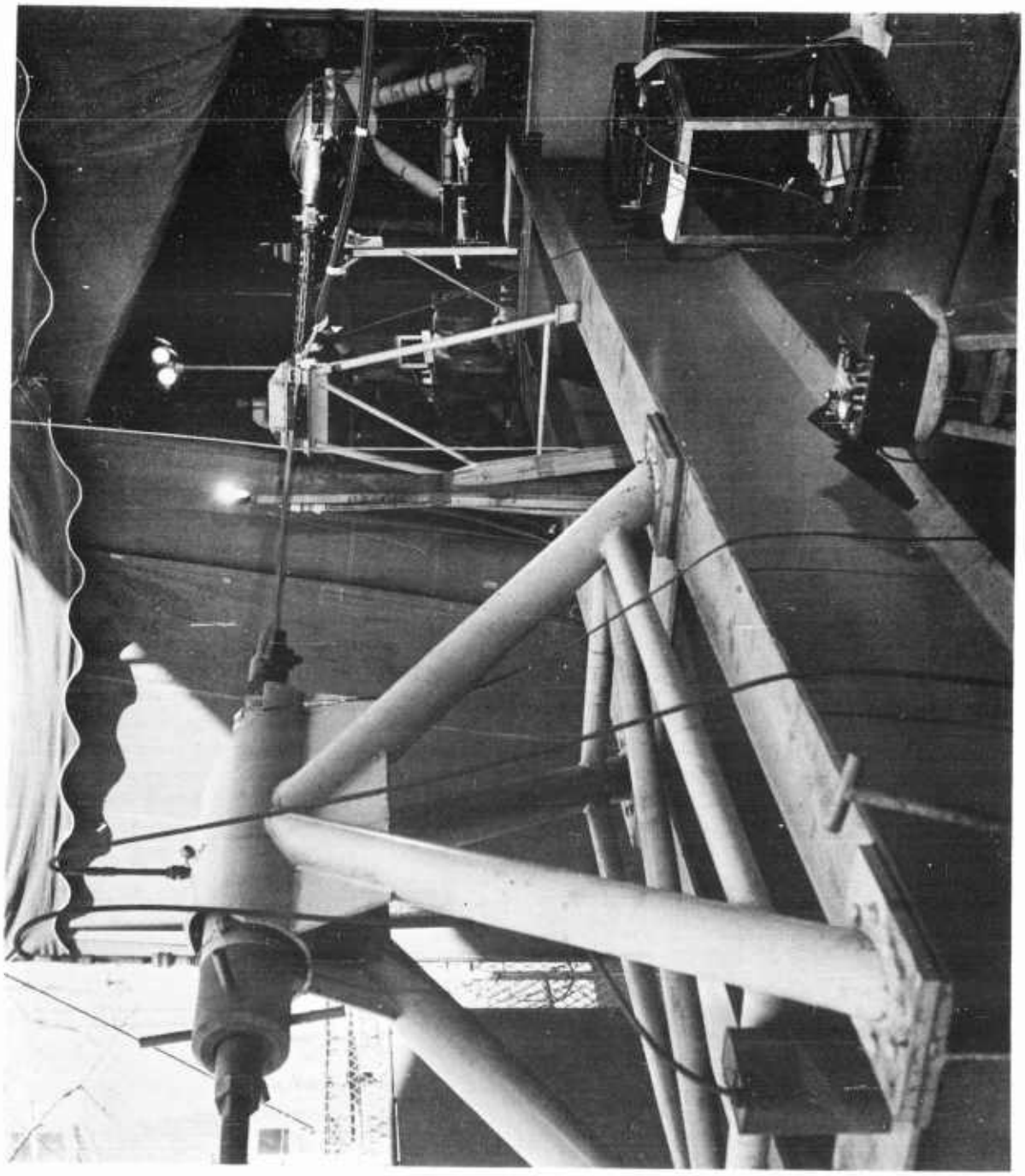

Figure 3-7. Test Setup Arrangement

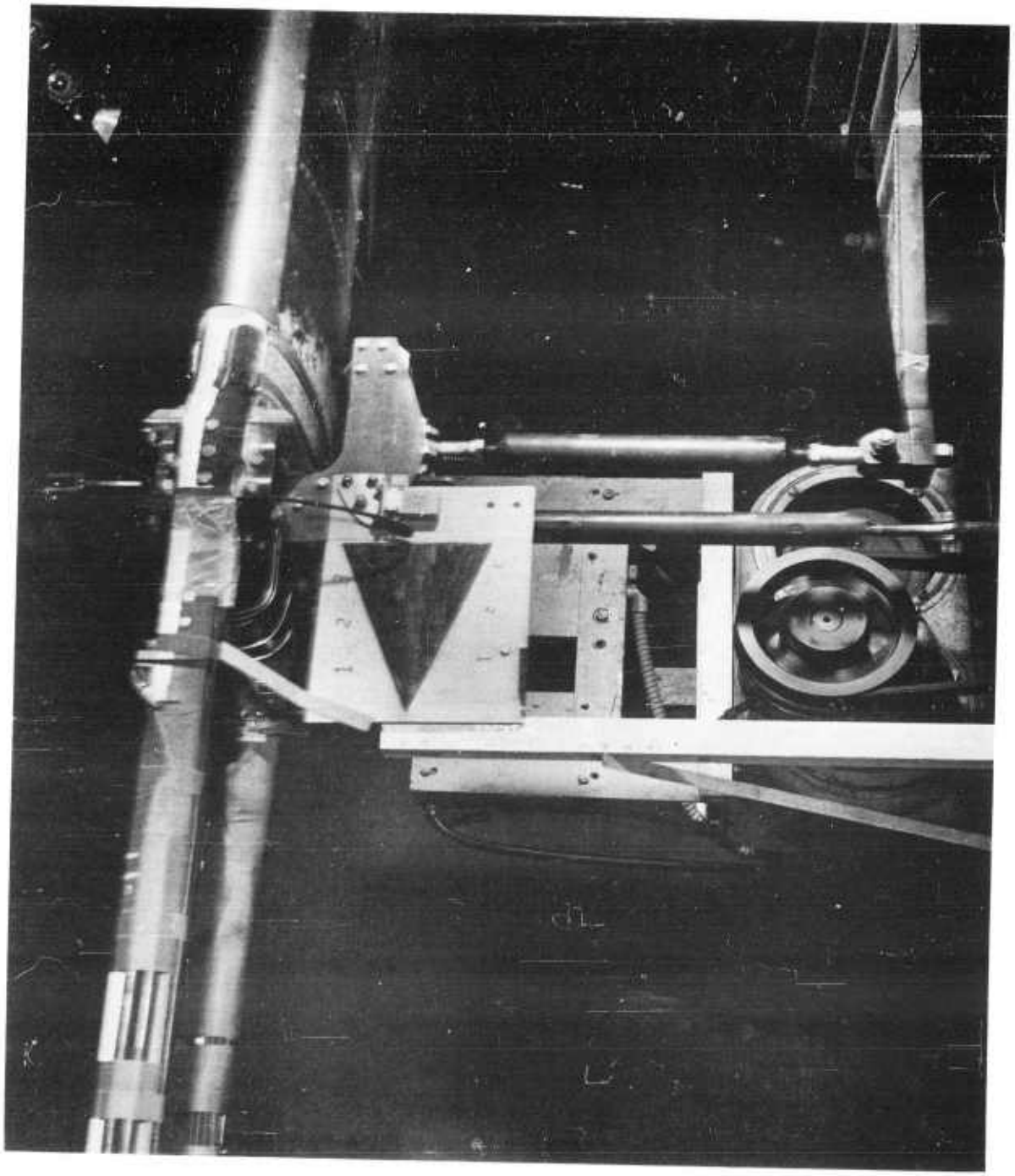

Figure 3-8. Flapwise Bending Exciter Arrangement

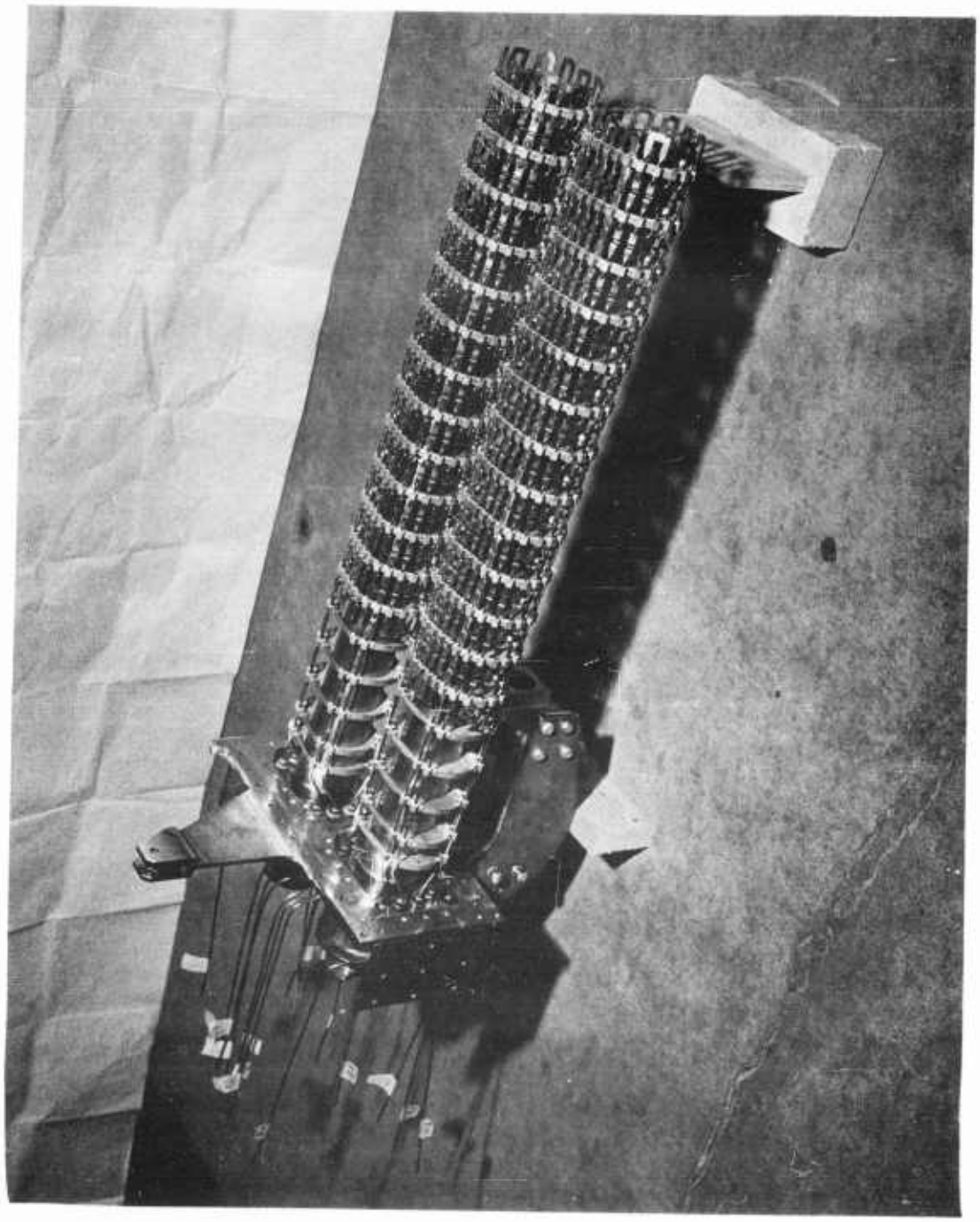

Figure 3-9. Forward and Aft Duct Heater Assembly

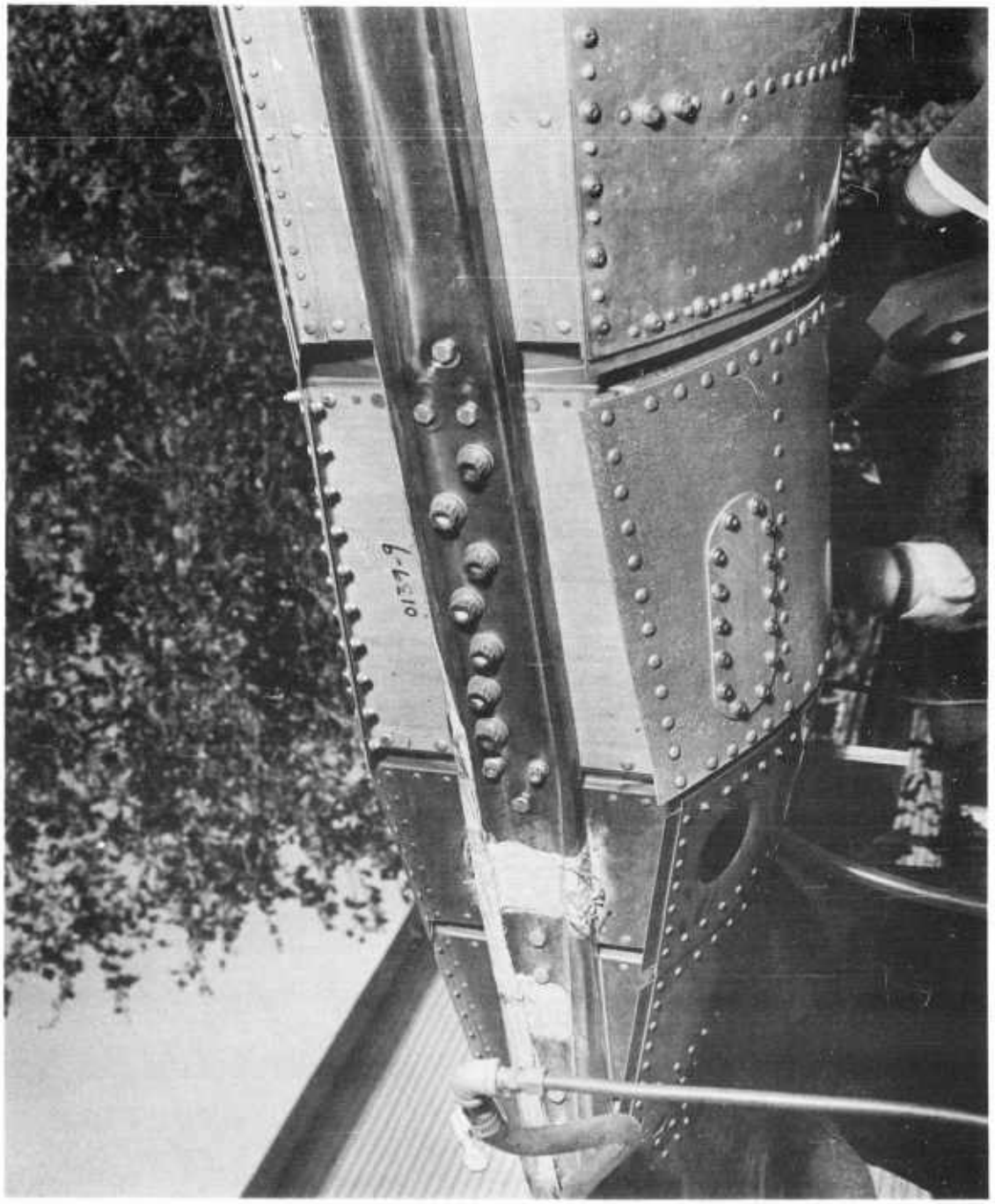

Figure 3-10. Front Spar Cooling Tube Arrangement and Typical Strain Gage Installation

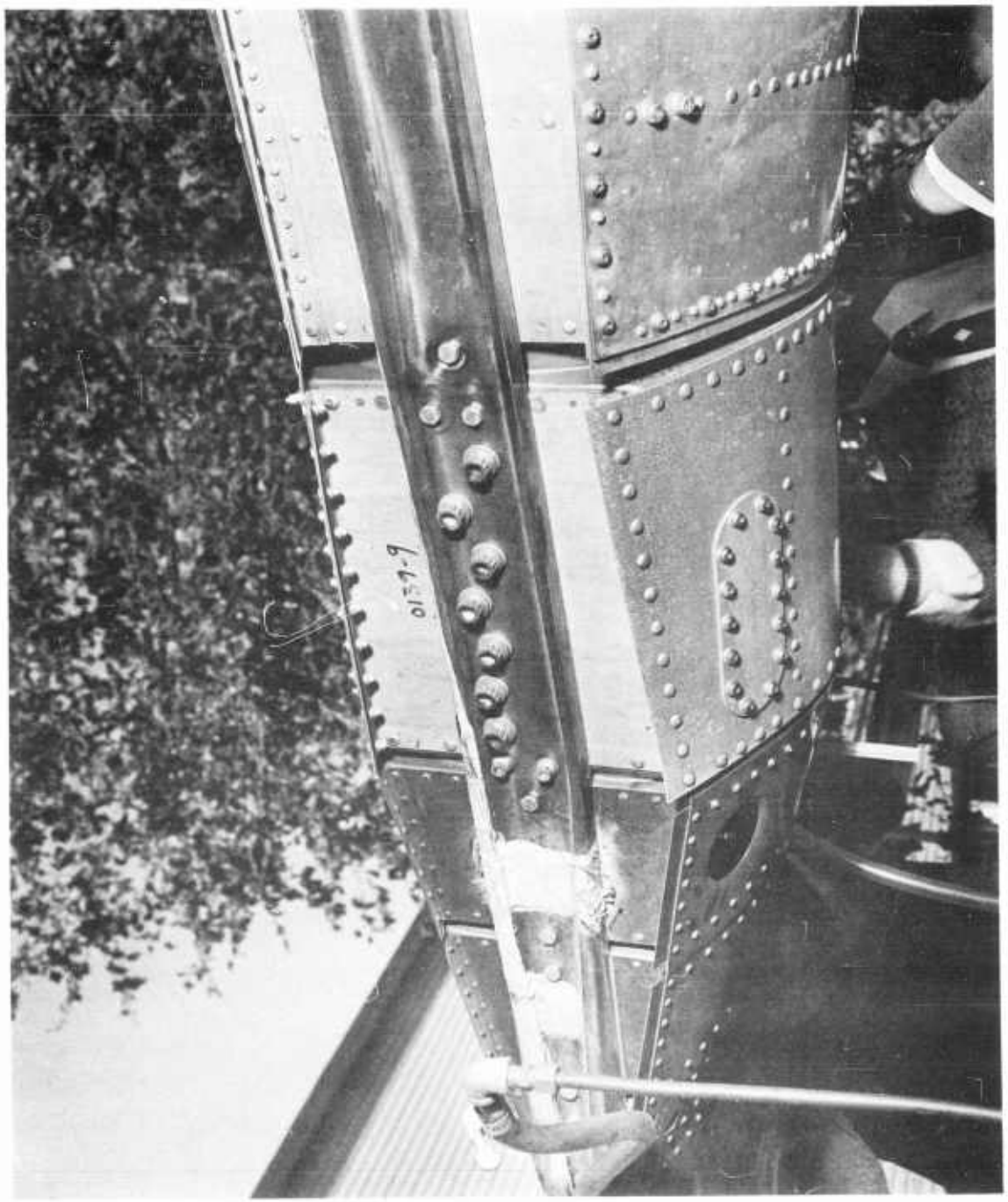

Figure 3-10. Front Spar Cooling Tube Arrangement and Typical Strain Gage Installation

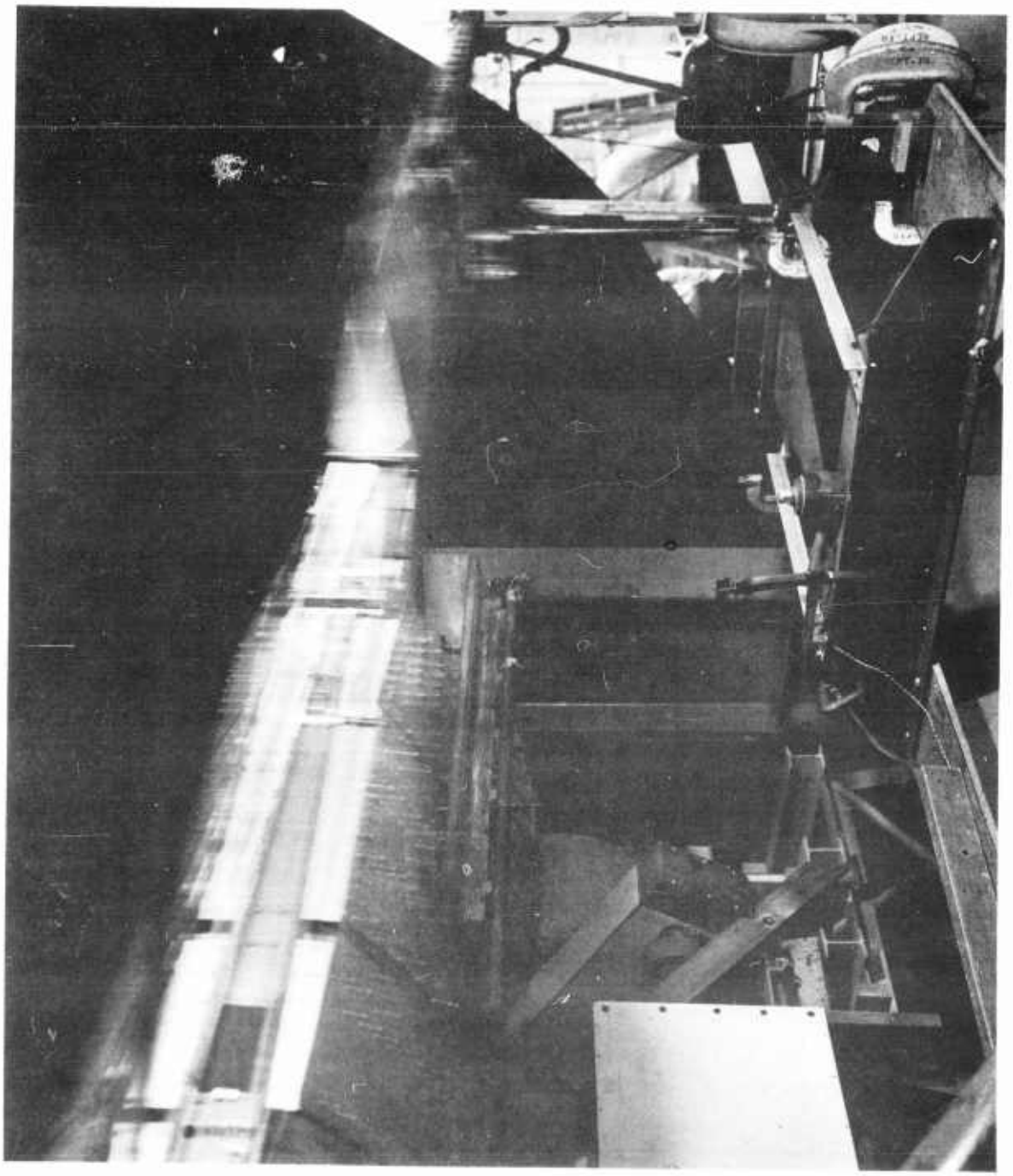

Figure 3-11. Fatigue Test Blade Assembly -- Test in Progress, View Looking Outboard at Rear Spar

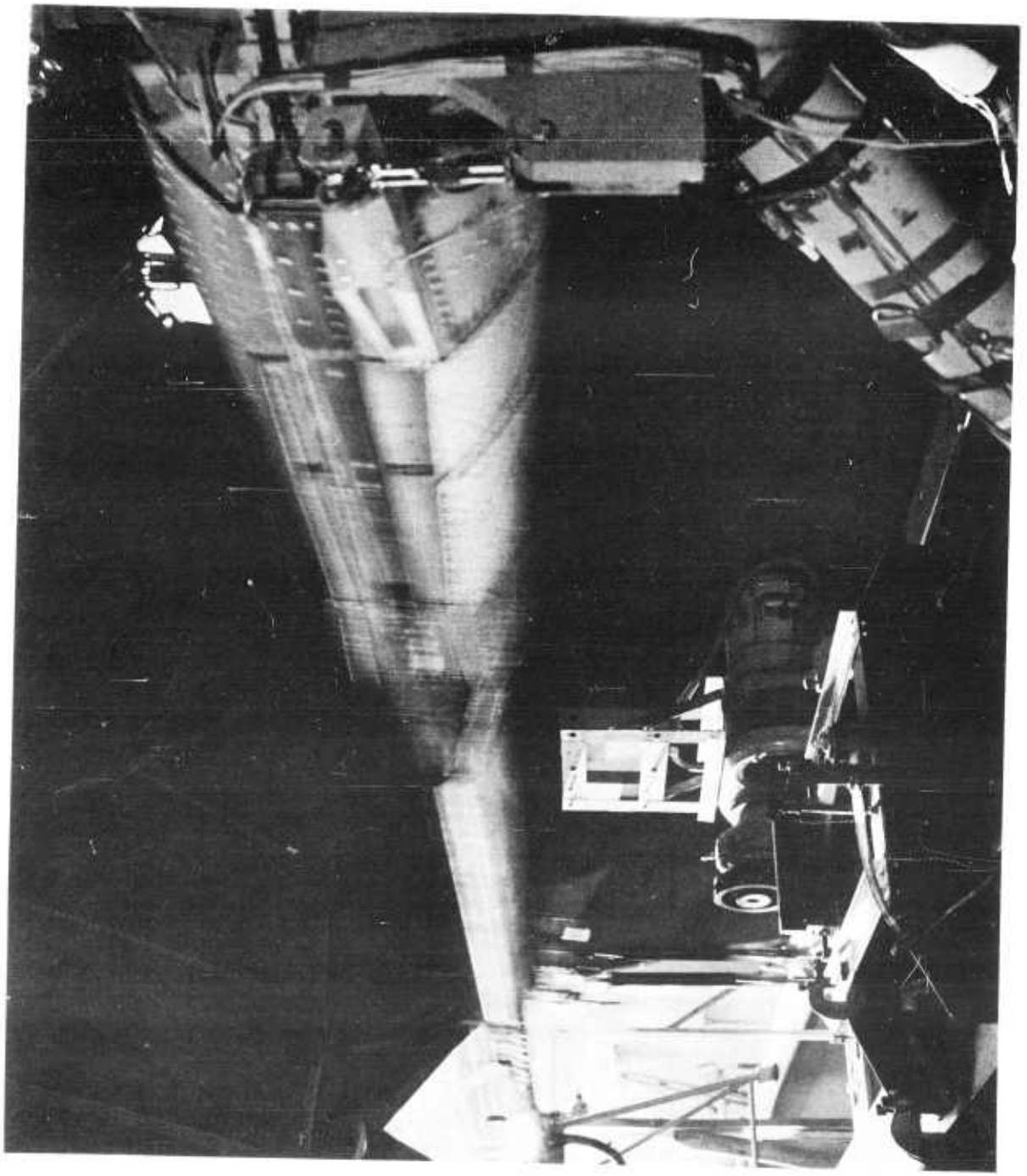

Figure 3-12. Fatigue Test Blade Assembly -- Test in Progress, View Looking Outboard at Front Spar

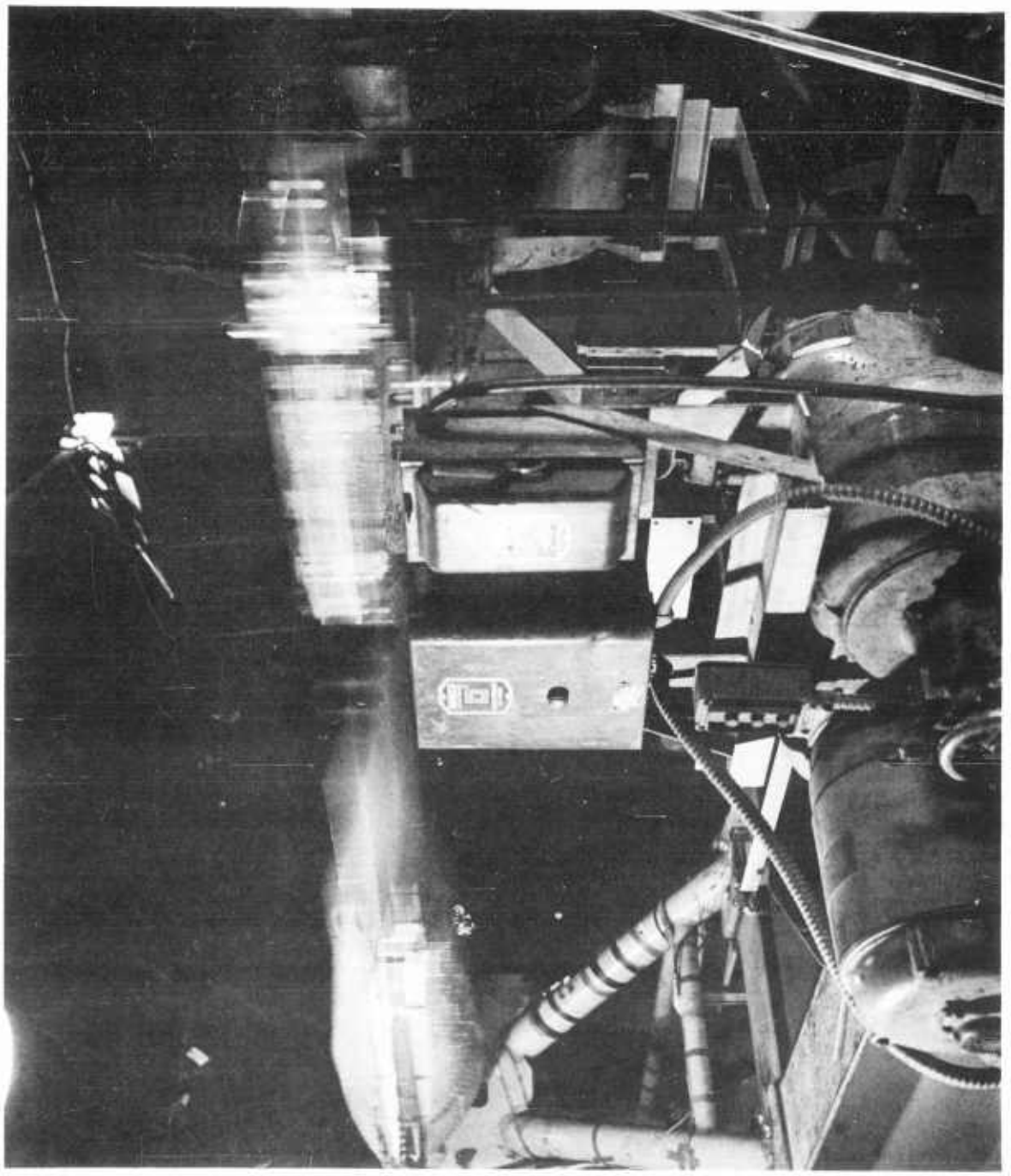

Figure 3-13. Fatigue Test Blade Assembly -- Test in Progress, View Looking Inboard at Rear Spar

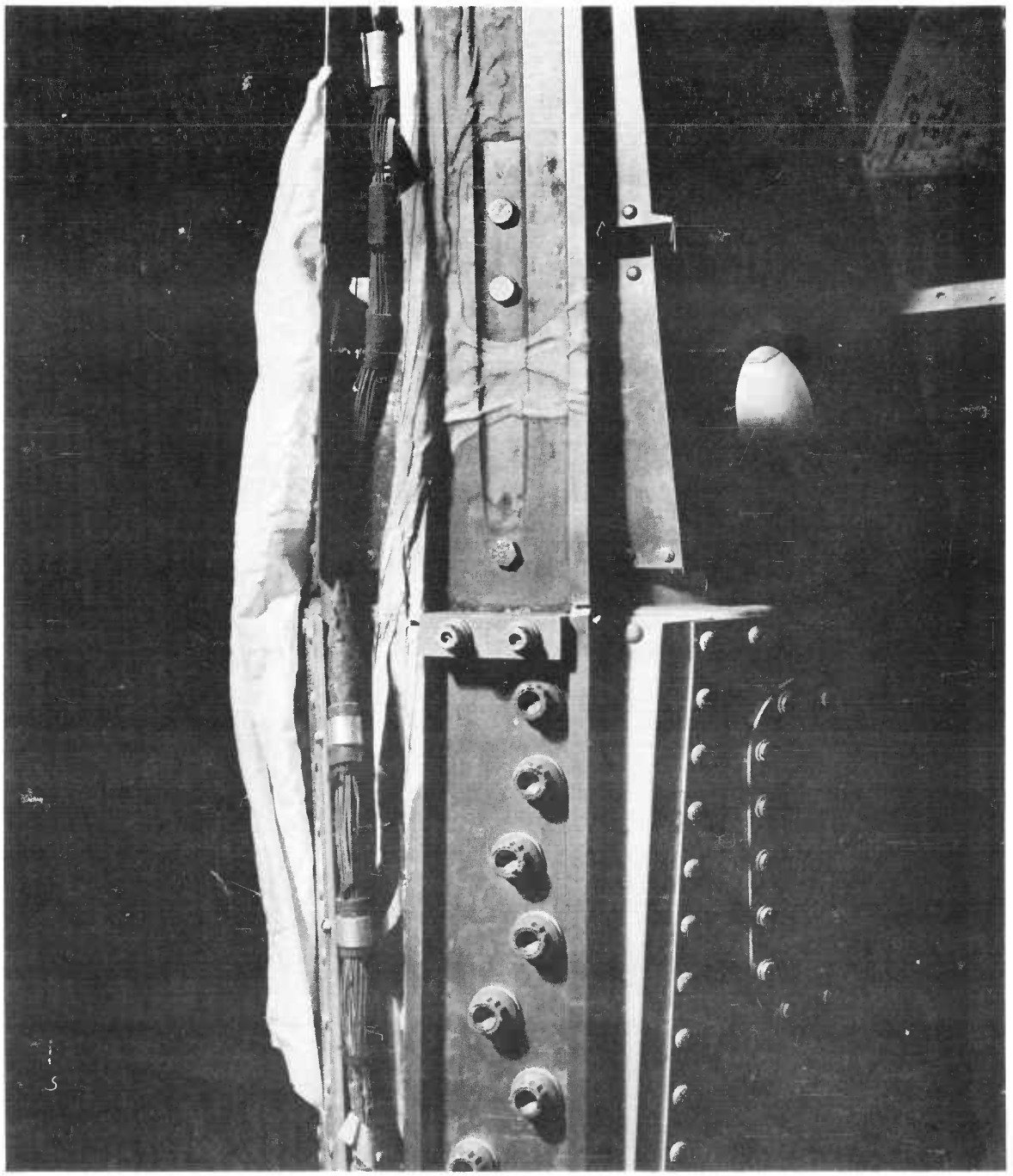

Figure 3-14. Rear Spar Failure at Station 73.0

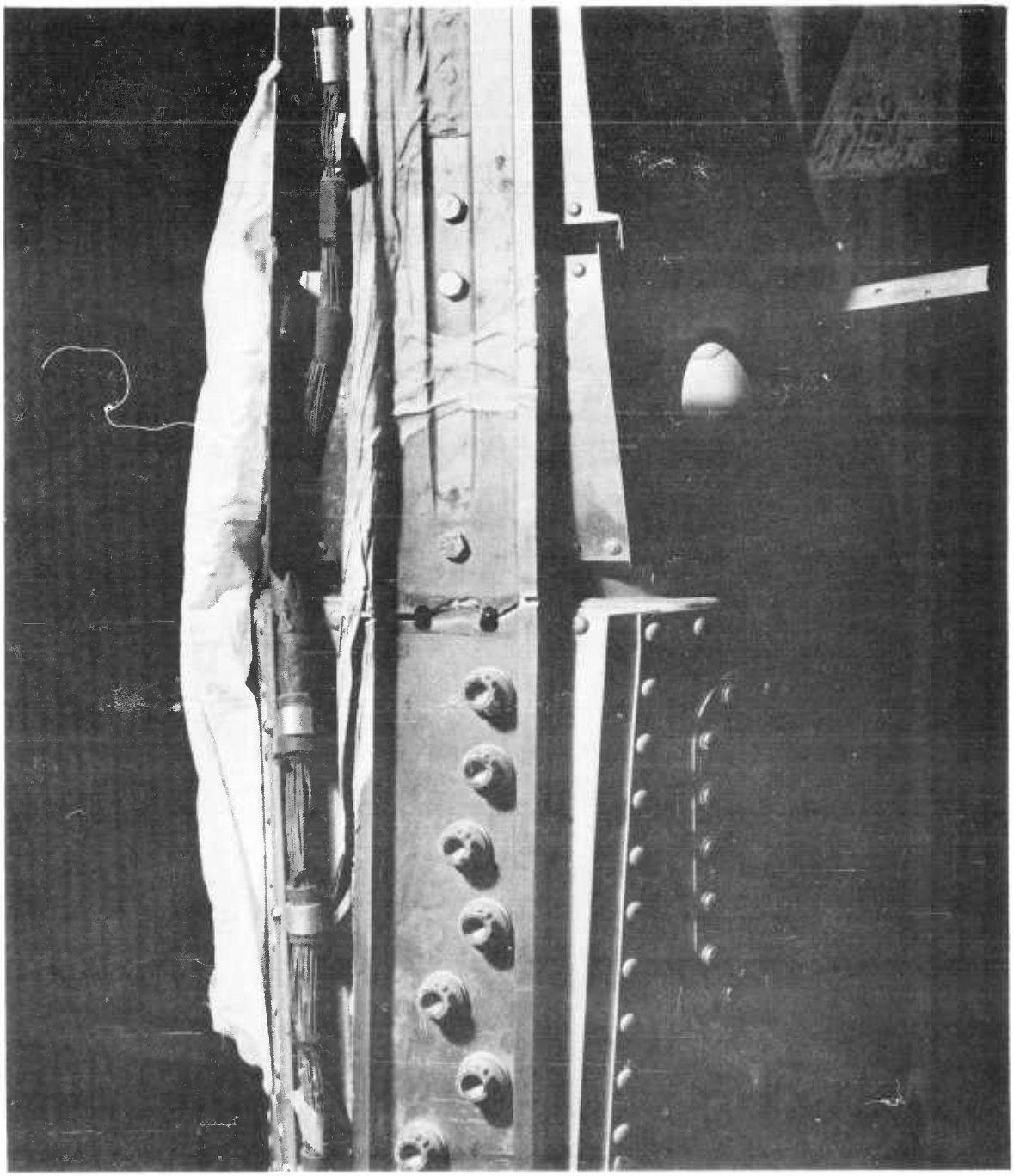

Figure 3-15. Rear Spar Failure at Station 73.0, Bolts Removed

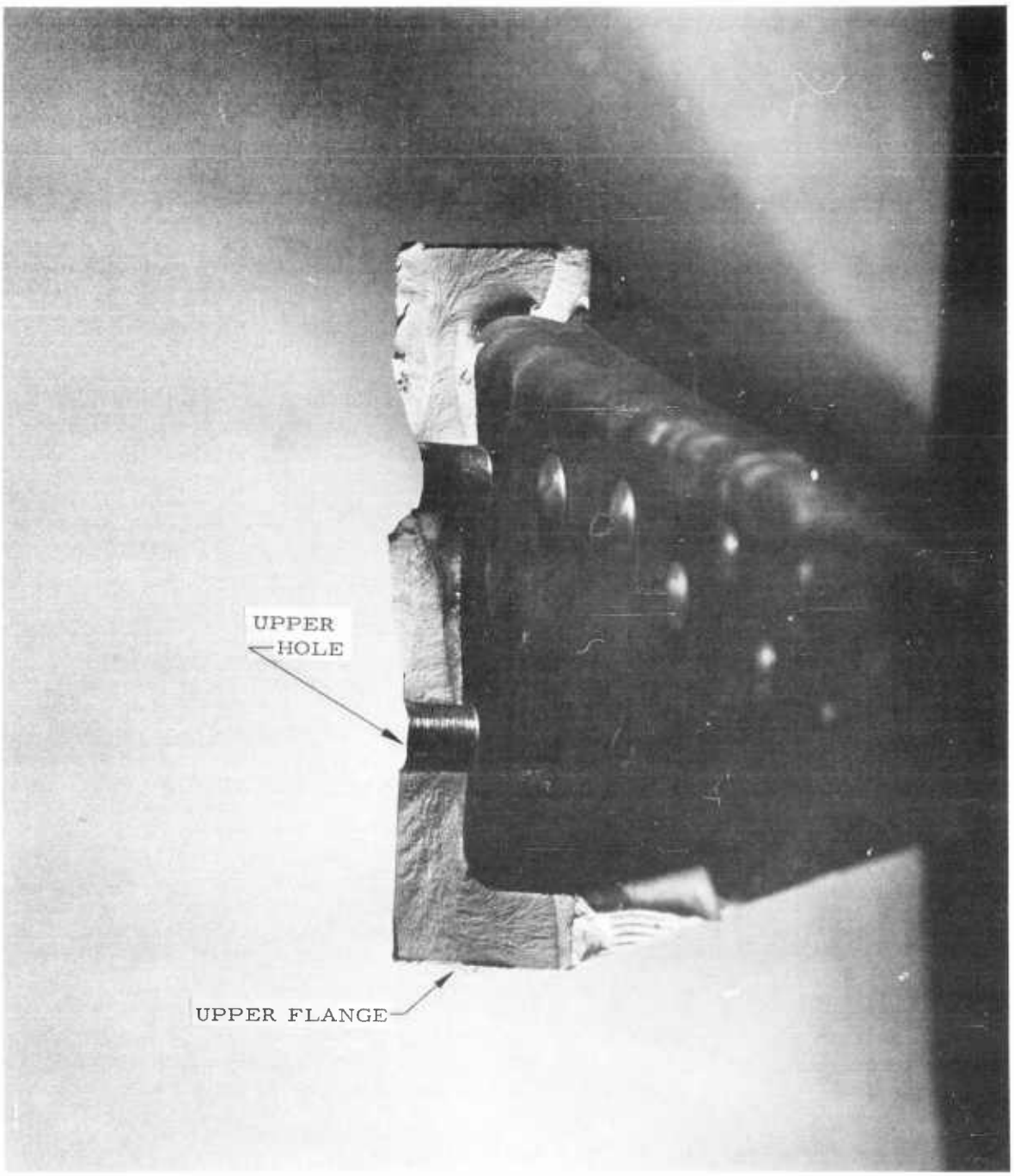

Figure 3-16. Rear Spar Fracture Area -- Inboard Portion

Figure 3-17. Rear Spar Fracture Area -- Inboard Portion

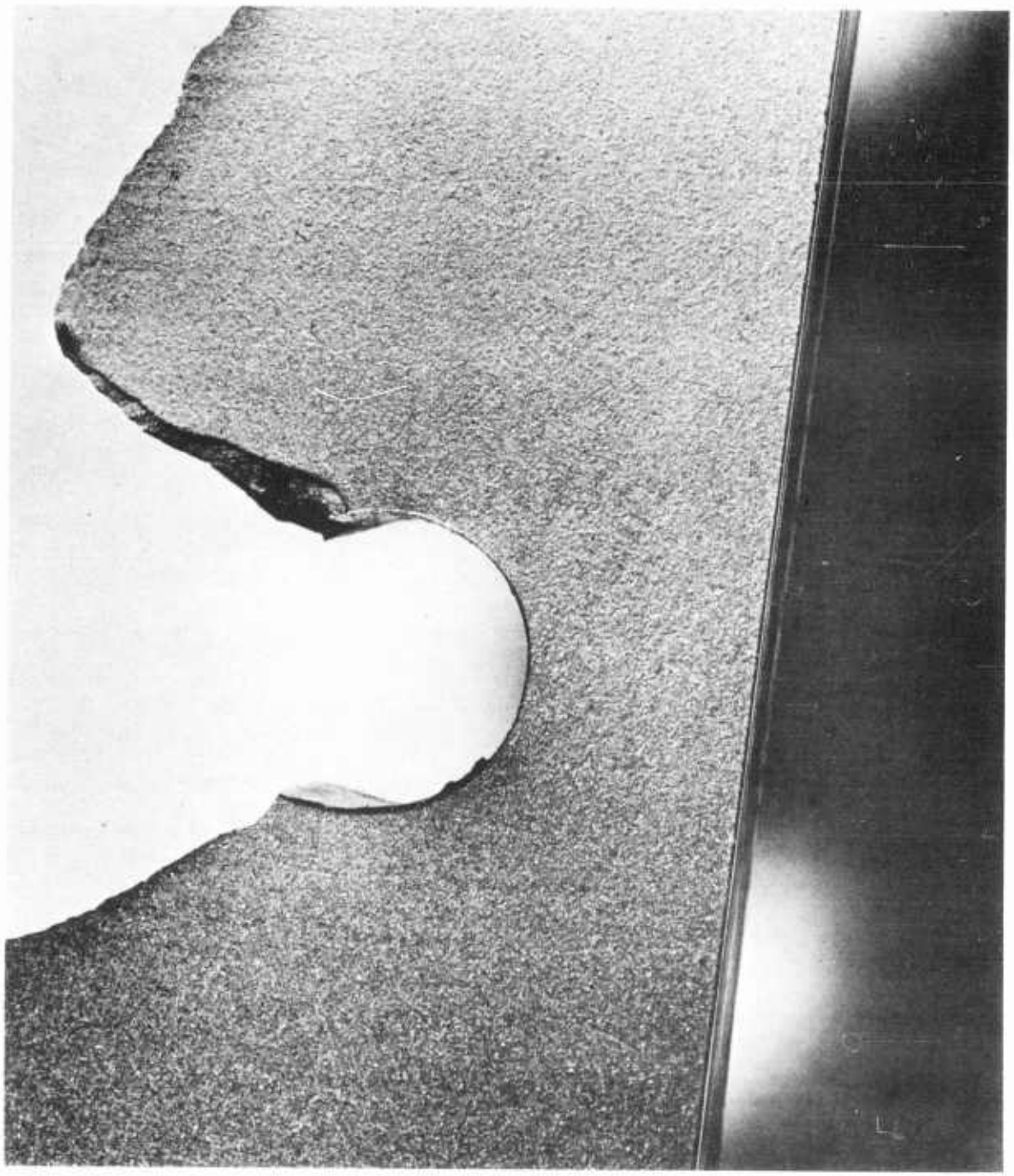

Figure 3-18. Rear Spar Fracture Area -- Burrs on Edge of Hole

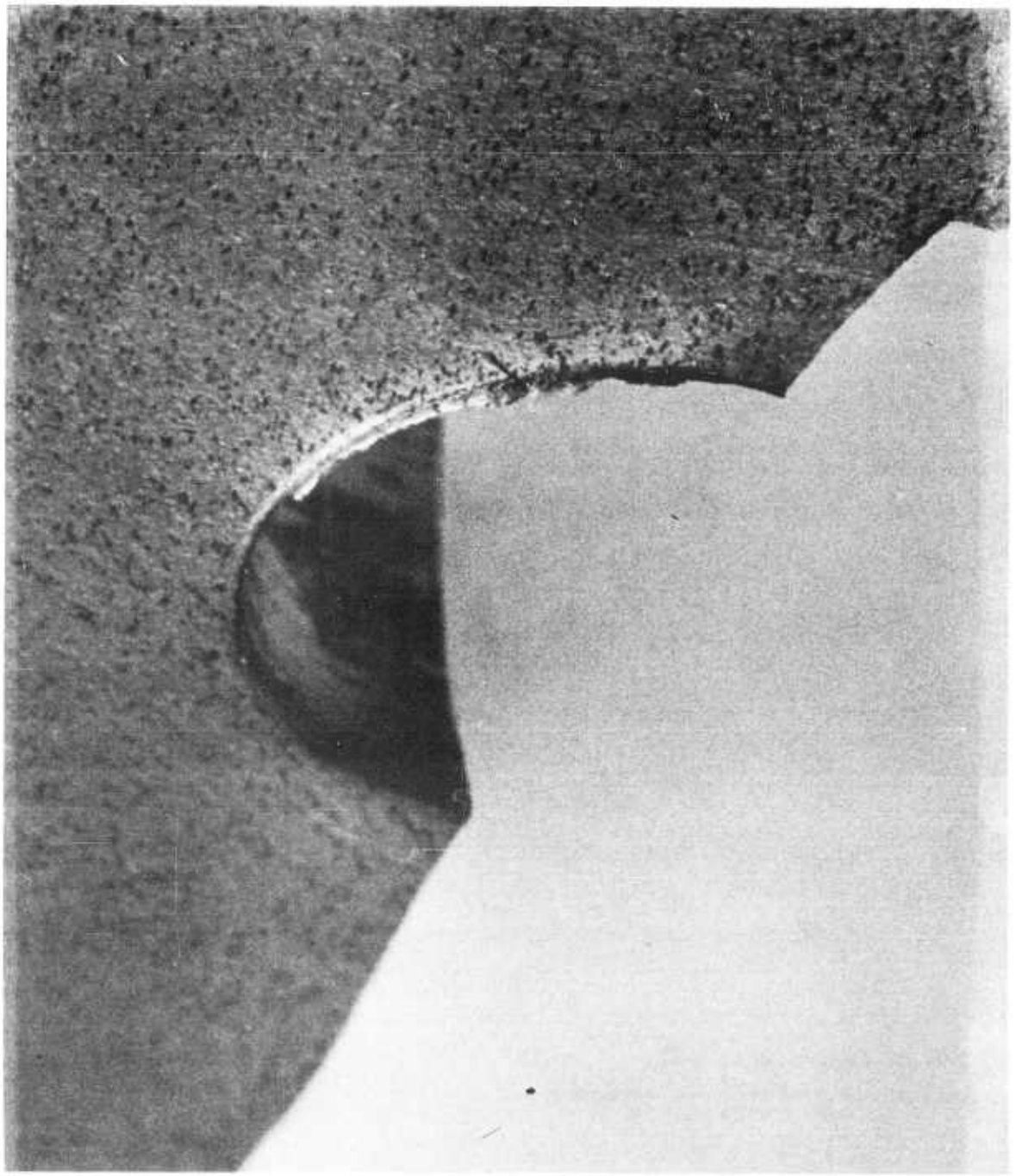

Figure 3-19. Rear Spar Fracture Area -- View of Crack in Burr

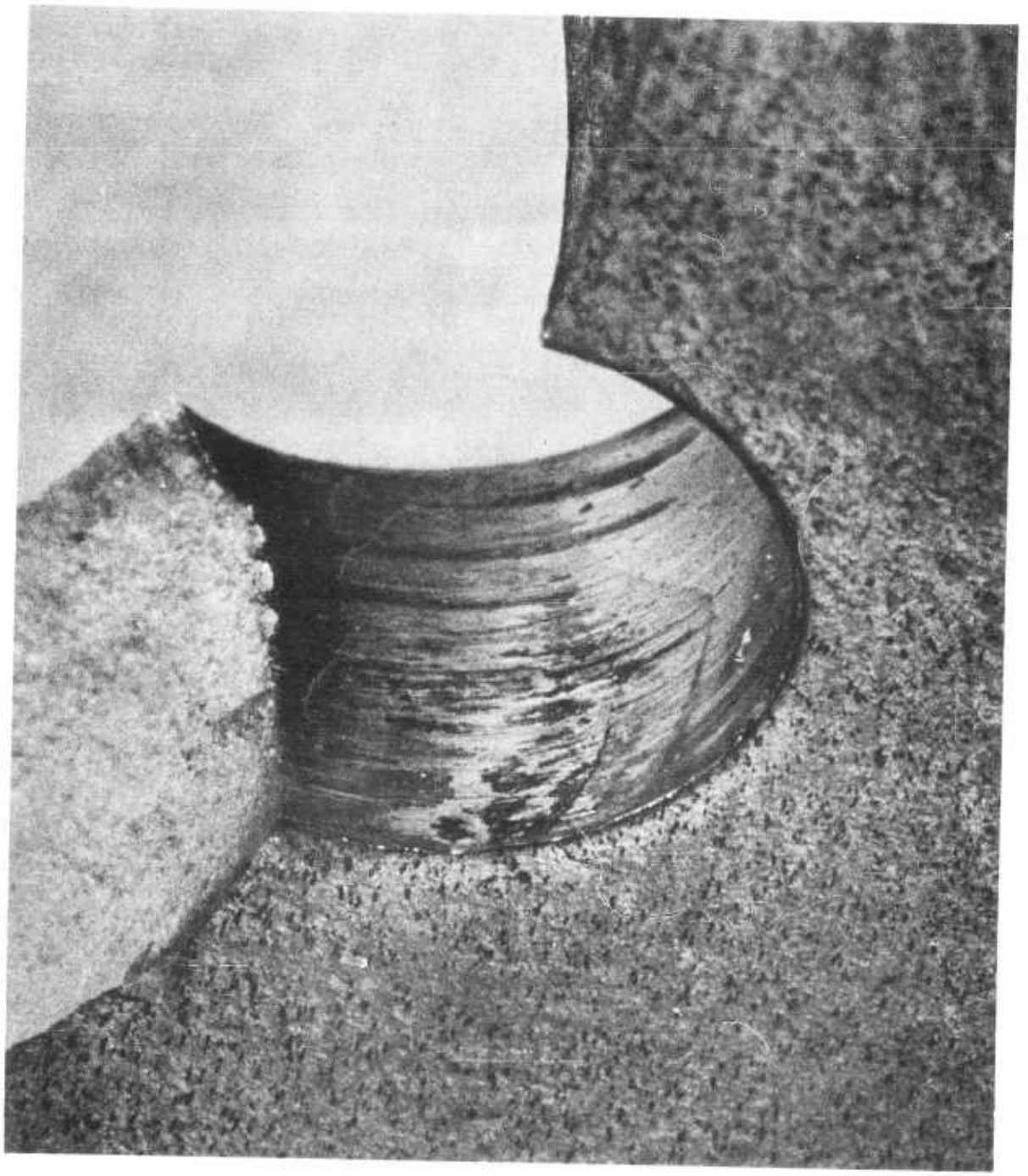

Figure 3-20. Rear Spar Fracture Area -- View of Crack in Burr

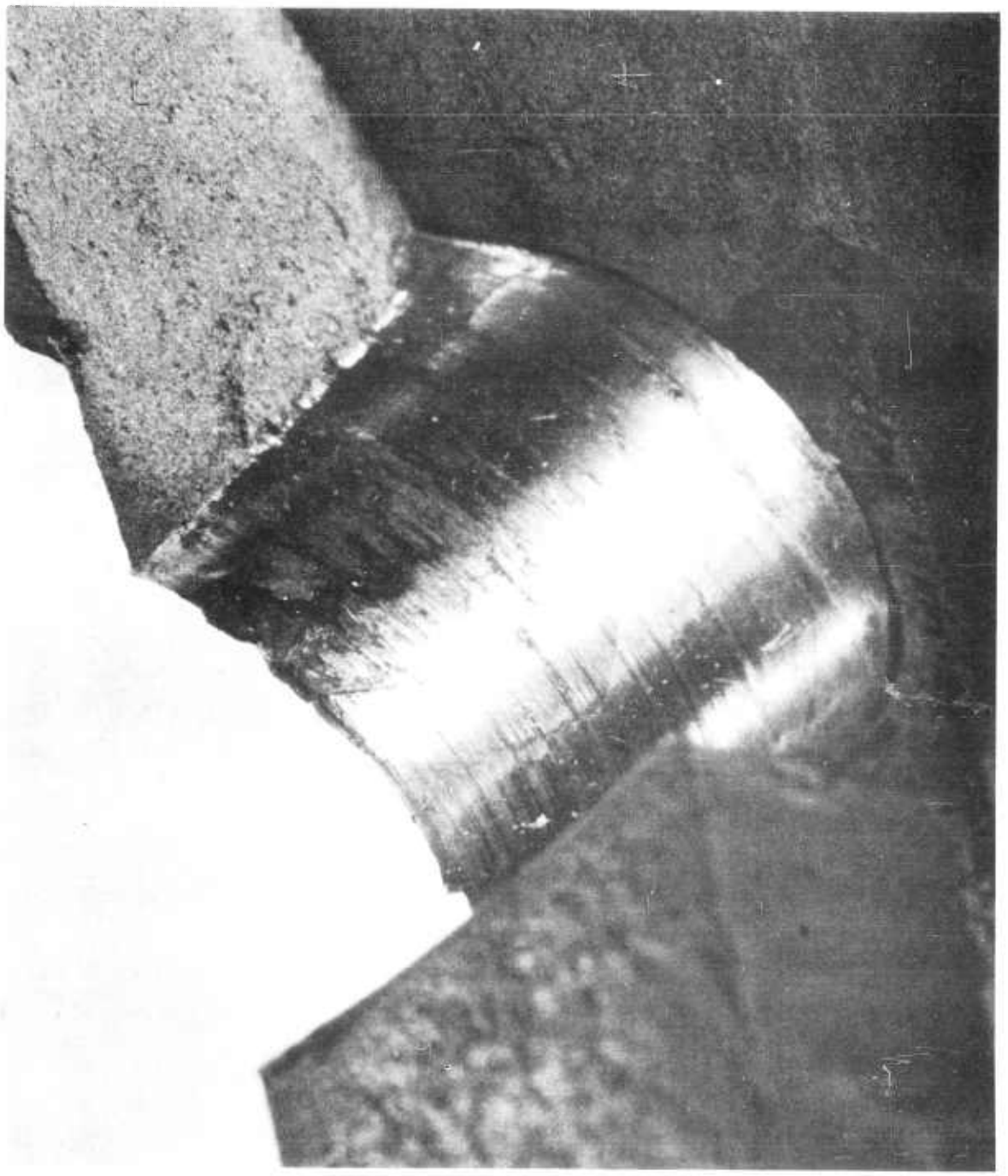

Figure 3-21. Rear Spar Fracture Area -- View of Crack in Burr

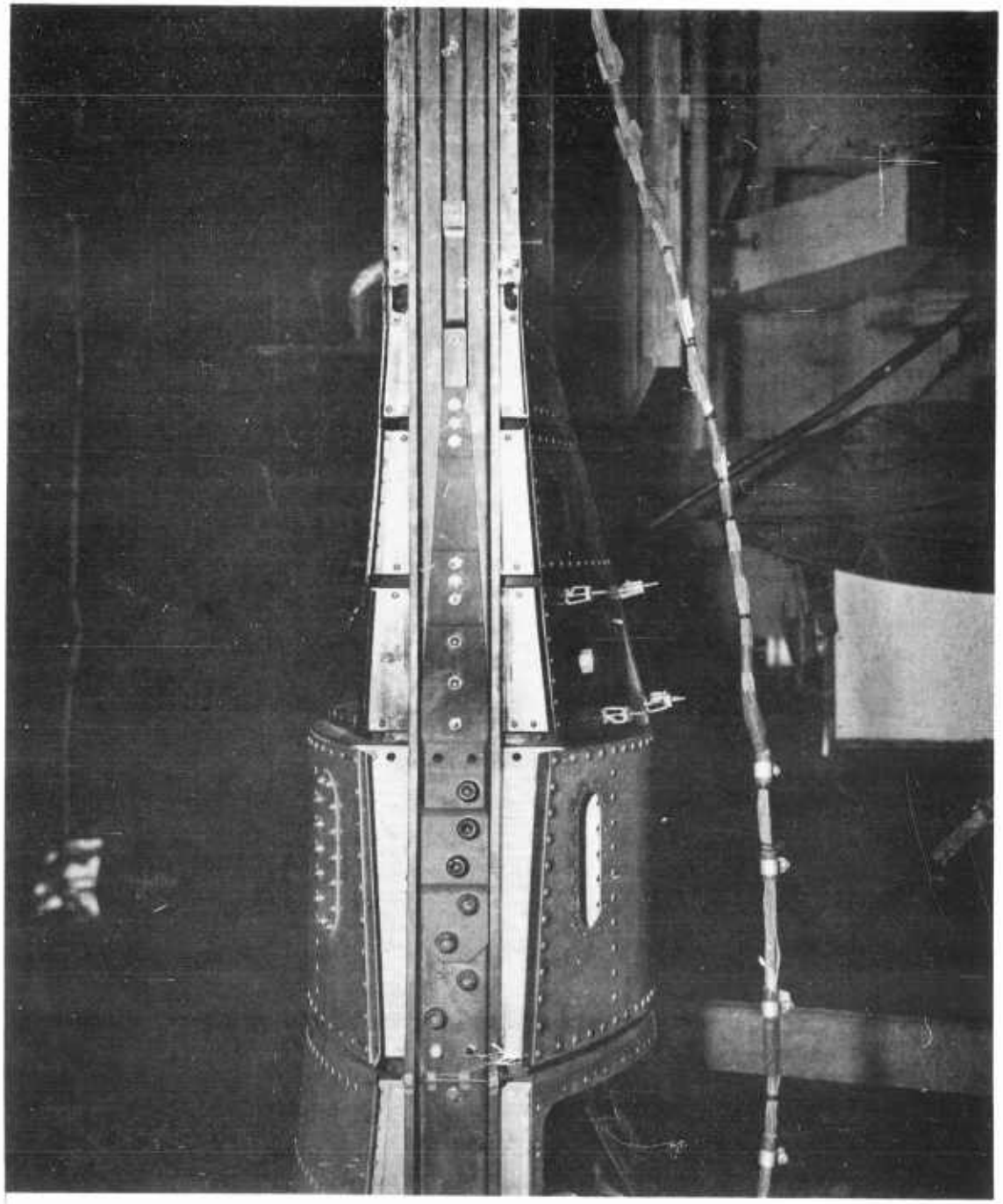

Figure 3-22. Inboard Area of Rear Spar Modification

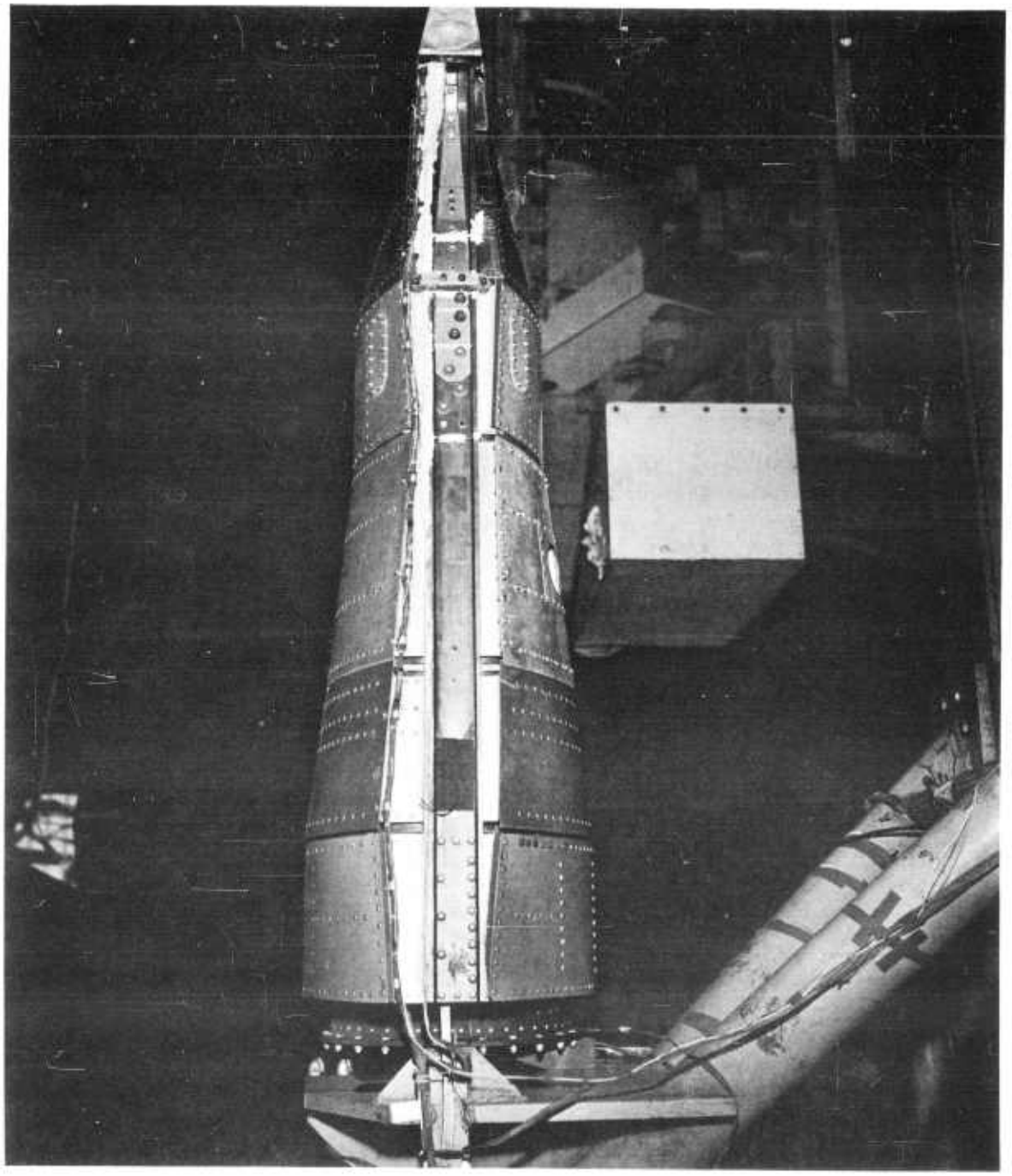

Figure 3-23. Inboard Area of Rear Spar Modification Prior to Retest

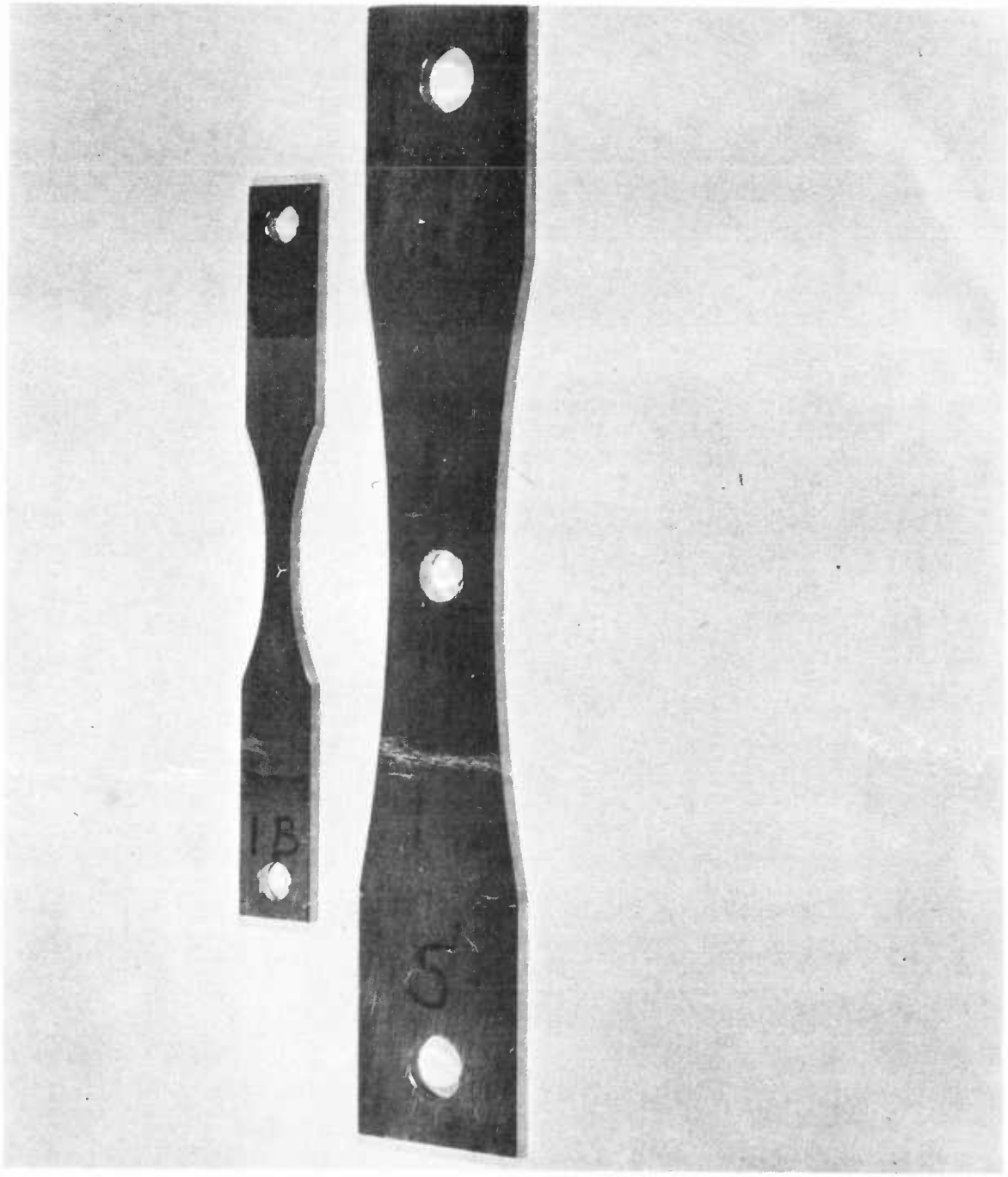

Figure 3-24. Aft Spar Titanium Fatigue Specimen Configuration

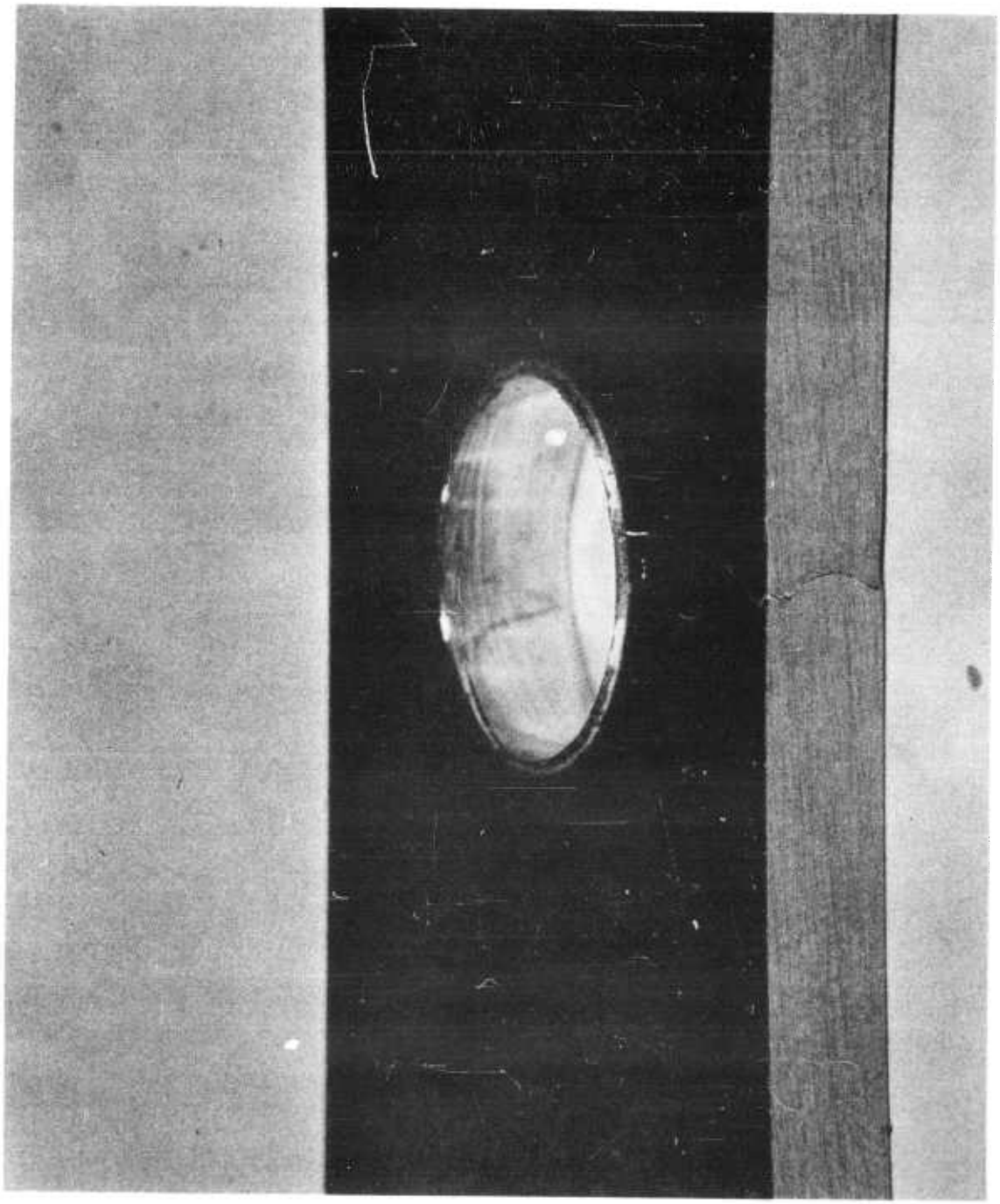

Figure 3-25. Typical Hole with Burr Titanium Fatigue Specimen

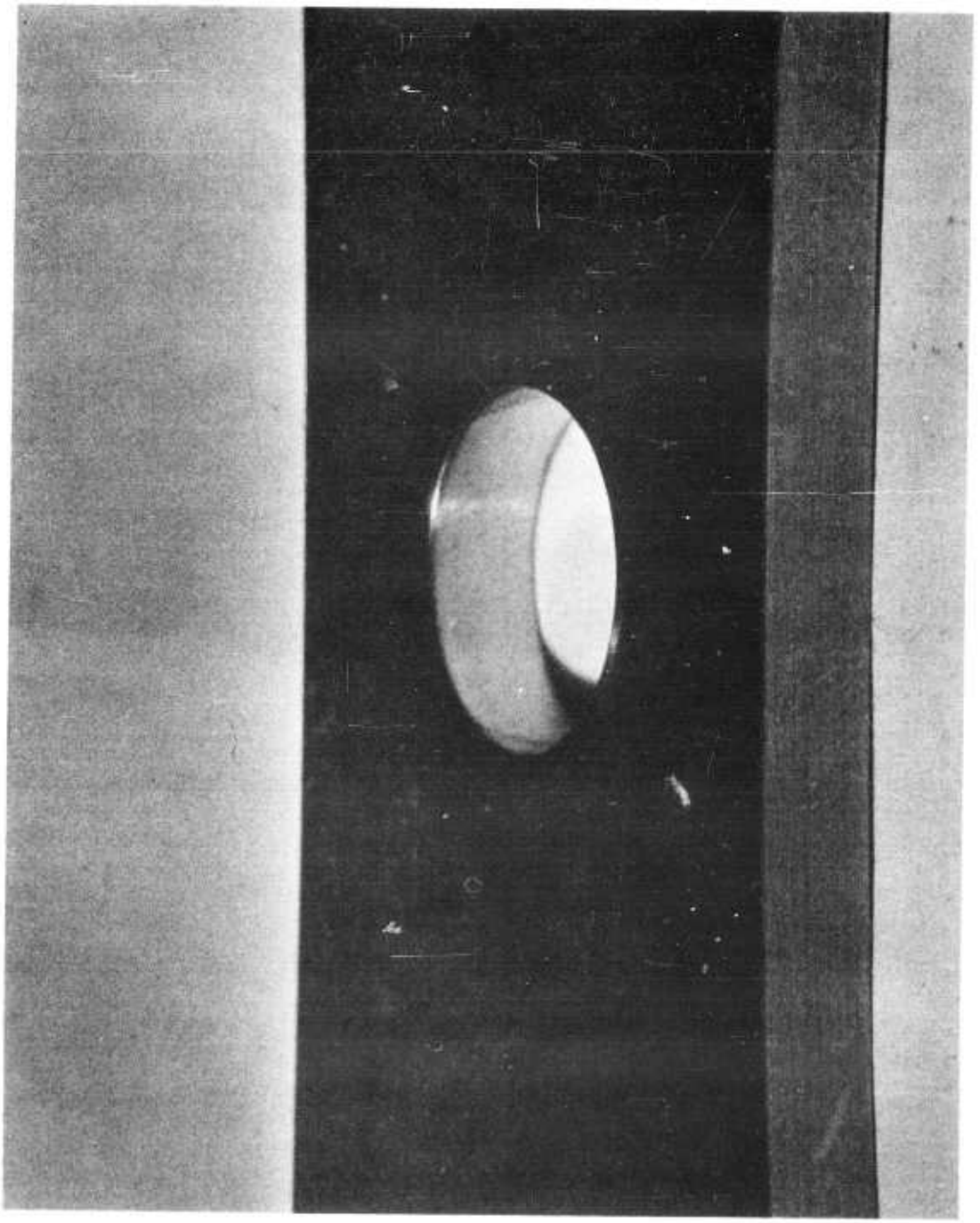

Figure 3-26. Typical Polished Hole Titanium Fatigue Specimen

SECTION 4

BLADE NATURAL FREQUENCY TESTS

4.1 PURPOSE

The purpose of these tests was to determine the non-rotating flapwise and chordwise bending frequencies for subsequent use in predicting blade natural frequencies during rotor operation.

4.2 TEST SETUP

4.2.1 Flapwise Frequency Determination

a. The instrumented blade was mounted in the blade support fixture, HTC-AD Drawing 285-0921, as shown on HTC-AD Drawing 285-0926 and Figure 4-3, and then attached to the gantry crane according to HTC-AD Drawing 285-0925 and Figure 4-4, the blade tip being 15 feet above the floor.

b. A medium force mechanical exciter assembly driven by a U. S. Motors Varidrive, was attached to the flapwise loading fixture, HTC-AD Drawing 285-0944, by a spring and a load cell. The loading fixture was attached to the blade by screws.

c. The transducers consisted of HTC designed and built strain gaged load cell of 1000 pounds capacity and 7 Statham type A-6 5G accelerometers. Six of the accelerometers, mounted at the following stations; 50, 100, 150, 200, 250 and 300 were attached to the blade in such a fashion as to be sensitive to acceleration in the flapwise direction only. In addition, an accelerometer was attached to the blade support fixture HTC-AD Drawing 285-0921, to detect accelerations which could possibly affect the test results. All accelerometers were calibrated for 2G's before installation. Preliminary runs made with two accelerometers attached to the blade support fixture indicated that the excitation of the support fixture in the direction normal to the test direction was neglible.

d. The output of the load cell and accelerometers was fed into individual bridge balance boxes and from there into a CEC 5-119P4-50 oscillograph equipped with a CEC 5-036C Datarite magazine. The CEC 7-339 galvanometers used have a flat frequency response from 0 to 30 cycles per second.

e. The natural frequency determination was made with the blade hanging vertically on the blade retention straps and capable of swinging freely. The loading fixture HTC-AD Drawing 285-0944, was

attached to the blade at Station 315 and the frequencies were swept by changing the speed of the U. S. Motors Varidrive unit. The speed sweeps ranged from 1 cycle per second to 100 cycles per second. The frequency at resonance could be read immediately from the oscillograph record.

4.2.2 Chordwise Frequency Determination Pin-End Condition

a. The pin end frequency determination was made using the same test setup as described in 4.2.1a and shown in Figures 4-3 and 4-4.

b. A medium force mechanical exciter driven by a U. S. Motor Varidrive was attached to the chordwise loading fixture HTC-AD Drawing 285-0944 by means of a spring and a load cell. The chordwise loading fixture was attached to the leading edge of the blade with screws.

c. The transducers attached to the blade are the same as those described in 4.2.1c except that the accelerometers were oriented so as to be sensitive to chordwise accelerations. An additional accelerometer was attached at the blade tip, Station 331. The accelerometer attached to the blade support fixture was also oriented so as to register accelerations in the chordwise direction. The signal input conditioning and recording equipment is the same as that described in 4.2.1d.

d. The pin end condition natural frequency was determined with the blade supported by the blade retention straps which were attached to the strap support beams, HTC-AD Drawing 285-0924. The blade beam combination was free to pivot about the bolt. A mechanical exciter was attached to the blade at Station 321. The speed of the varidrive was swept through the range of one cycle per second to sixty cycles per second. The weight of the test fixtures attached to the blade was about the same as that of the parts which had not been installed. The frequency at resonance could be read immediately from the oscillograph record.

4.2.3 Chordwise Frequency Determination, Cantilevered Condition

a. The cantilever natural frequency was obtained using basically the same test setup described in 4.2.1a and shown in Figures 4-3 and 4-4.

b. A medium force mechanical exciter driven by a U. S. Motors varidrive was attached to the chordwise loading fixture, HTC-AD Drawing 285-0944, by means of a spring and a load cell. In addition, the 285-0923-3 tip loading fixture was attached to the tip of the blade to maintain tension in the straps. A cable ran from the tip loading fixture to a

hydraulic cylinder, load cell, and load ring which were anchored to the floor by an I-beam loaded with lead weights.

c. The arrangement of the transducers is the same as that described in 4. 2. 2c with the exception of the tip accelerometer which was attached at Station 321, and the load cell attached to tip load fixture.

The signal input conditioning equipment is the same as that described in 4. 2. 1d.

d. The natural frequency for the cantilevered condition was determined with the blade supported by the blade retention straps which were attached to the strap support beams, HTC-AD Drawing 285-0924. Unlike the pin-end test however, the 285-0924 strap support beams were rigidly fixed by using the 285-0926-5 shim and additional shims as required. A small chordwise force applied at the tip of the blade was enough to cause the blade retention straps to buckle. An axial load therefore was required to prevent strap buckling during the frequency determination. The axial load was applied in the following steps: 0, 2000, 4000, 5000, 6000 7, 000 and 8000 pounds. The axial load was monitored by use of a load ring which had been recently calibrated. In addition the output of the load cell was recorded on the oscillograph. The chordwise loading fixutre was attached to the blade at Station 321. The frequencies were swept from one cycle per second to seventy-five cycles per second by changing the speed of the varidrive. The frequency at resonance and the axial load on the blade were read from the oscillograph record. The measured frequency was corrected for the effect of the axial load.

4. 3 TEST RESULTS

The results of the Hot Cycle blade natural frequency tests are as follows:

4. 3. 1 Flapwise Frequencies

Figures 4-1 and 4-2 present the first and second mode natural frequencies respectively. It can be seen that the natural frequency is reduced by an increase in amplitude. This effect is assumed to arise from the slip joint configuration of the blade section. For small amplitudes of vibration, some of the slip joints probably do not move, resulting in an increase in blade stiffness and, hence, in frequencies. It can be seen that the first mode frequencies vary from 2. 6 to 3. 3 cps and the second mode frequencies vary from 8. 7 to 11. 1 cps. When applying these frequencies to predictions of operating natural frequencies, a correction must be made for the reduction in modulus of elasticity of the titanium spars from the room temperature

Figure 4-1. Hot Cycle Rotor First Mode Flapwise
Natural Frequency Vs. Amplitude

Tests of 20 March 1961

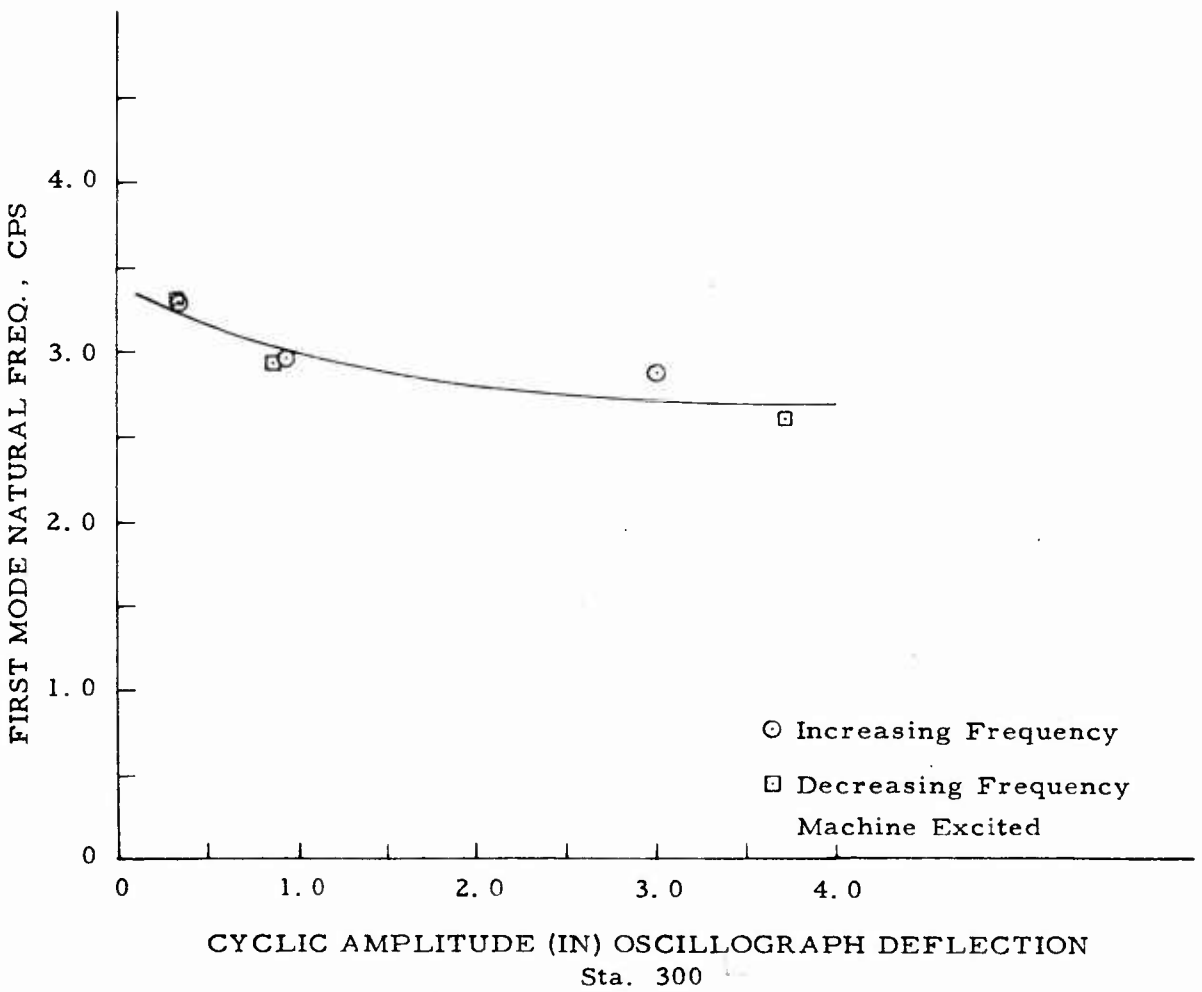

Figure 4-2. Hot Cycle Rotor Second Mode Flapwise Natural Frequency vs Amplitude

Tests of 21 March 1961

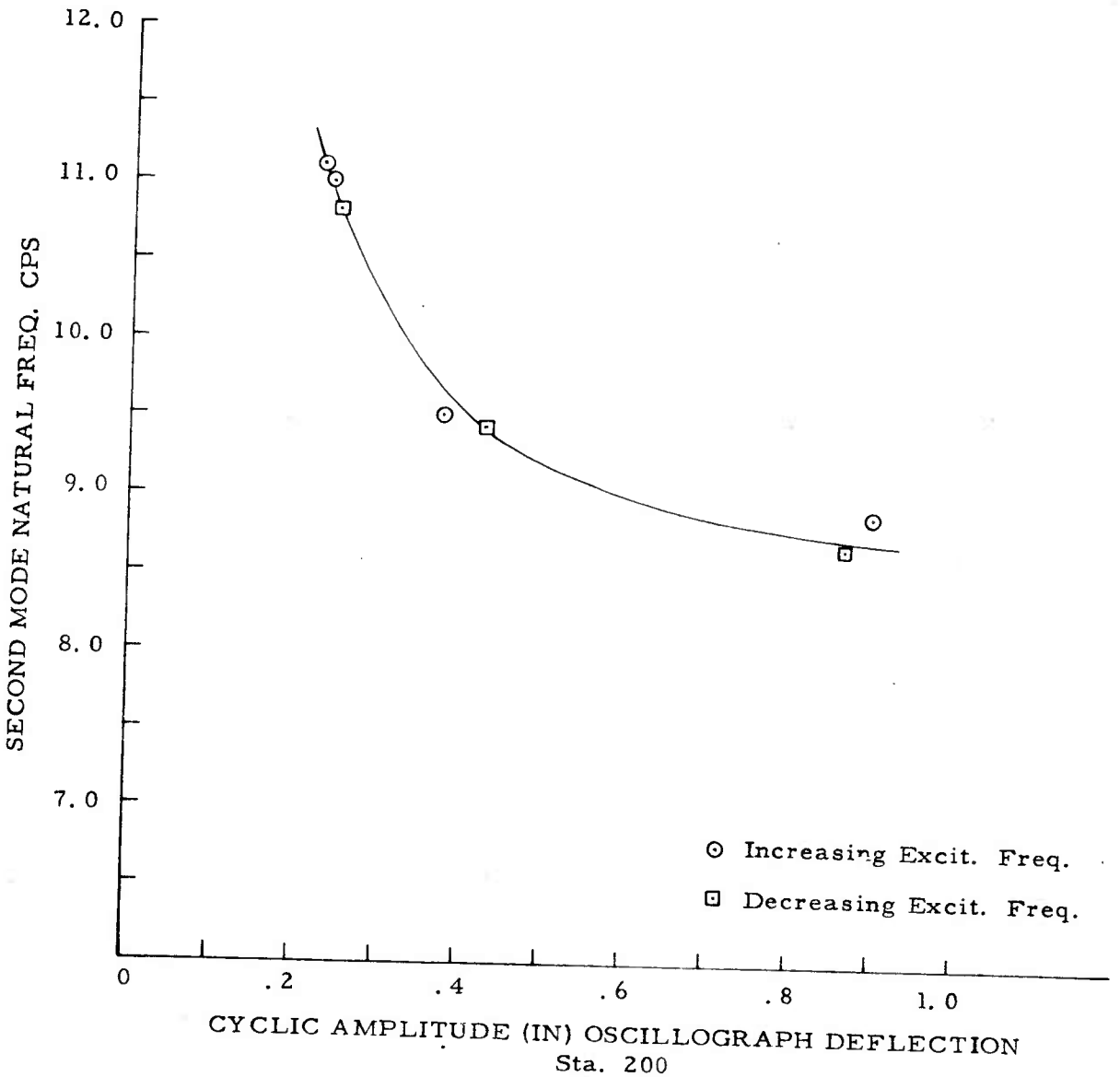

value where the vibration tests were performed to the values when the spars are at operational temperature. The factor is:

$$\sqrt{\frac{14 \times 10^6}{16 \times 10^6}}$$

Applying this factor results in a frequency range of 2.5 to 3.1 cps for the first mode and 8.2 to 10.4 cps for the second mode.

4.3.1.1 Flapwise damping. Whenever the excitation was cut off it was noted that the blade motion damped out rather quickly. From the measured rates of decay, an estimate was made of the blade structural damping of 8% of critical. NACA Technical Note 3862 presents measured values of structural damping for blades of conventional construction which are of the order of 1% of critical. Thus, it appears that the Hot Cycle blade has 8 times as much structural damping as a conventional rotor blade. This is attributed to the additional damping introduced by the slip joint construction. This additional damping should be very valuable in minimizing amplification when passing through resonance during rotor rev up and shut down or when reducing rotor speed to operate as a compound helicopter.

4.3.2 Chordwise Natural Frequencies (Cantilever)

Measurements were made of the first and second mode chordwise cantilever natural frequencies. These measurements were corrected for the effect of temperature, as above, as well as for the effect of tension applied at the blade tip to prevent buckling of the straps. Applying these two corrections resulted in a frequency range of 5.3 to 5.5 cps for the first mode and 21.5 to 22.5 cps for the second mode.

4.3.3 Chordwise Frequency (Pinned)

A measurement of chordwise frequency was made in which the blade was permitted to rotate about a pinned fitting just inboard of the feathering ball. This measured frequency was corrected for temperature, as above, as well for movement of the point of rotation to the main rotor shaft. During operation of the rotor, the pin ended mode involves simultaneous bending of all three blades and rotation of the hub and shaft. Applying these corrections resulted in a frequency of 18.3 cps.

4.4 CONCLUSIONS

Measurements have been made of the non-rotating natural frequencies of the hot cycle rotor blade. The results are as follows:

Flapwise, 1st mode	2.5 - 3.1 cps
Flapwise, 2nd mode	8.2 - 10.4 cps
Chordwise, cantilever, 1st mode	5.3 - 5.5 cps
Chordwise, cantilever, 2nd mode	21.5 - 22.5 cps
Chordwise, pin-end	18.3 cps

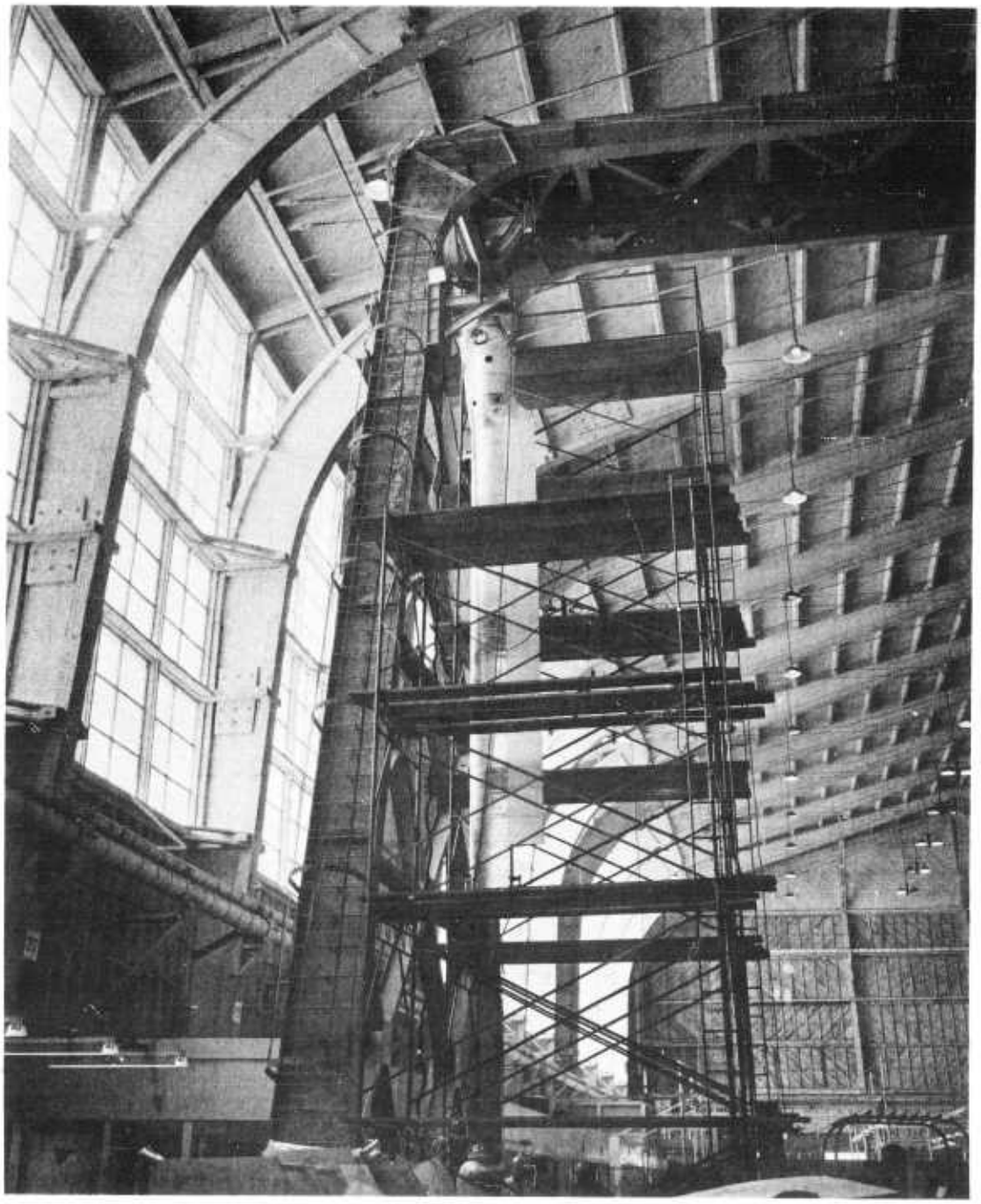

Figure 4-3. View of Instrumented Whirl Blade in Calibration Fixture

Figure 4-4. View of Instrumented Whirl Blade in Calibration Fixture

SECTION 5

MATERIAL EVALUATION TESTS

5.1 PURPOSE

To determine the mechanical **static room temperature tensile** properties of the blade spar, titanium, AMS4928, and the room temperature and elevated temperature tensile properties of Rene' 41.

5.2 SPECIMEN

The titanium static tensile coupons were machined in a longitudinal direction from the ends of one of the production spars. The Rene' 41 coupons were machined from sheet stock of various stock thicknesses. The static tensile coupons were machined according to Federal Methods Standard Number 151.

5.3 TEST SETUP

The room temperature tensile coupons were tested in a Baldwin 5000 pound Test Machine. The elevated temperature tests of Rene' 41 were conducted in the HTC-AD elevated temperature test machine.

5.4 TEST RESULTS

The results of the room temperature tensile tests of the titanium and Rene' 41 coupons are given in Tables 5-1 and 5-2. The results of the elevated temperature tests of Rene' 41 coupons are given in Table 5-3. These coupons were transverse tensile specimens machined per HTC-AD Drawing 326-0011 and aged at 1400°F for 16 hours and air cooled. The specimens were soaked at 1100°F for 15 minutes (± 30 seconds). Tension was applied at an elongation rate of 100 microinches per inch per second. After yield, the rate was increased to 1000 micro-inches per inch per second.

TABLE 5-1

TENSILE PROPERTIES OF TITANIUM SPAR STOCK
LONGITUDINAL SPECIMENS ONLY

SPECIMEN NUMBER	SPECIMEN AREA	SPECIMEN THICKNESS	YIELD STRESS .2% OFFSET	ULTIMATE STRESS	ELONGATION % (1 inch gage length)
		SPECIMENS FROM SPAR BILLET No. 7			
7-1	.0286	.0570	136,800	151,000	14
7-2	.0314	.0625	126,500	146,300	15
7-3	.0288	.0576	133,000	148,200	15
7-4	.0315	.0629	121,200	145,000	18
7-5	.0312	.0621	141,000	156,900	16
7-6	.0304	.0609	141,500	154,300	15
		SPECIMENS FROM SPAR BILLET No. 8			
8-1	.0298	.0594	142,500	155,300	15
8-2	.0289	.0576	136,500	148,400	15
8-3	.0325	.0648	145,000	159,500	15
8-4	.0290	.0579	149,000	162,000	15
8-5	.0302	.0603	139,200	152,800	15
8-6	.0301	.0601	137,900	149,000	15

TABLE 5-2

TENSILE PROPERTIES OF AGED RENE' 41

SPECIMEN NUMBER	SPECIMEN AREA	SPECIMEN THICKNESS	YIELD STRESS .2% OFFSET PSI	ULTIMATE STRESS PSI	ELONGATION %
SPECIMENS AGED FOR 16 HOURS AT 1400°F, AIR COOL					
LONGITUDINAL SPECIMENS					
61-1	.00555	.0111	140,000	171,000	8
61-2	.00545	.0109	142,500	165,500	7
61-3	.00542	.0108	142,000	184,000	17
62-1	.00866	.0174	140,300	188,000	Failed Outside of Test Section
62-2	.00866	.0174	139,200	192,500	18
62-3	.00865	.0174	141,800	193,500	21
TRANSVERSE SPECIMENS					
61-4	.00500	.0100	140,600	184,000	15
61-5	.00499	.0100	142,100	185,000	16
61-6	.00492	.0099	143,200	187,000	15
62-4	.00885	.0177	139,700	190,500	15
62-5	.00883	.0177	143,400	190,000	15
62-6	.00885	.0177	142,500	181,000	Failed Outside of Test Section

TABLE 5-2 (continued)

TENSILE PROPERTIES OF AGED RENE' 41

SPECIMEN NUMBER	SPECIMEN AREA	SPECIMEN THICKNESS	YIELD STRESS .2% OFFSET PSI	ULTIMATE STRESS PSI	ELONGATION %
		SPECIMENS AGED FOR 4 HOURS AT 1650°F, AIR COOL			
		LONGITUDINAL SPECIMENS			
61-7	.00468	.0096	119,200	154,000	8
61-8	.00462	.0095	119,300	154,000	12
61-9	.00460	.0095	119,200	164,000	Failed Outside of Test Section
62-7	.00823	.0172	123,500	183,000	Failed Outside of Test Section
62-8	.00819	.0172	127,100	185,000	19
62-9	.00829	.0172	120,100	185,000	22
		TRANSVERSE SPECIMENS			
61-10	.00475	.0099	123,700	162,500	10
61-11	.00480	.0099	121,900	153,000	7
61-12	.00481	.0099	122,800	166,000	11
62-10	.00845	.0174	126,700	182,000	16
62-11	.00845	.0175	127,500	182,700	16
62-12	.00845	.0176	127,500	172,500	Failed Outside of Test Section

TABLE 5-3

ELEVATED TEMPERATURE TENSILE TESTS OF RENE' 41 TRANSVERSE SPECIMENS

SPECIMEN NO.	DIMENSIONS (IN.)	YIELD STRESS (0.2% OFFSET) (PSI)	ULTIMATE STRESS (PSI)	PERCENT ELONGATION	MODULUS (E) (PSI)
1	.010 x .50	123,000	144,000	7.2	24×10^6
2	.010 x .50	120,000	148,000	10.6	24.5×10^6
3	.010 x .50	116,000	145,000	11.5	26.1×10^6
4	.010 x .50	122,000	153,000	18.4	22.6×10^6
5	.020 x .50	125,000	161,000	13.6	27.4×10^6
6	.020 x .50	144,000	173,000	12.9	24.1×10^6
7	.020 x .50	123,000	159,000	10.0	24.5×10^6
8	.020 x .50	123,000	161,000	16.3	24.9×10^6
9	.020 x .50	132,000	163,000	(10. +)*	24.6×10^6
10	.020 x .50	127,000	165,000	16.4	26.0×10^6
11	.020 x .50	143,000	170,000	7.5	23.7×10^6

*Break occurred outside of gaged area

SECTION 6

ARTICULATE DUCT OUTBOARD SEAL TEST

6.1 PURPOSE

To determine the ability of the articulate duct outboard seal to withstand pressure and thermal environments.

6.2 TEST SPECIMEN

The test specimen described in this report represents the current design of the outboard duct seal, HTC-AD Drawing 285-0217B. Earlier versions were found to bind at misalignment angles of greater than three degrees. The duct seal, as installed in the whirl test blades, is an assembly of three nested conical lip seals with staggered slots and two nesting backup leaves in the direction of maximum side load. The material of this assembly is Rene' 41 alloy sheet, solution heat treated condition. The three nesting seals are .010 inch in thickness and the two backup leaves are .020 inch in thickness. The seals were formed one inside the other on a hydro-press machine in order to obtain the closest possible fit between the seals. The seals were then separated and slotted. After reassembly between an inner and an outer mandrel, the seal rubbing surface was ground to match the diameter of the mating articulate duct ring.

6.3 TEST SETUP

The test setup consisted of a fatigue test fixture, HTC-AD Drawing 285-0831, designed to produce the condition of weighted fatigue rotor operation with a gas pressure of 24.0 psig and temperature of 1050°F. This fixture is shown in Figures 6-1, 6-2, 6-3 and 6-4. The instrumentation for recording duct temperatures and friction loads, and heat and gas temperature control instruments are shown in Figure 6-3.

6.4 TEST RESULTS

The duct seal was subjected to a cyclic angular motion of $\pm$ 3 degrees flapping and $\pm$ 12 degrees feathering. The cyclic rate was 550 rpm. The duct seal was cycled for twenty hours. Inspection of the seal occurred at the ten hour period and at the end of the test run. At each inspection period the seal was disassembled and inspected for wear and fatigue crack indications. No malfunctions were noted and wear was negligible. The leakage rate varied from 1.1 to 2.8 cubic feet per minute flow. The load required to oscillate the seal varied from a break-in load of 400 pounds for the first three hours to an average of 240 pounds for the remainder of the test.

All seals installed on the whirl test blades were initially tested in the fatigue test fixture by cycling for one hour for break-in and checking for bind-up and excessive leakage.

The typical breakaway torque required to move the lip seal assembly at various angles of misalignment are as follows;

Misalignment Angle	Breakaway Torque (in-lbs)
0°	550.
3°	580.
6°	680.
9°	840.

These tests were conducted at a temperature of 1050° and pressure of 24. 0 psig.

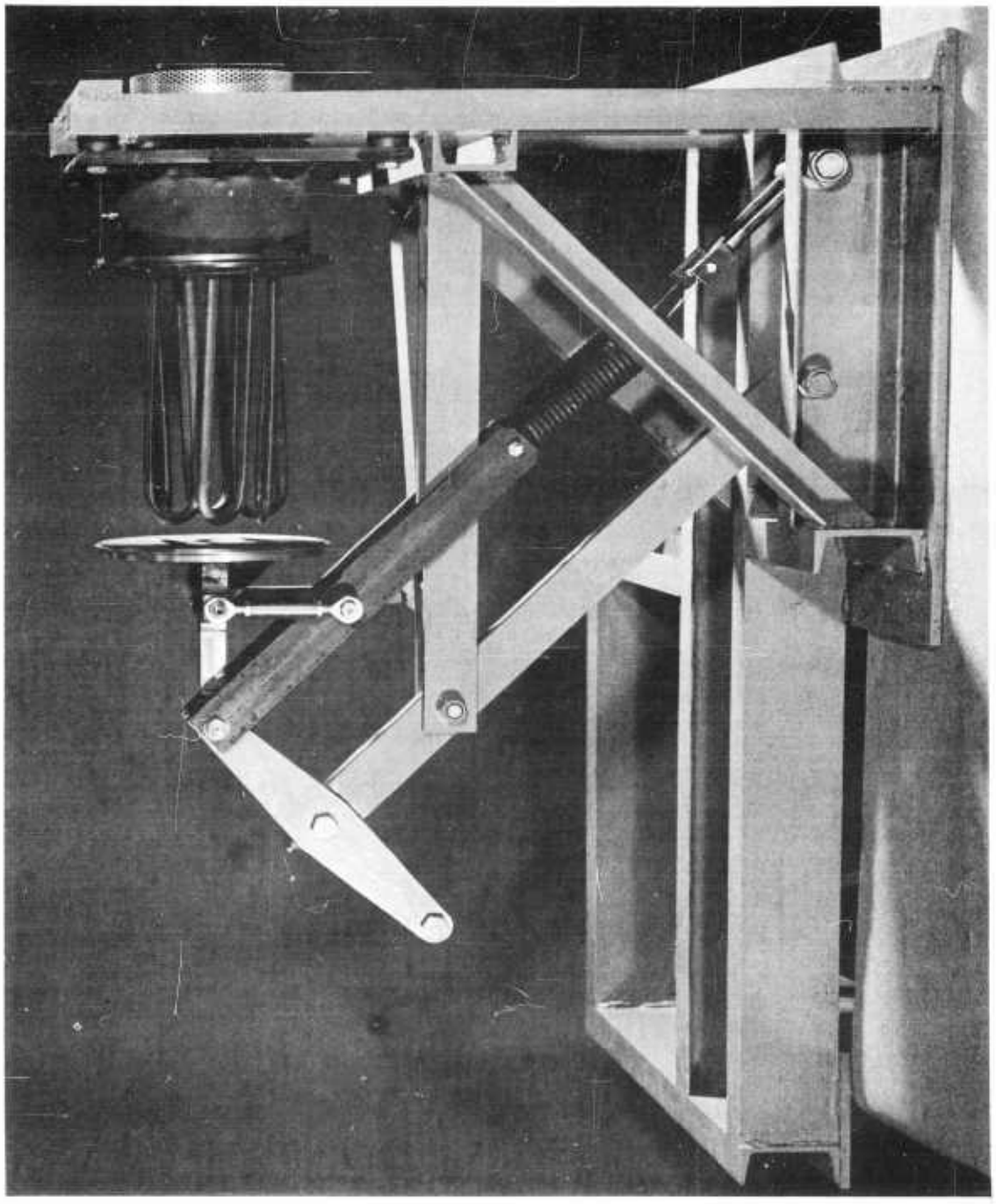

Figure 6-1. Fixture for Articulate Duct Outboard Seal Test with Electric Heater in Place

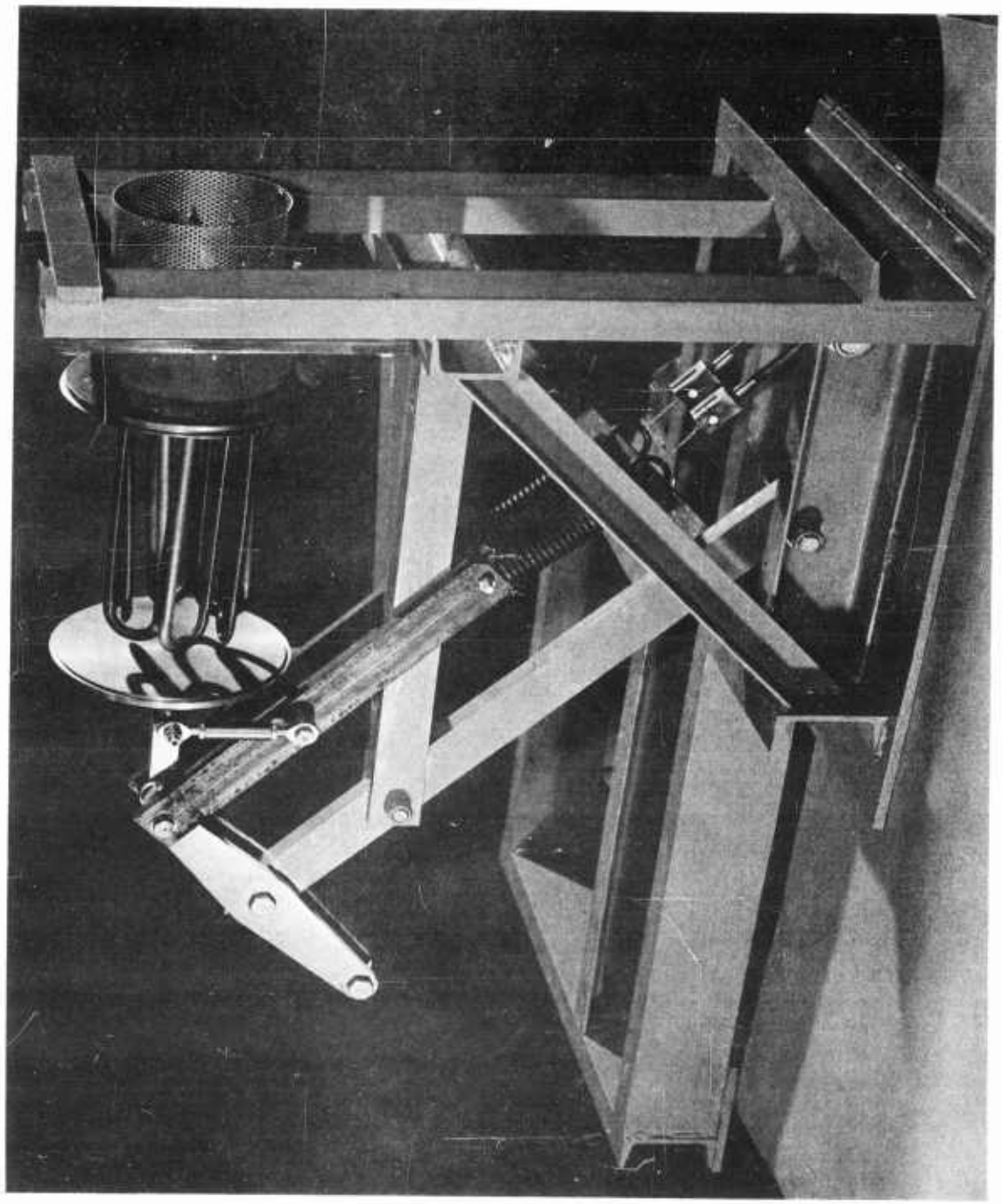

Figure 6-2. Fixture for Articulate Duct Outboard Seal Test with Electric Heater in Place

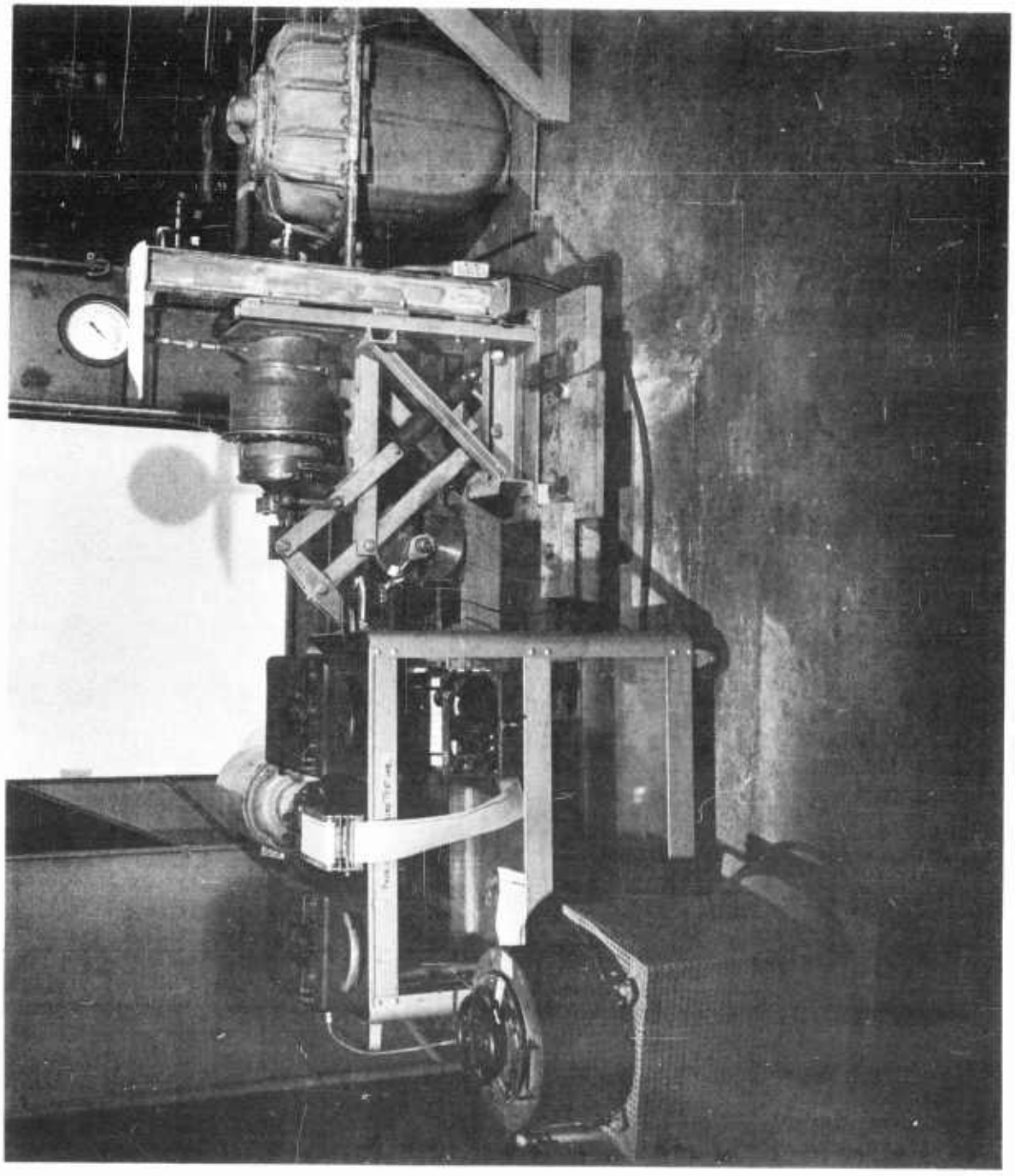

Figure 6-3. Test Setup -- Outboard Articulate Duct Seal Test

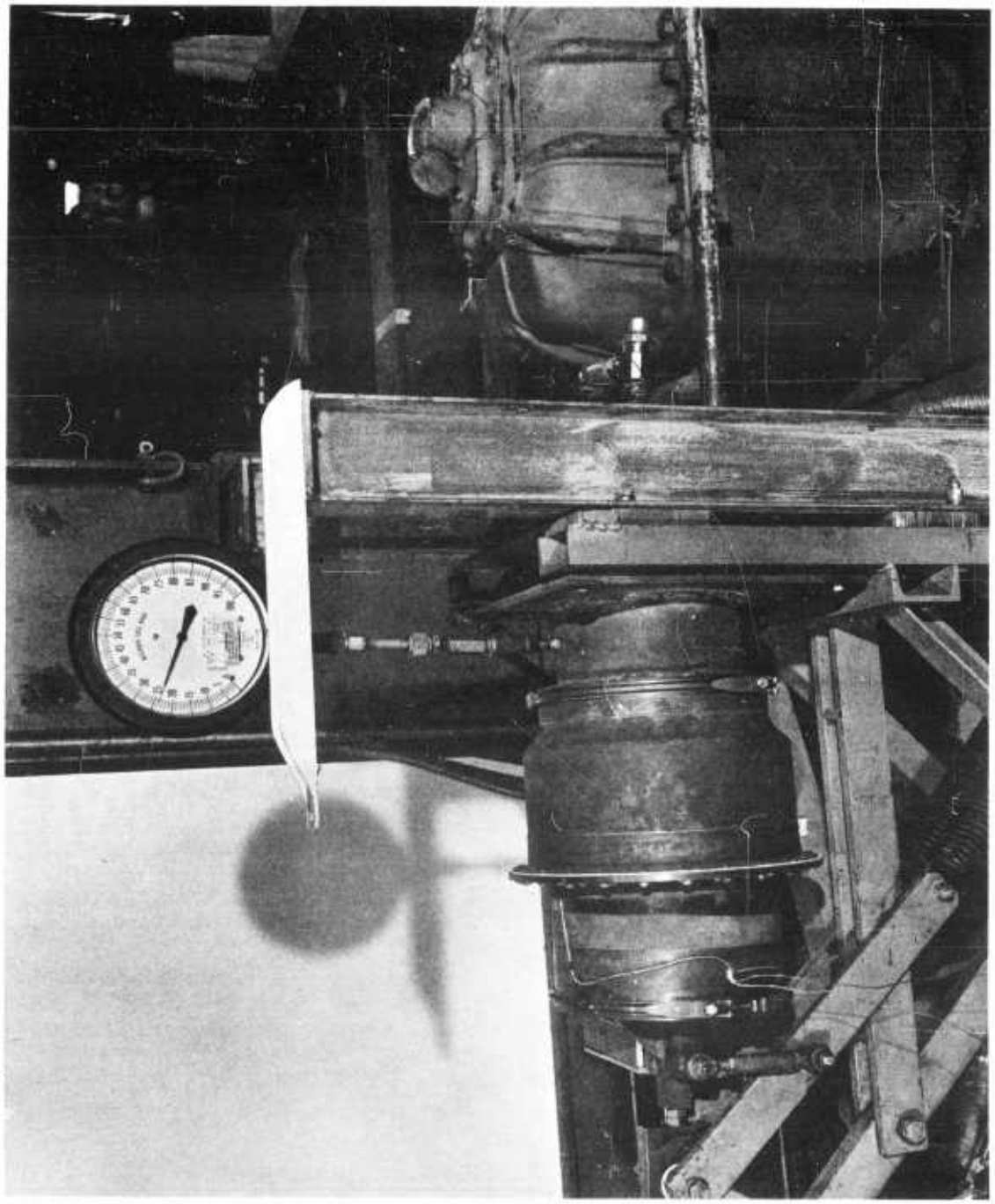

Figure 6-4. Duct Assembly and Pressure Arrangement -- Outboard Articulate Duct Seal Test

8.3 TEST RESULTS

8.3.1 Phase I Ten Hour Soak at 800°F. and 24.0 PSIG

The specimen was heated until 800°F. was attained on the inner duct walls. This condition was maintained for five hours. For the remaining five hours a flow of air was maintained through the ducts which averaged 1.2 scfm at 24.0 psig. The outside skin temperatures were held below 550°F. It was noted that a white powdery residue from the sealant compound was escaping from the air flow control valve orifice.

8.3.2 Phase II Four Hour Soak at 1150°F. and 24.0 PSIG

The specimen was heated until 1150°F was attained on the inner duct walls. A flow of air was maintained through the duct area of approximately 1.5 scfm. This condition was maintained for three hours and 45 minutes. For the remaining 15 minutes the temperature on the inner duct walls was increased to 1235°F. The outside skin temperatures did not exceed 600°F. The white residue was noted, similar to the Phase I test.

8.3.3 Phase III One Hour Soak at 1150°F. and 24.0 PSIG with holes through the duct

This test phase was similar to Phase II except the air leakage was through two drilled holes in the forward and aft ducts and the duration of this phase was one hour. The two holes were drilled through the outside skin, the flexural coupling and the duct. The location of the holes is shown in Figure 8-1. The hole through the forward duct was increased in diameter from .046 to .068 to .10 inch in approximately 15 minute intervals. The hole through the aft duct was drilled at the same time as the forward .10 inch diameter hole.

Thermocouples were installed into each hole to record the air temperature in the sealant area. The forward hole temperature was 960°F. The aft hole temperature was 1125°F. The air leakage through the two .10 inch diameter holes was approximately 3.0 scfm. Inspection of these holes after test revealed that the sealant compound had partially clogged the holes in the outside skin.

8.3.4 General

The temperature distribution in the specimen for each test phase is given in Figure 8-1. The condition of the sealant compound after test is shown in Figures 8-4, 8-5, 8-6, 8-7 and 8-8.

SECTION 7

FEATHERING - FLAPPING BEARING WEAR TEST

7.1 PURPOSE

To determine the ability of the feather-flapping bearing to withstand the normal and cordwise shear load components from the blade to the hub structure.

7.2 TEST SETUP

The spherical bearing and seal, consisting of a cast aluminum alloy ball, Drawing 285-0155-501, and a metal retainer bonded with "Fabroid", Figure 7-4, was inserted in a test fixture shown in Figure 7-1 and 7-2. The test fixture subjected the bearing to oscillatory motion simulating flapping and feathering, blade changes. Bearing test temperatures were applied with radiant heat coils mounted inside the test assembly. The instrumentation used for recording bearing temperatures and the cyclic test loads is shown in Figure 7-3. The test installation is shown in HTC-AD Drawing 285-0821.

7.3 TEST CONDITIONS

The test conditions applied to the bearing assembly were as follows:

1.	Feathering rotation	$\pm$ 6 degrees,
2.	Flapping rotation	$\pm$ .33 degrees,
3.	Axial movement	$\pm$ .010 inch,
4.	Shear load	500 $\pm$ 2100 pounds,
5.	Frequency	4.1 cps,
6.	Bearing temperature	292 $\pm$ 15°F.

7.4 TEST RESULTS

The spherical bearing and retainer was subject to 26.5 hours of cycling. Inspection of the bearing and Fabroid bonded retainer revealed that a small amount of flaking of teflon fibers had occurred. No indication of increased clearance or damage of any kind was noted. The bearing and retainer after test is shown in Figures 7-5, 7-6, 7-7 and 7-8.

The whirl test blade feathering-flapping bearings were inspected after 60. hours of whirl tests. No indication of increased clearance or damage was noted.

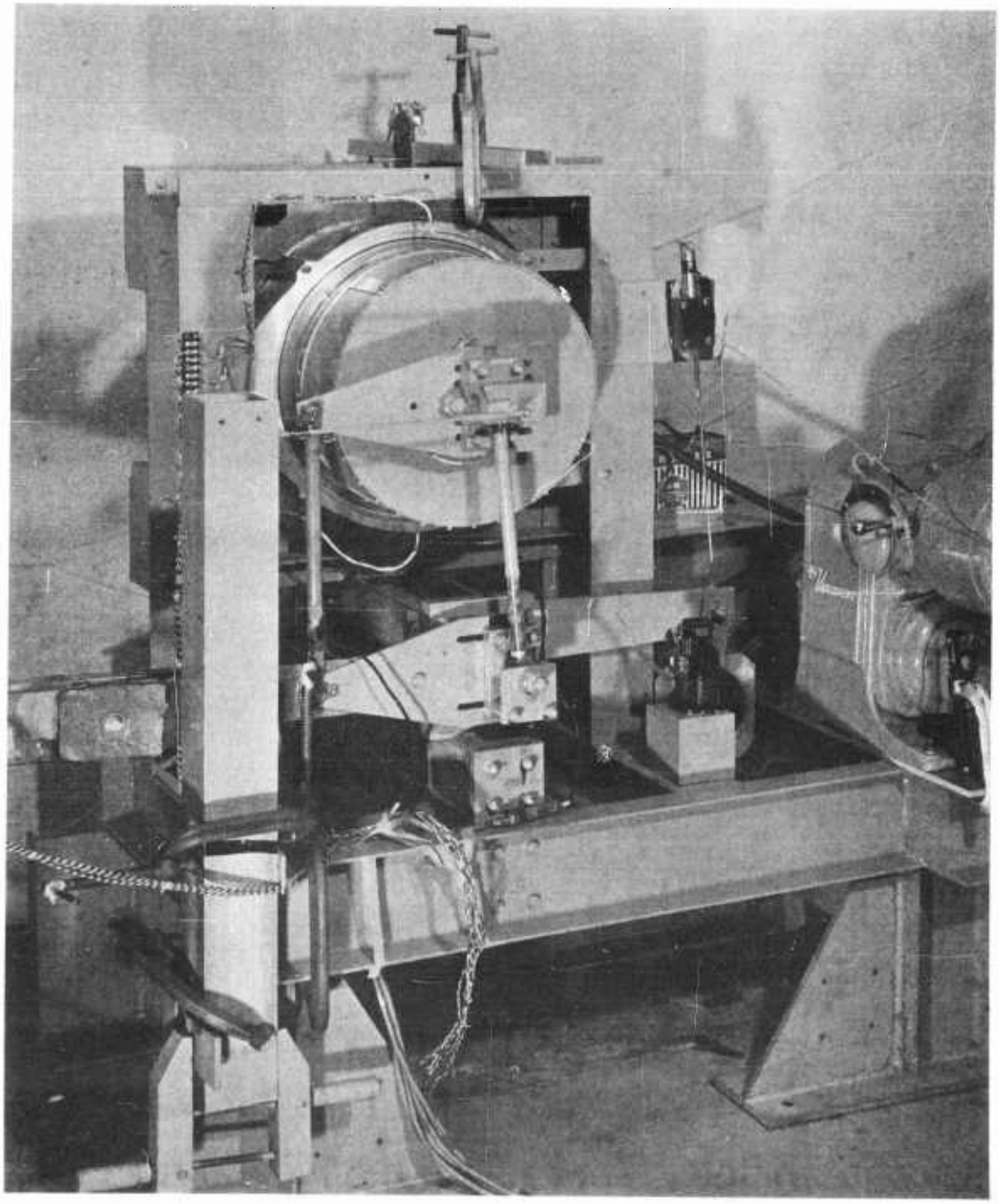

Figure 7-1. Test Fixture -- Feathering-Flapping Bearing Wear Test

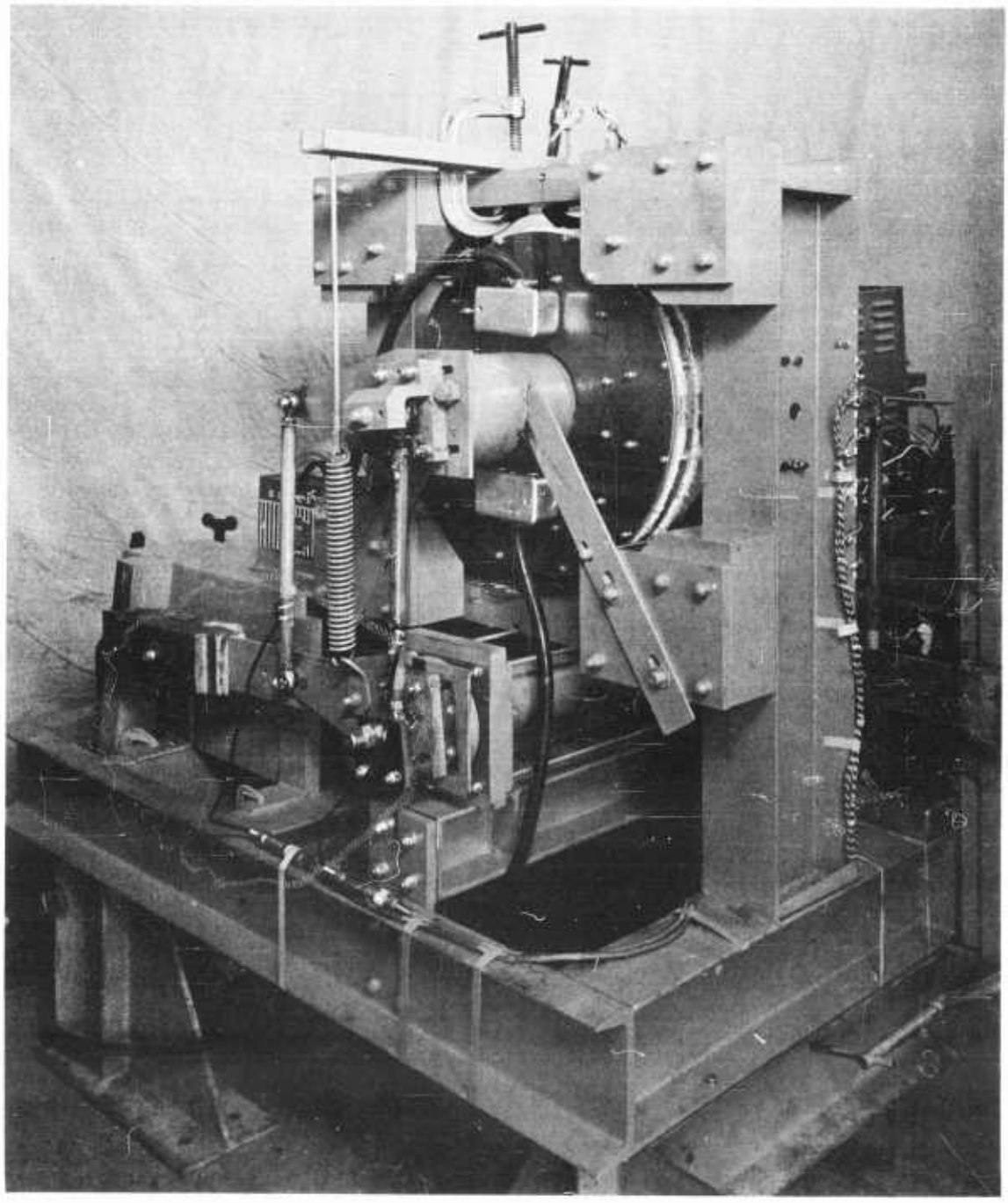

Figure 7-2. Test Fixture -- Feathering-Flapping Bearing Wear Test

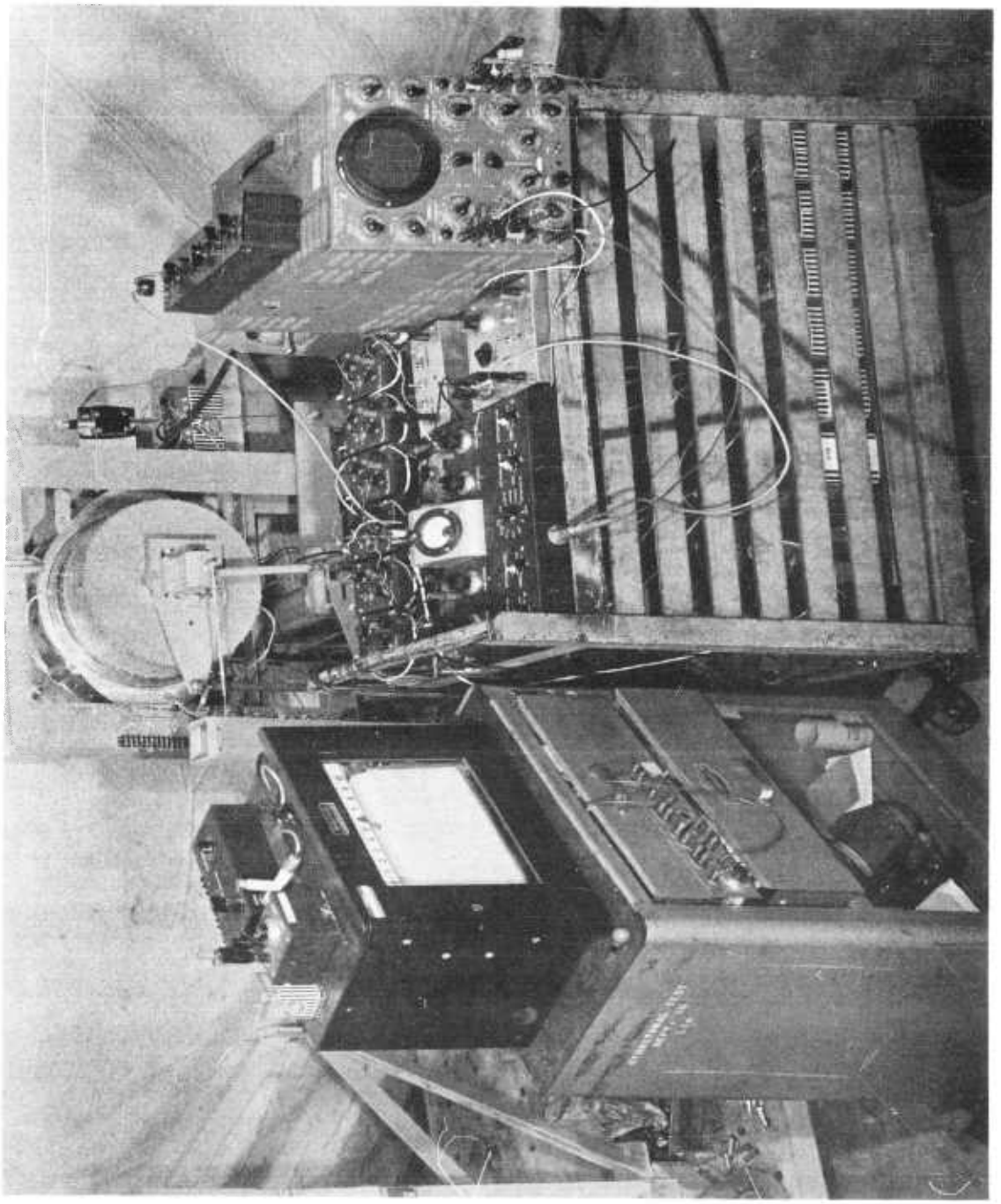

Figure 7-3. Instrumentation -- Feathering-Flapping Bearing Wear Test

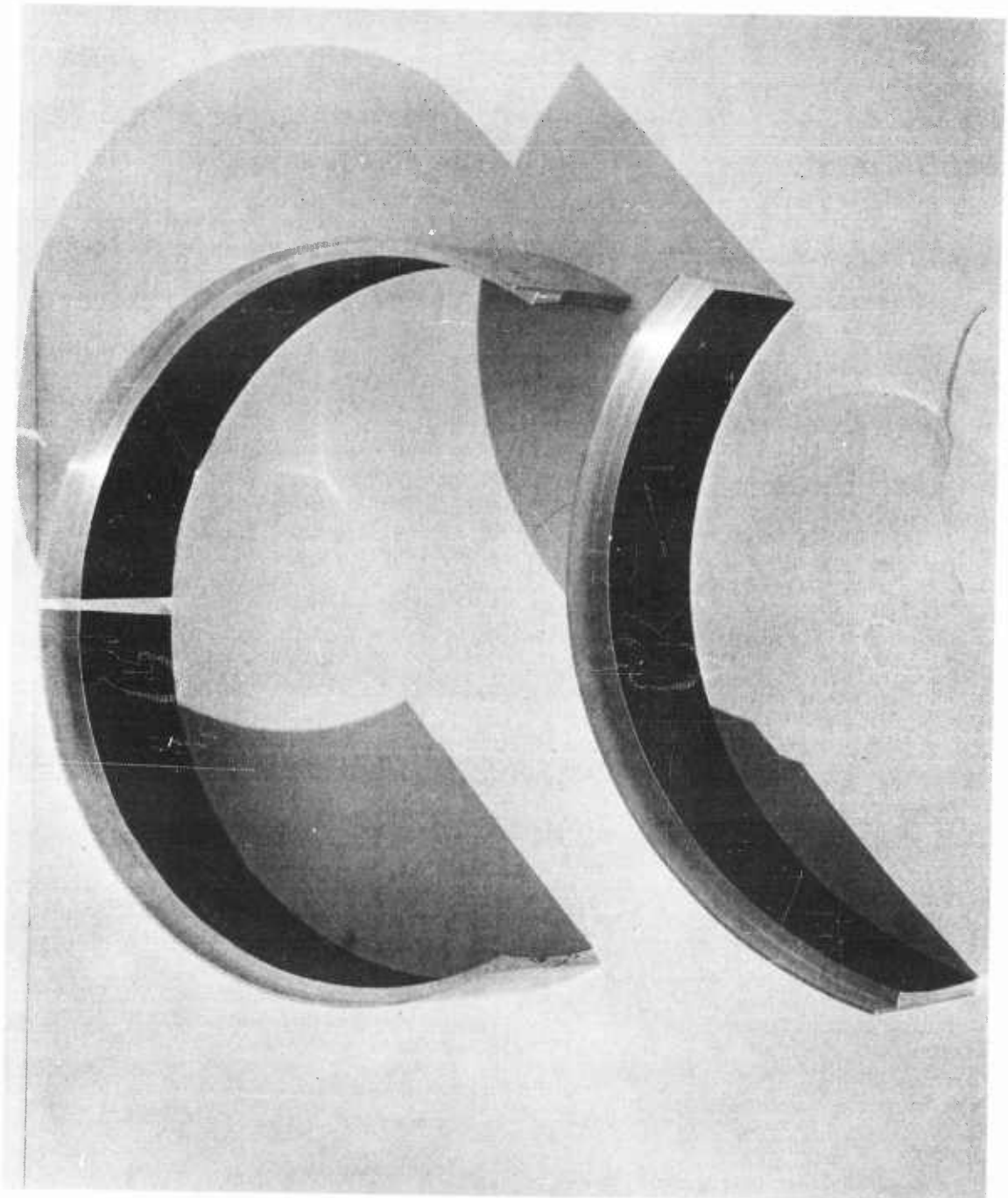

Figure 7-4. Metal Retainer Bonded with "Fabroid"

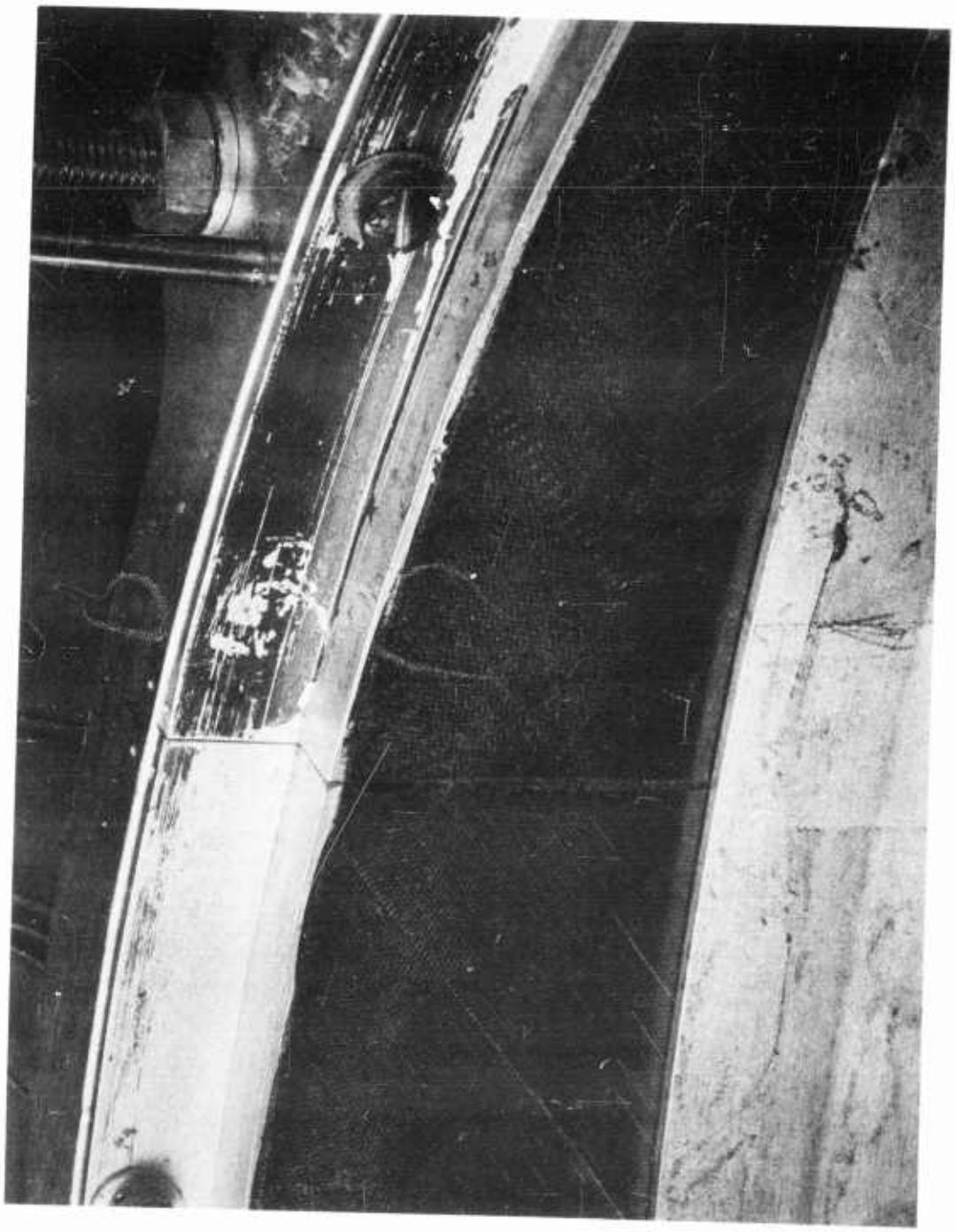

Figure 7-5. Fabroid Bearing after 26.5 hrs. of Test (no apparent damage)
Lower Left in Fixture

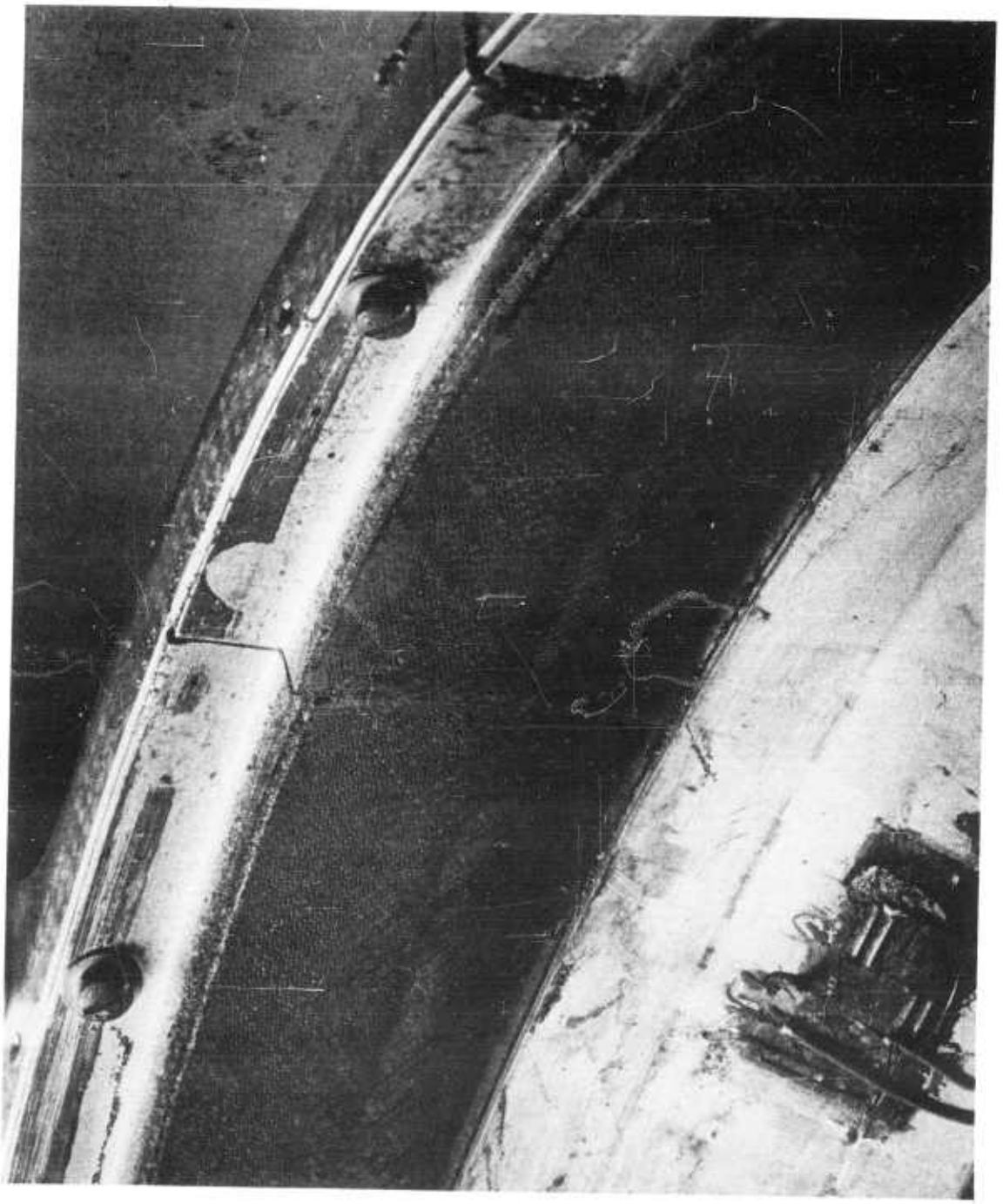

Figure 7-6. Fabroid Bearing after 26.5 hrs. of Test (no apparent damage)
Upper Left in Fixture

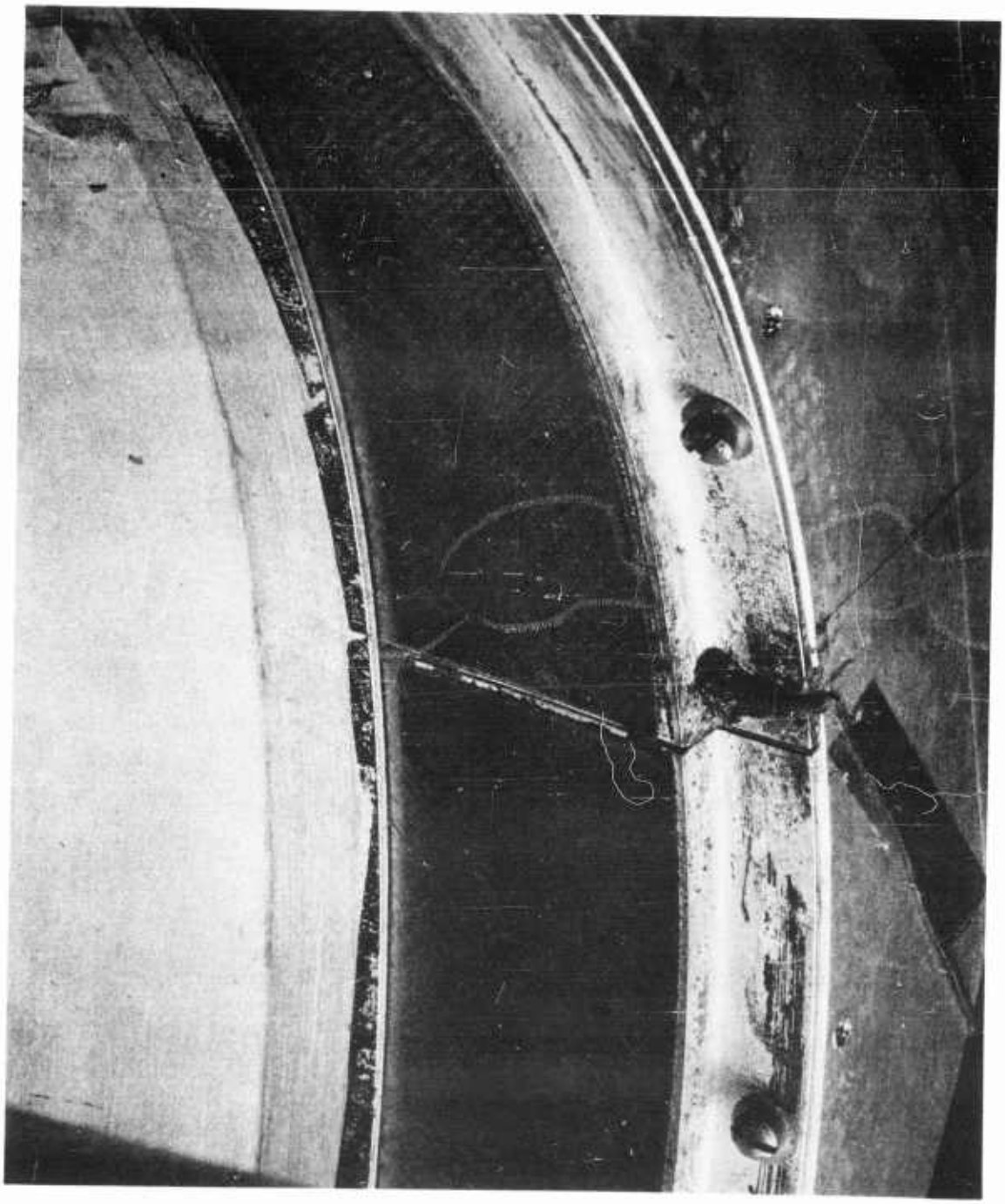

Figure 7-7. Fabroid Bearing after 26.5 hrs. of Test (no apparent damage)
Right Side in Fixture

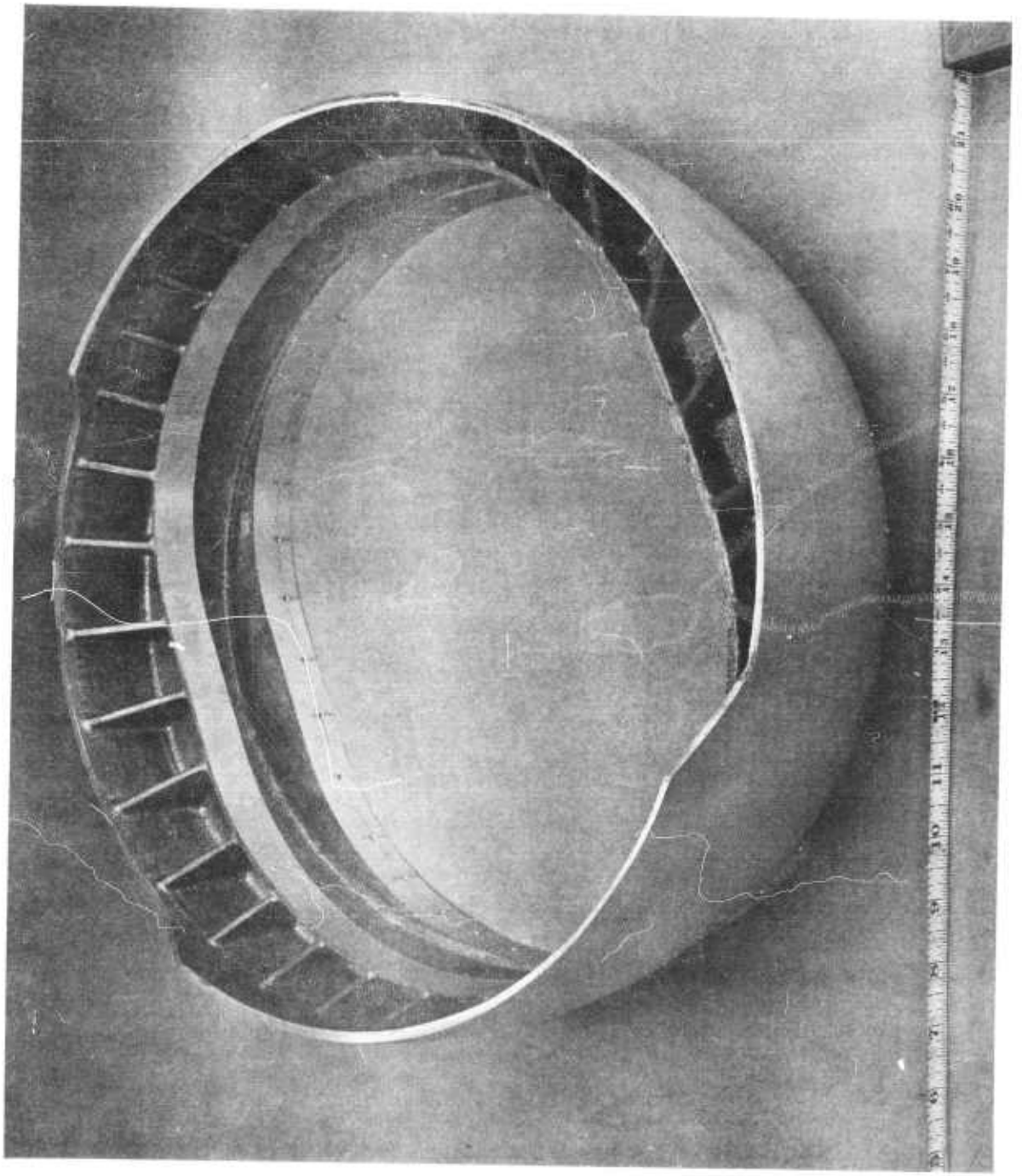

Figure 7-8. Bearing Ball

SECTION 8

TWO SEGMENT DUCT ASSEMBLY SEALANT TEST

8.1 PURPOSE

To determine the ability of RTV-601 sealant compound in the flexural joint between two duct segments to withstand thermal and pressure environments.

8.2 TEST SETUP

8.2.1 Test Specimen

The test specimen consisted of a two segment duct assembly, HTC-AD Drawing 285-0957. This assembly included two duct segments, HTC-AD Drawing 285-0113, assembled at the flexural joint per drawing 285-0167. Steel bulkheads at each end of the segment assembly contained the pressure environment and also provided support for air pressure lines and gage, and, rod-type radiant heat coils inserted into each duct approximately 19.0 inches. See Figure 8-2. A centrifugal blower mounted in front of the test assembly simulated air flow across the segments and prevented the outer skin temperatures from exceeding 600°F. This blower is shown in Figure 8-3.

8.2.2 Sealant Application

All leaks at the flexural joint were sealed with RTV-601 silastic rubber compound, manufactured by the Dow Corning Corporation. The sealant was applied on the faying surfaces of the outer skins and the flanges of the flexural joint. After most of the rivets were installed, additional sealant compound was applied to the inner surface of the flexural coupling and outer skin by means of long tubes inserted through rivet holes. This sealant application technique was identical to the sealant repair operation used on the whirl test blades.

8.2.3 Instrumentation

Thermocouples were installed in the ducts, flexural coupling and outer skin areas. Figure 8-1 shows these locations. Temperature measurements were recorded from a Leeds and Northrup Potentiometer. The leakage rate of air was measured with a Fisher - Porter rotatometer.

Figure 8-1. Temperature Distribution

PHASE 1

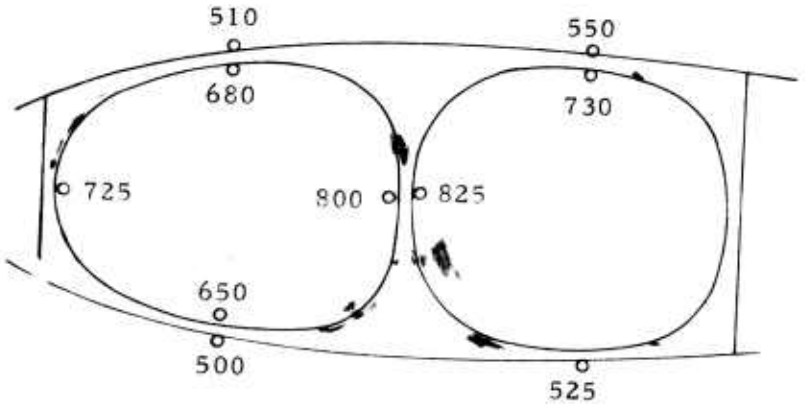

Up

Fwd

PHASE 2

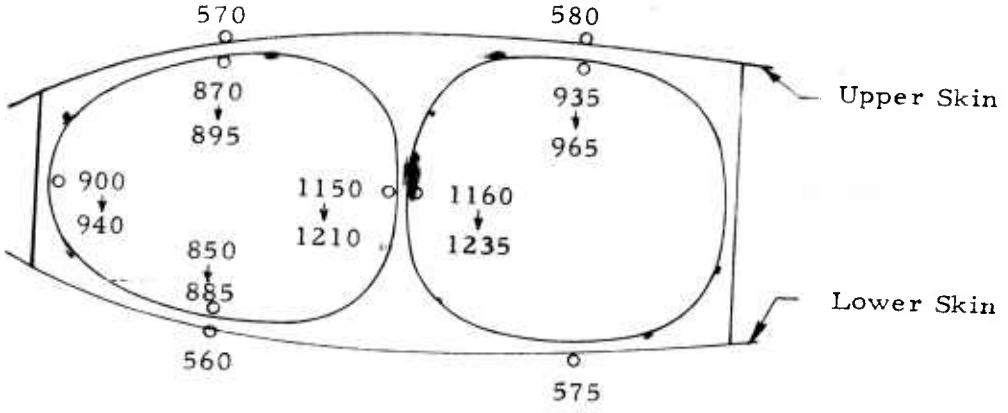

PHASE 3

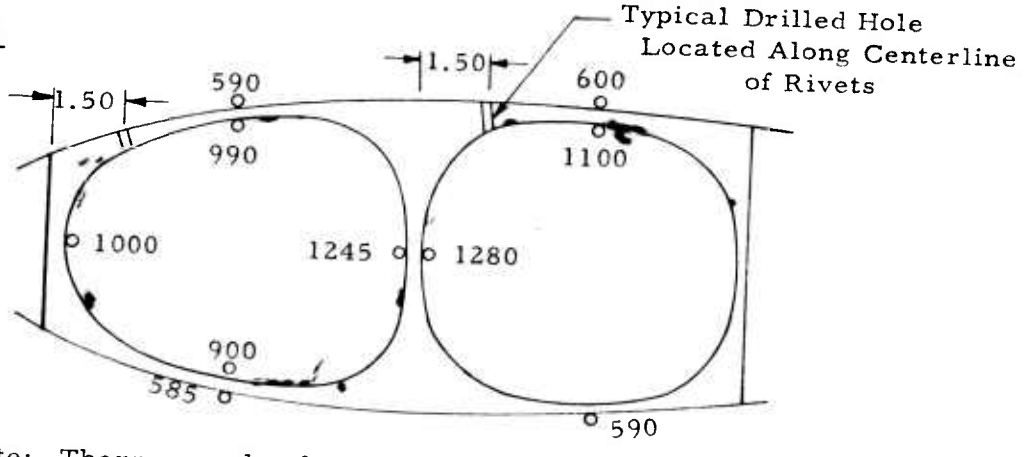

Note: Thermocouples located on Inner Wall of Ducts and Along Centerline of Flexural Coupling

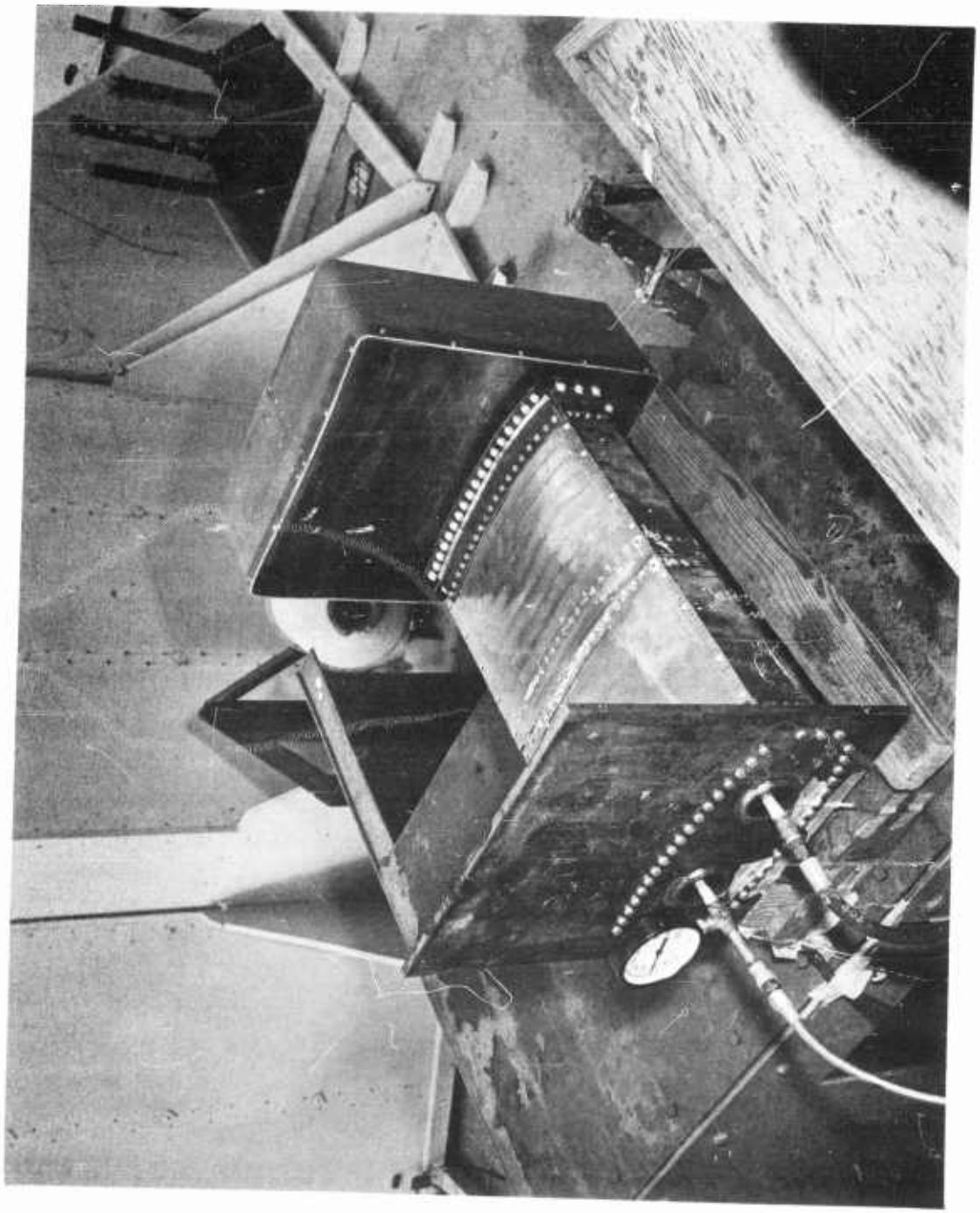

Figure 8-2. Test Setup -- Two Segment Duct Assembly

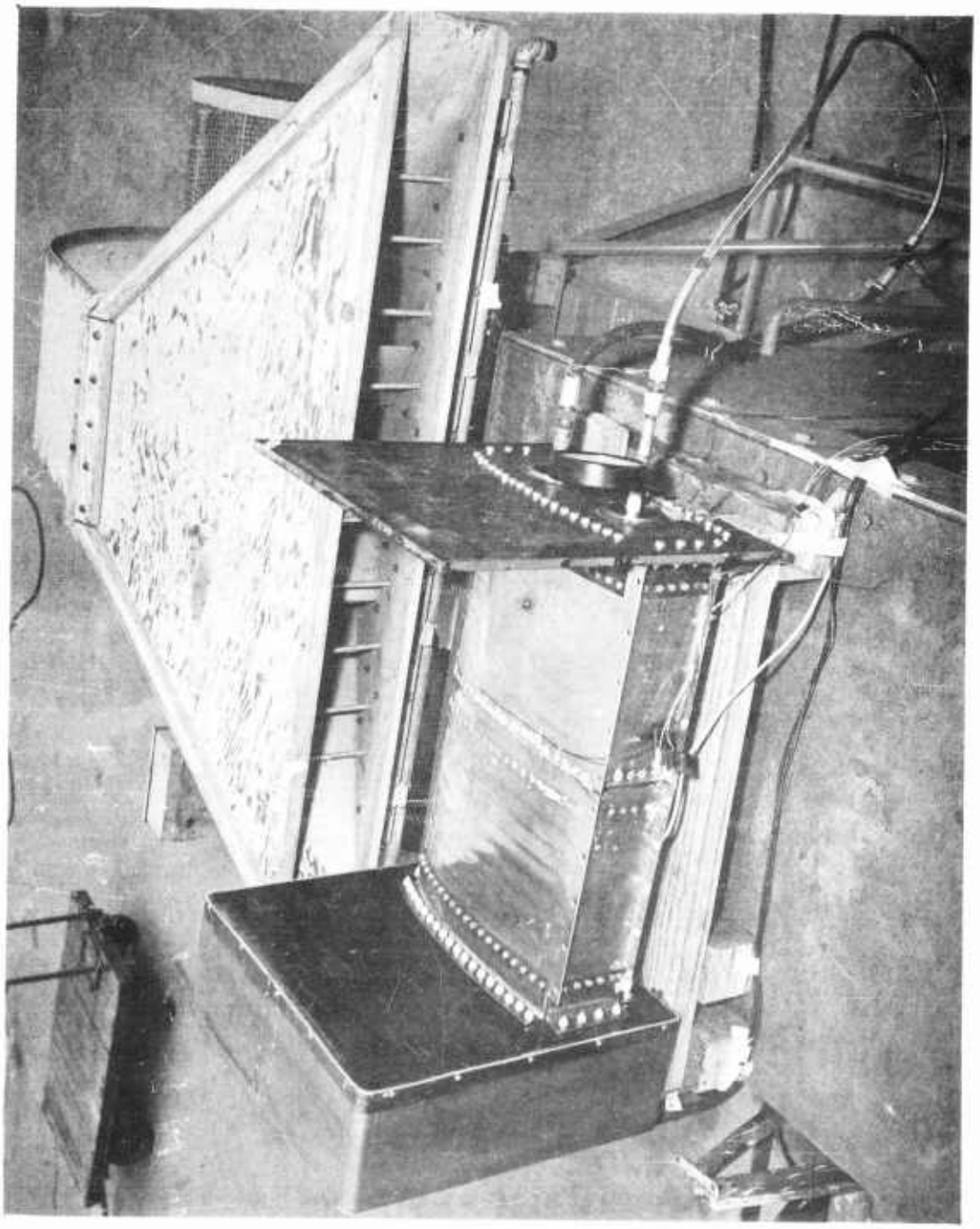

Figure 8-3. Test Setup -- Two Segment Duct Assembly

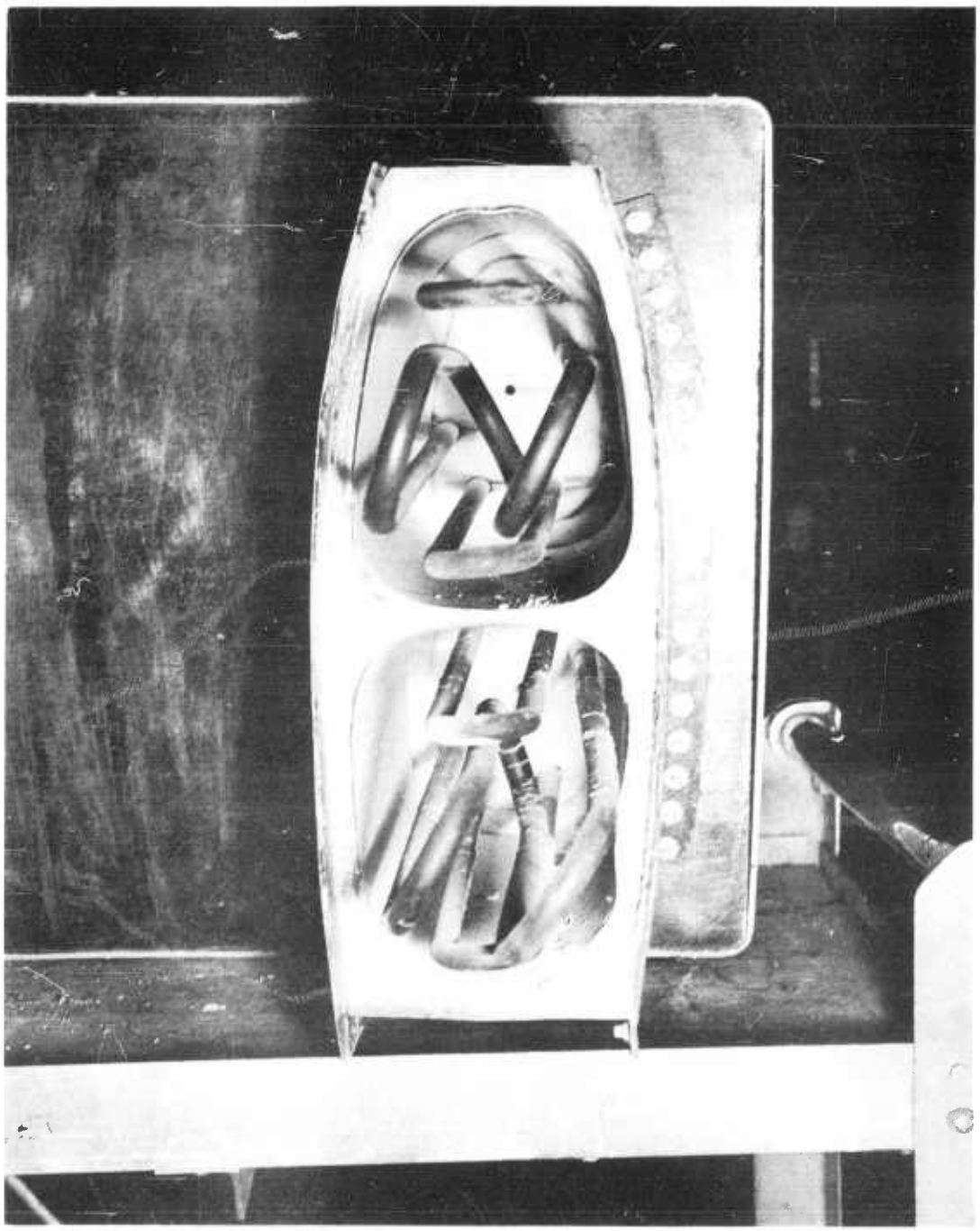

Figure 8-4. View of Flexural Coupling and Sealant

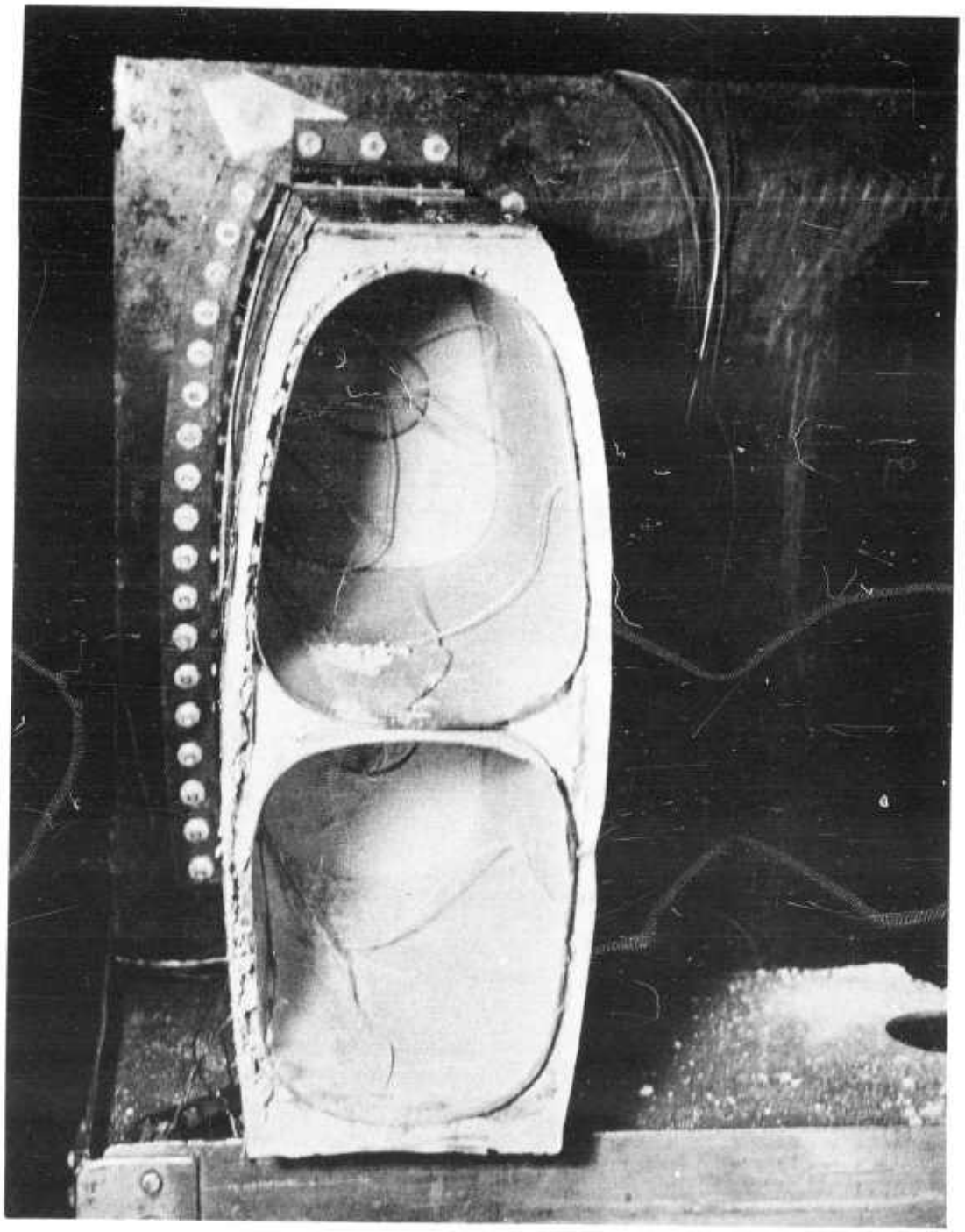

Figure 8-5. View of Duct and Joint Area

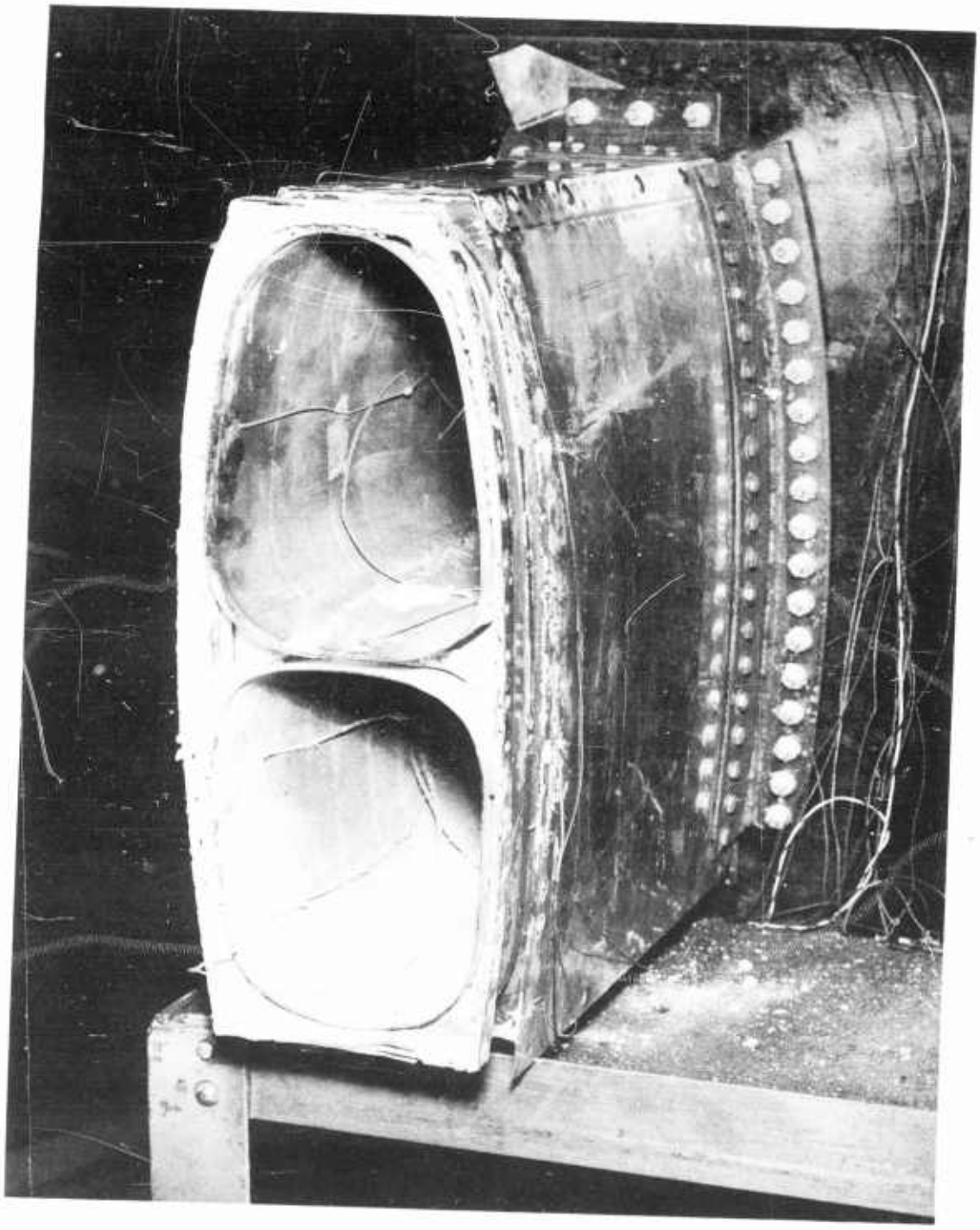

Figure 8-6. View of Duct and Joint Area

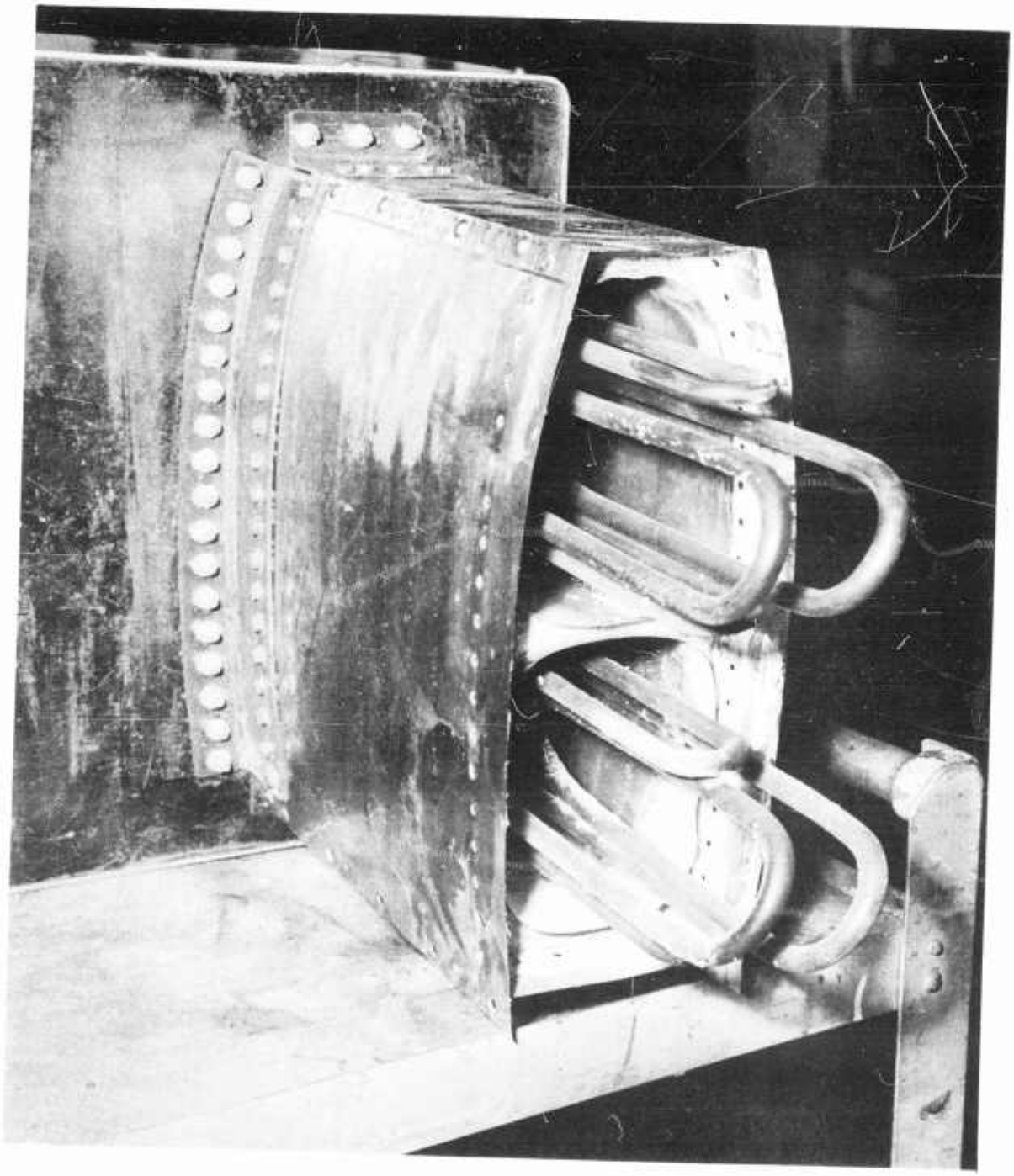

Figure 8-7. View of Joint Area

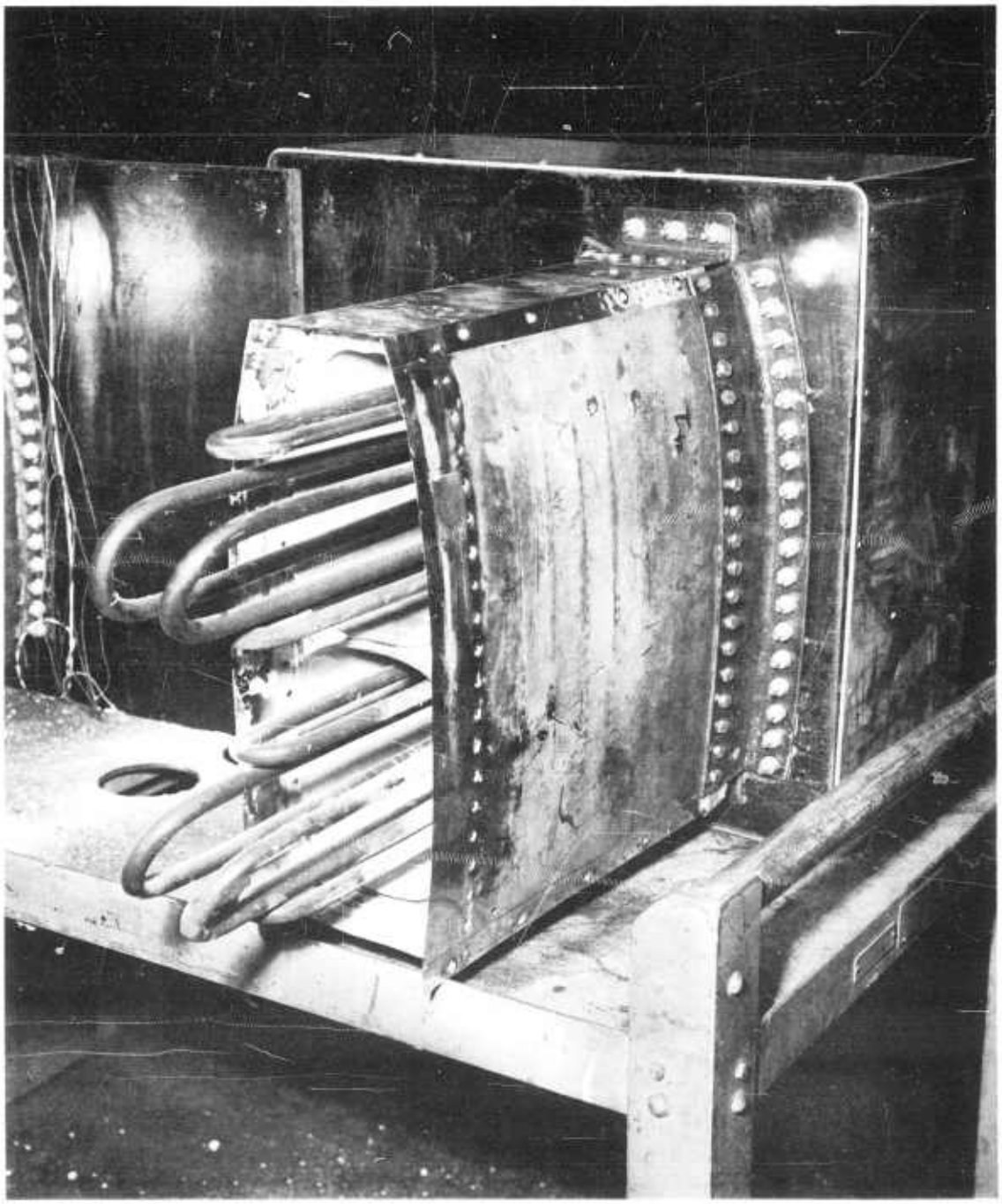

Figure 8-8. View of Joint Area

Initial sealant tests were conducted to determine the combustion characteristics of the RTV-601 sealant. These tests are presented in the Materials and Processes Report, #285-18 (62-18). The two segment Duct Assembly Sealant Test showed that the sealant did not ignite under design conditions of pressure and high temperature.

UNCLASSIFIED